Université de Montréal

Methods and Physical Chemistry of Resin-based Dental Composites

Par Eric Habib

Département de Chimie
Faculté des arts et des sciences

Thèse présentée en vue de l'obtention du grade de philosophiæ doctor (Ph.D.) en chimie

Août 2017

Résumé

Les propriétés des composites dentaires ont été nettement améliorées depuis leur invention, mais la compréhension de la physique qui guide leurs propriétés est toujours obscure. L'objectif de cette thèse est de découvrir les tendances et relations qui régissent l'effet des agents de remplissage sur les propriétés du composite qui en résulte.

La photocalorimétrie (pDSC) a déjà été utilisée pour mesurer le degré de conversion des résines dentaires, mais les paramètres de mesure n'ont jamais été adéquatement définis. En utilisant des variations systématiques dans la séquence d'analyse, la température, la masse d'échantillon, l'intensité lumineuse ou la composition atmosphérique, un protocole optimisé a été établi pour obtenir des résultats fiables et reproductibles.

Une série de composites dentaires a ensuite été formulée avec de la silice sphérique à basse dispersité de tailles gradées de 75 à 1000 nanomètres à différents taux de chargement. La viscosité de ces composites avant la polymérisation a été mesurée et utilisée pour améliorer le modèle classique Krieger-Dougherty de viscosité des suspensions de façon à ce qu'il inclue l'aire de surface des particules en plus du taux de chargement. Ce model étendu (EKD) a aussi été utilisé pour calculer la conversion du composite. C'est le premier modèle unifié qui permet de calculer la viscosité et la conversion des composites en utilisant seulement la taille des agents de remplissage et la composition de la résine.

Le chargement maximal et les propriétés mécaniques de ces mêmes composites ont aussi été étudiées. Bien que le chargement maximal fonctionnel varie selon la taille des particules, la force flexurale ultime des composites dépend seulement du taux de chargement des particules et non de leur taille. D'autres tests avec ces composites ont démontré que la taille des particules est directement liée à la transparence des matériaux, ainsi l'opacité augmente avec la taille des particules.

Cet œuvre avance les limites de la compréhension des matériaux dentaires. Le nouveau protocole de pDSC permet des mesures plus fiables de conversion et le model EKD nous permet de prédire plus précisément les propriétés des composites par leurs composantes seules. Les règles établies dans cette thèse peuvent donc être utilisées pour concevoir des composites avec les propriétés désirées de viscosité avant polymérisation, de conversion, de propriétés mécaniques et de transparence.

Mots clés : photocalorimétrie, technique pDSC, viscosité, chargement, silice sphérique, aire de surface, transparence, formulations, composite dentaire, compréhension technique.

Abstract

The properties of dental resin composites have improved significantly since their inception, but the fundamental physics behind their properties remain to be explained or modeled comprehensively. The aim of this thesis is therefore to study the fundamental trends and relationships between the filler particles constituting these materials and the resulting properties.

Photocalorimetry (pDSC) methods have been used previously to measure the degree of conversion in dental resins, but the measurement parameters have never been adequately assessed. Through systematic variations of the analysis sequence, sample mass, temperature, light intensity, and atmospheric composition, an optimized protocol was established to yield reliable and reproducible results.

A series of dental composites was then formulated with spherical silica particles of graded sizes from 75 to 1000 nanometers at different loading levels. The viscosity of these composites before polymerization was measured and used to expand the classic Krieger-Dougherty suspension viscosity model to account for filler surface area in addition to filler loading. This extended model (EKD) was also used to model composite conversion, resulting in the first unified model of composite viscosity and conversion using only filler size and resin composition.

The maximum loading and post-cure mechanical properties of these same composites were also examined. Although the maximum functional filler loading varied according to the filler size, the ultimate flexural strength of the materials depended only on the filler loading. Further tests with these composites showed that filler size was directly responsible for transparency of the materials, with opacity increasing as a function of filler size.

This work pushes the boundaries of understanding in dental composites. The newly established protocol for pDSC measurements yields more reliable conversion data, and the EKD model allows for more accurate predictions of dental composite properties directly from their component parts. The guidelines established here can now be used to design new composites with the desired properties of viscosity, conversion, mechanical strength, and transparency.

Keywords: photocalorimetry, pDSC technique, viscosity, loading, spherical silica, surface area, transparency, formulations, guidance, technical understanding.

Table of Contents

List of Tables

Table of Figures

List of Symbols and Abbreviations

φ	volume fraction loading
φ_M	maximum volume fraction loading
Φ	mass fraction loading
η	viscosity sometimes used to mean the amplitude of complex viscosity ($\|\eta^*\|$)
η_c	continous phase (resin) viscosity
η^*	complex viscosity (Pa.s)
$\|\eta^*\|$	magnitude of the complex viscosity vector (eq 4.5)
$[\eta]$	intrinsic viscosity (in Krieger-Dougherty equation)
λ	wavelength
ρ	density (g/cm^3)
A	area, or Arrhenius equation coefficient
B	constant in conversion equation for EKD (eq 4.11)
BisEMA	ethoxylated BisPhenol A glycerolate dimethacrylate
Bis-GMA	bisphenol A glycerolate dimetharylate
c	surface interaction constant
CAD-CAM	computer aided design – computer aided manufacturing
Conv	conversion
CQ	camphorquinone
d	diameter
E_A	transition or activation energy
EDMAB	ethyl dimethylaminobenzoate
HAP	hydroxyapatite
POSS	polymeric oligomeric silsesquioxane
R	gas constant ($8.314\ JK^{-1}mol^{-1}$)
R^2	correlation coefficient
RAFT	reversible addition fragmentation chain transfer
RBC	resin-based composites

t	time
T	temperature
TEGDMA	triethylene glycol dimethacrylate
UDMA	diurethane dimethacrylate

To my wife, who has supported me throughout my extensive scholastic life.

Acknowledgements

I would like to thank Prof Zhu for his support and guidance throughout my doctorate, and particularly for taking a risk on me, to transition from biochemistry into polymer and composite science. Despite sometimes getting into heated arguments, they always led to productive outcomes, and it was always for the best! Thanks to Dr Daniel Fortin for all his feedback on the project and the information, as well as the support for my work and conference presentations. I would also like to thank Wilms Baille for his guidance and mentorship in all things business and entrepreneurship (and chemistry), which I hope will continue to develop into something fun and productive.

I would also like to thank my colleagues, particularly those with whom I shared an office, where we shared many interesting discussions: scholastic, philosophical, or just friendly. Thanks to Frantz Ledévédec for introducing me in the lab and showing me the ropes, to Nicolas Lévarray for his laid-back attitude and interesting brainstorming sessions, Rémi Vachon for his impressive level of organization and always sincere feedback, Meng Zhang for his enthusiasm and determination in the face of difficulties, Edgar Alberto Ortiz for his sharp wits and quick drinks; last, but not least is Ruili Wang for all of the different discussions and feedback between us for our publications and work on dental materials.

Thanks to Pierre Ménard and Sylvain Essiembre for all their help in the use of instruments and the best ways to use the data coming out of them.

Thanks to Prof Meifang Zhu as well as the other professors at Donghua University that allowed me that three-month internship in Songjiang, and to meet many new people, and make new friends.

Finally, I would like to thank my committee members for their time and thoughts about my work and thesis.

Foreword

Most of my academic career thus far has been a transition from one philosophical extreme of science to another, going from fully fundamental research in membrane protein topology to highly applied research in dental composites. Part of my initial attraction to material chemistry was that although it remains research in chemistry - the science of matter - it was decidedly applicable and could directly be used to make new products for any purpose. Truly, one need only look around the house to see all the advances in the last century that have allowed plastics to become omnipresent. Even previously domain specific words such as carbon fiber and polypropylene have become part of the mainstream language.

Many a chemistry thesis has lingered on a library shelf, unread due to its complexity and lack of accessibility to the general public. However, a large majority of North Americans have had an experience with dental fillings, having lived the moment of bright blue illumination while dental professionals tinker in their mouths. For this reason, dental composites are a topic that is accessible to everyone. Beyond their direct experience with these materials, their accessibility comes from their simplicity: a liquid resin with some solid particles in it; a concept that anyone can grasp. This thesis strives to explain how such a simple mix results in the complex properties that are observed and exploited for the treatment of cavities.

Whether you are a seasoned chemist or simply someone with an interest in what dentists are putting into your teeth, I hope that this thesis will give you an idea of the state of the art in dental resin composites and the current understanding of their composition and function.

Chapter 1 - Introduction

Dental caries are a world-wide health problem. A Health Canada survey from 2007-2009 revealed that 95% of Canadians adults have a history of cavities (*1*), totalling 12.5 B$ in expenses in 2013 (*2*). These problems have been a concern for people for a very long time. While tooth decay was rare in pre-agricultural society, the development of farming, circa 10,000 BCE, led to an increase in the frequency of decay in teeth to upwards of 10% of the population (*3*). Dentistry evolved soon after, with evidence of dental drilling as far back as 12000 BCE (*4-6*). Even more intriguingly, a 2012 study (*7*) discovered evidence that even as far back as 6500 BCE, honeybee wax was used as a dental filling. Moving forward in time, there is anecdotal evidence indicating that dental amalgam was used as early as 618 CE in the Tang Dynasty (*8-9*), using alloys of tin and silver. However, only by the 16th or 19th century did the more modern mercury-containing version of dental amalgams appear, alongside other metals like tin, gold, and even lead and thorium.

1.1 Dental Restorations

Dental restorations today have developed significantly since their infancy in the Neolithic period, and encompass a wide range of materials including metals, polymers, ceramics, and composites. The materials used for these restorations are separated into indirect and direct restorations.

Indirect restorations include inlays or onlays, crowns, bridges, and veneers. These restorations are fabricated in a dental laboratory, and then are cemented or otherwise permanently bonded to the teeth to restore appearance or function. Recent advances in computer aided design and computer aided manufacturing (CAD-CAM) has allowed many of these traditionally slow-process restorations to become more convenient, if more expensive (*10-11*).

1.2 Direct Dental Restorative Materials

Direct restorations consist of materials that start out as soft and pliable substances that can be shaped as desired or used to fill gaps, and are subsequently hardened to their final properties. Several types of materials exist within this category, the most prominent of which are metal alloys, glass ionomer cements, and resin composites.

1.2.1 Dental Metal Alloys

Historically, the material of choice for this type of restoration has been amalgam. This mercury alloy consists of a 4:6 mix of mercury and other metals, a mix of silver, tin, zinc, and copper (*12*). These come in a capsule in separate phases that are mixed to obtain a paste that hardens over 2.5-4.5 minutes. Amalgam restorations have a very long history of use, as mentioned previously, and their performance has also historically been very good, with a mean survival time of 11.4 years (*13*).

Amalgams are used for occlusal and proximal restorations, including the occlusal surfaces (the tooth's mastication surface), where the forces are the strongest (*14*). The main reason for these particular clinical indications are that amalgam restorations do not bind to the tooth surface; all their retention is mechanical. The main drawbacks associated with amalgam fillings are their poor aesthetic quality due to the metallic finish of the material, in addition to the darker finish that results from the oxidation of the amalgam. Furthermore, there have been recent health concerns about the presence of mercury in these products, though most authorities in dental materials maintain that these materials are safe and release negligible amounts of mercury (*15-16*).

1.2.2 Glass Ionomeric Restoratives

Glass ionomer cements are composed of separate fluoroaluminosilicate glass particles and water soluble polymers or copolymers of carboxylic acids. The setting reaction that occurs upon mixing these two components involves dissolution and then coordination of the glass particles with the acidic polymers, resulting in a highly cross-linked network (Figure 1.1). This setting reaction advances sufficiently in 4-6 minutes for stiffness; however, it takes approximately 24 hours for it to be complete. In order to improve their mechanical properties and shorten the setting time, ionomers can be combined with methacrylate resins for a dual cure free radical/coordination setting mechanism.

Due to their calcium-coordination properties, these materials exhibit strong adhesion to tooth tissue, and therefore do not require additional adhesive preparation; they are indicated for use as cements and luting agents. Furthermore, the fluoride release in the setting reaction is very useful for restorations in high carie-risk areas. The biggest drawback of these materials, however, is that their mechanical properties are not sufficient for high stress restoration areas, such as those where amalgam and resin composites can be used. These

materials are therefore mostly used for side restorations and for restoring primary (children's) teeth.

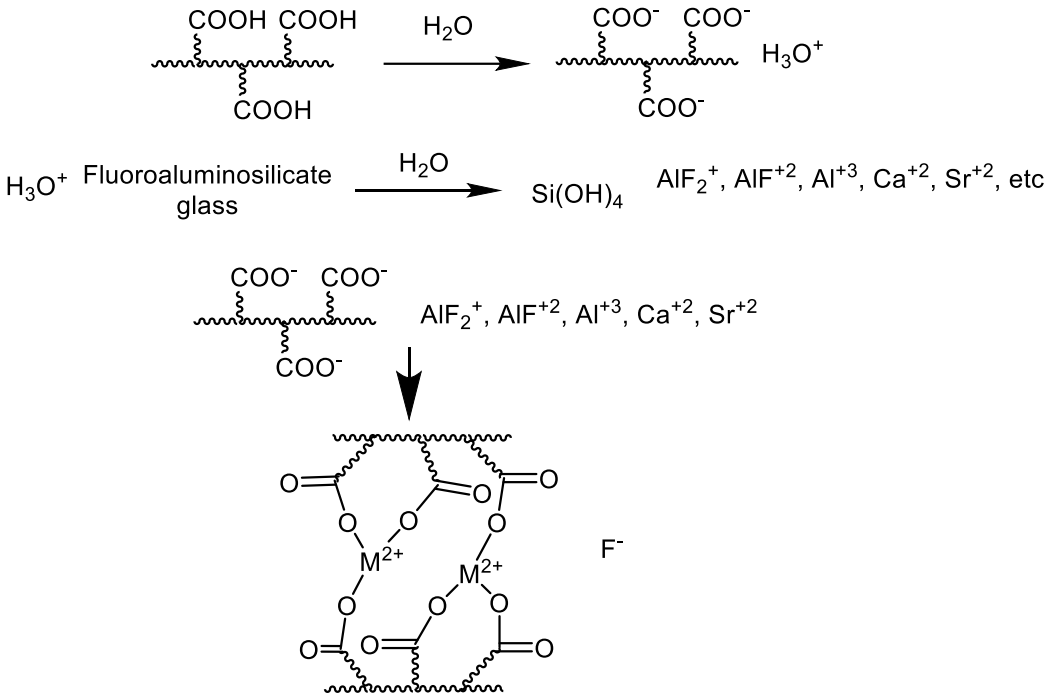

Figure 1.1 - Setting reaction for glass ionomers from (*17*).

1.3 Dental Resin Composites

The main alternative to dental amalgam for high stress restorations comes in the form of dental resin composites. These materials are sometimes called "white fillings", and are often confused with ceramics (which are an entirely other class of fully inorganic materials). These composites are made from a mix of inorganic particles (fillers) and a resin matrix that can be polymerized once in place. This class of dental materials was initially developed in the 1960s by Raphael Bowen, using vinyl-modified vitreous silica particles and a resin composed of bisphenol A glycerolate dimethacrylate (Bis-GMA, Figure 1.2), methyl methacrylate, and tetraethylene glycol dimethacrylate, with benzoyl peroxide and 4,N,N-trimethylaniline as radical initiator and co-initiator, respectively (*18*). These materials were separated into powder and liquid, with the initiation starting upon mixing of the two.

Despite the advancements, the general formulation for these materials has remained similar throughout their development: they are composed of a mix of resin monomers,

including initiators and co-initiators, and surface modified filler particles. Though some composites still exist at a two-part mix for self-curing (thermal curing) materials, most of them now use blue light-initiated curing reactions, where no mixing is required.

1.3.1 Common Resin Monomers

Most of the resin monomers that are in use today remain similar to the original Bis-GMA and tetraethylene glycol dimethacrylate monomers; the two most frequently used ones today being Bis-GMA and triethylene glycol dimethacrylate (TEGDMA, Figure 1.2). Bis-GMA-based resins produce good mechanical and polymerization performance, but due to the very high inherent viscosity of Bis-GMA, it must be diluted with a more liquid monomer, hence the use of TEGDMA. To remedy the high viscosity of Bis-GMA, many derivatives have been developed, mainly modifying the glycidyl hydroxyl group to dramatically reduce the resin viscosity (*19-25*).

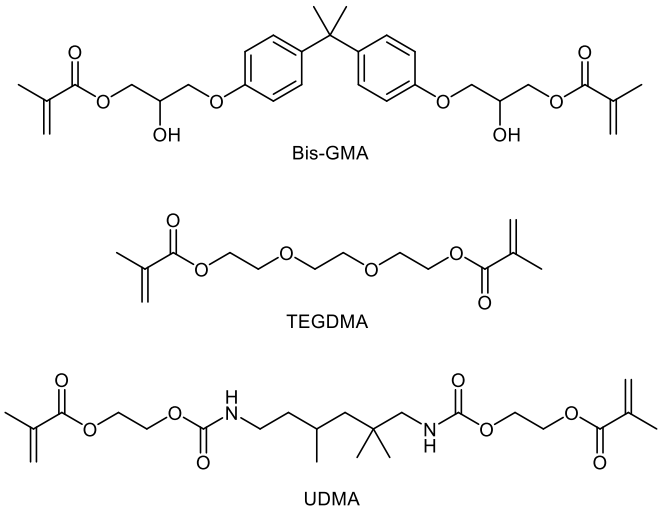

Figure 1.2 – Monomers commonly used for dental composites. Bisphenol A glycerolate dimethacrylate (Bis-GMA) is often diluted with triethylene glycol dimethacrylate (TEGDMA). Bis-GMA is is often replaced with diurethane dimethacrylate (UDMA) due to its high viscosity.

Another strategy to circumvent the viscosity problem of Bis-GMA was the development of a class of urethane methacrylates (UDMA, Figure 1.2). These compounds bare a mostly linear aliphatic chain, including some carbamate bonds, hence the 'urethane'

nomenclature. These compounds exhibit lower viscosity than Bis-GMA, though higher than that of TEGDMA, resulting in properties intermediate between the two.

1.3.2 State of the Art in Resin Monomers

While the majority of resins that are being used still resemble Bis-GMA and TEGDMA, there has been extensive work on developing alternatives to these compounds, due to the high shrinkage of methacrylate monomers (*26-27*) and toxicity of Bis-GMA and TEGDMA resins (*28-30*). Some of the more radically different monomers include a 'silorane' class of cyclic monomers (Figure 1.3A) that were meant to revolutionize the dental industry, but ultimately fell short in their mission due to lack of market adoption (*31*). Another class of materials that has emerged are the natural product-based resins, using isosorbides (Figure 1.3B)(*32-33*), or even bile acids (Figure 1.3C)(*34-36*); these products showed promising properties for sustainable and lower toxicity monomers. Aside from these, there have not been any true leaps in the advancement of these resins; this led the US National Institute of Health call for proposals with a 2.8 M$ grant for new longer-lasting dental materials in 2013, which was awarded to several groups that have made significant progress in this area (*37*).

Most of the work directed at increasing the lifetime of these materials seeks to move away from methacrylate chemistry, and their water-sensitive ester bonds. In turn, several new types of chemistries are being explored: thiol-ene radical reactions (*38-42*); base-catalyzed thiol-vinyl Michael-addition reactions (*43-45*); alkyne-azide cycloaddition with copper catalysis; epoxide-acrylate interpenetrating networks (*46-48*); and higher stability methacrylamide monomers (*49*). Thiol-ene radical polymerization monomers (Figure 1.4A) have shown some very promising results, with similar mechanical properties to traditional methacrylate monomers (*42*), albeit with slower polymerization kinetics (*41*). Photobase-catalyzed thiol alkene Michael addition (Figure 1.4B) served as an alternative to radical thiol reactions, but the kinetics are even slower than the former (*44, 50*). Epoxide-acrylate interpenetrating networks (Figure 1.4C) show that they can achieve properties that are similar, although their performance is ultimately inferior to the current dental material technologies. Finally, the use of acrylamides has been studied as methacrylate resins cross-linkers for their theoretically longer life span (due to the increased hydrolytic stability). These studies have shown that they do not significantly compromise composite strength,

however showed slower kinetics (*49*). These new resin chemistries show promise for more resilient resins in the future, but presently are still behind in terms of performance relative to the traditional composites.

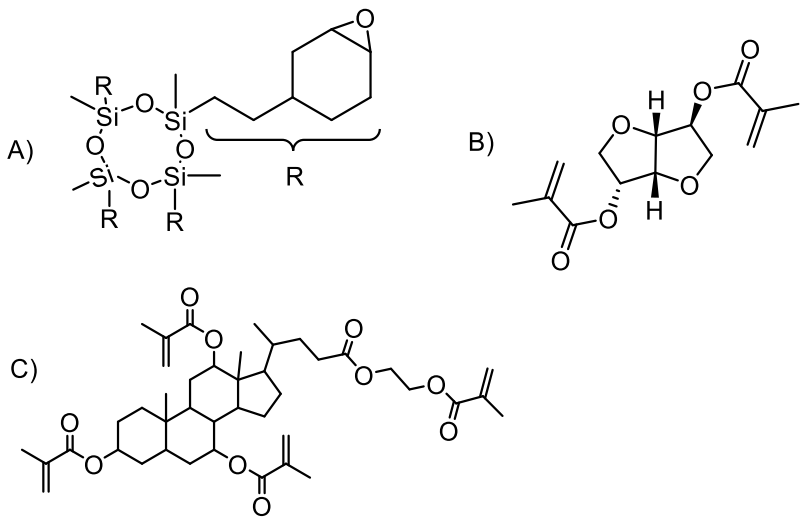

Figure 1.3 - Experimental Monomers A) 3M's silorane resins; B) Isosorbide dimethacrylate, sugar-based monomer; and C) ethylene glycol cholate tetramethacrylate, based on bile acids.

There have also been monomer developments in the use of stress-relaxing monomers, where a reversible addition-fragmentation chain transfer (RAFT) capability is included in the monomer to relieve stresses over time (*51*). These are mainly designed to reduce shrinkage stress that is caused by polymerization contraction of these materials. This type of monomer is currently used by 3M's Filtek Bulk Fill restoratives that are currently available on the market, but are still being actively studied and optimized in the literature (*43, 51-53*).

Finally, Antonucci *et al* previously investigated the use of quaternary ammonium monomers as antibacterial agents that had promising results, including increased conversion with the charged monomers (*54*). More recent work at 3M suggested that ionic liquid methacrylate monomers are capable of reducing the oxygen inhibition layer that forms on the surface of methacrylate polymerization reactions (*55*), presumably due to the low gas solubility in these materials. Further work including such monomers may become more commonplace if their properties turn out to be useful.

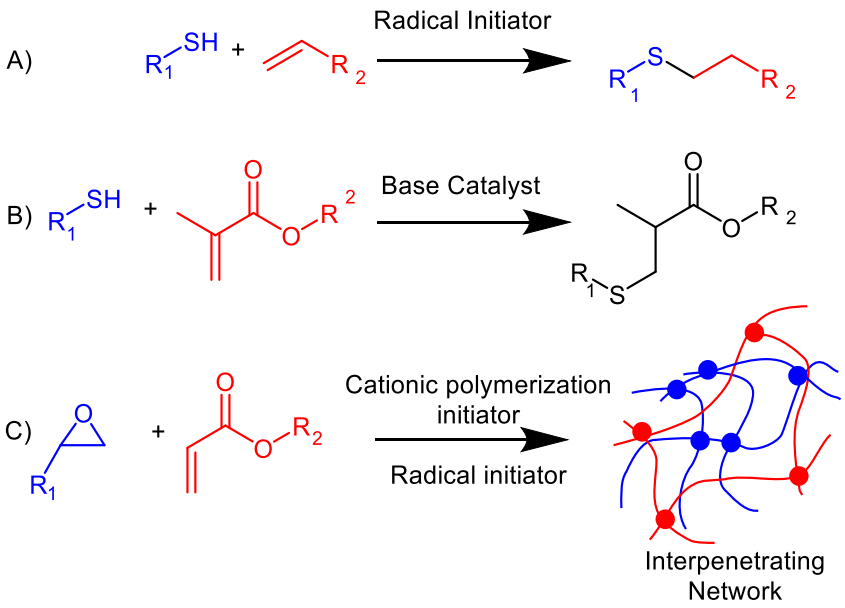

Figure 1.4 - Alternate chemistries used for new dental composites: A) Thiol-ene radical reactions, B) Thiol-Michael addition reactions, C) epoxide-acrylate interpenetrating networks with dual reaction chemistry.

1.3.3 Filler Particles

The inorganic filler particles that are used in dental resin composites are typically silicates, which range from simple silicon dioxide to alkaline silicates (e.g. barium glass) and blends with other oxides (e.g. aluminium oxide or zirconium dioxide). There have been many variations around the chemical compositions of these fillers, but most of the advancements in filler technologies have revolved around particle size (*31*) and morphology (*56*).

Despite the large amount of literature examining the commercial materials, due to the large number of possible filler variations in composition, morphology, size, and size distribution, there is still a gap in the understanding of the direct effect of these variables on the final properties of these materials. Wang *et al* (*57*) and Habib *et al* (Chapter 5) have been pushing the fundamental understanding of these material effects through theoretical and systematic experimental studies. Through theoretical understanding of filler packing (*58*), and empirical understanding of the resulting mechanical properties of these highly loaded composite materials (*59*), the existing particles can be used to obtain superior mechanical and optical properties.

In an effort to obtain properties similar to both resin and fillers, Stansbury and others have been working on fillers termed ‘nanogels’. These particles are pre-polymers that are synthesized by solution synthesis, and are then included into the composite mix along with resin and traditional filler particles (*60-66*). Composites formulated with these nanogels showed similar mechanical properties to normal composites, but exhibited up to 23% decrease in volumetric shrinkage (*60*). This improvement suggests that such materials would have a much lower failure rate due to marginal leakage (*59*).

1.3.4 Shortcomings of Dental Resin Composites

While these materials are the most used direct dental restoratives in North America, they still suffer from several shortcomings. The main pitfalls of these materials are their polymerization shrinkage, their fracture toughness, their pre-polymerization viscosity, and their biocompatibility.

Though it has improved significantly over time, the polymerization shrinkage of the materials remains its greatest flaw. This contraction can cause marginal separation and leakage, and ultimately the failure of the restoration, either due to detachment or to secondary caries.

The low fracture toughness of dental composites can amplify defects in the restorations, such that small damage can perpetuate and ultimately cause the failure of the material. The nature of the surrounding dental hard tissue requires materials with very high moduli; such materials are then very brittle, and prone to fracture. Therefore, a challenge remains to produce these very stiff materials, while increasing their toughness to reduce their tendency to crack.

The mechanical properties of the composites are closely related to their filler loading. Their loading, however, is limited by the viscosity of the material before polymerization. Therefore, by finding ways to decrease the viscosity of the pastes before polymerization, a higher loading could be achieved, leading to superior mechanical performance.

The biocompatibility of the composites has historically not been a significant problem, however, several studies examining the most common resins have shown that these have pronounced cytotoxicity effects (*28-30*). In turn, several natural product-based alternative resin monomers have been proposed, but as of yet, to our knowledge, none of these has been used commercially.

1.4 Objectives of this Work

These novel resins with alternate chemistries (**1.3.2**) are being designed to address the problems of shrinkage, toxicity, and stability in dental composites to bring these materials to the next level of performance. Both the resins and fillers are designed to increase the material's fracture toughness, minimize its shrinkage, increase its durability, and improve its biocompatibility. Since composites are heterogeneous blends though, their properties emerge from not only the component parts, but also from the interactions and synergy between them. However, the number of possible formulations is virtually unlimited, and so a fundamental understanding is necessary to narrow the parameter space to optimize them. Despite the large body of research documenting the properties of most of the commercially available composites and the effect of formulation changes in experimental composites, there has not been a consensus as to the relationships underlying these properties and processes. Therefore, most of the work in the field thus far lacks models with sufficient predictive power to have any real usefulness in designing better composites.

The main objective of this thesis was to systematically assess different formulations in order to understand the factors contributing to the properties of the composite pastes and polymerized composite materials. To this end, it was necessary to develop a more precise characterization method for composite conversion. This method and many more were then used to evaluate the influence of filler particle size on the initial and final properties of the dental resin composites.

1.5 Scope and Structure of the Present Work

This thesis consists of six chapters including an introduction and a conclusion. All of the work presented here was performed by the author of the thesis under the supervision of professor Julian X.X. Zhu.

Chapter 2 is a review on the fillers that have been explored in the use of dental resin composites, both experimental and commercial. Existing fillers types were reviewed and the properties of the resulting composites are described, both in the context of dental composites and in the broader context of industrial composite blends. (Eric Habib, Ruili Wang, Yazi Wang, Meifang Zhu, and X. X. Zhu, Inorganic Fillers for Dental Resin Composites: Present and Future, *ACS Biomaterials Science & Engineering* 2016, 2 (1), 1-11. The sections on

particle clusters and HAP were written by Ruili Wang and Yazi Wang, respectively, the rest was written by Eric Habib, manuscript revision was done by X.X. Zhu and Meifang Zhu.)

Chapter 3 describes the optimization of a photocalorimetric method for the measurement of photopolymerization reactions. Variations in mass, light intensity, temperature, protocol, and nitrogen purge time affected the polymerization kinetics, temperature, as well as the overall conversion. This work was accepted as a research article on December 1, 2017 (Eric Habib, X.X. Zhu, Photo-calorimetry Method Optimization for the Study of Light-initiated Radical Polymerization of Dental Resins, *Polymer*. The experimental design, all the experimental work and writing was done by Eric Habib, manuscript revision was done by X.X. Zhu.)

Chapter 4 explores the rheological behaviour of unpolymerized polymer pastes and their degree of conversion using composites with spherical silica fillers of graded sizes. The well-established Krieger-Dougherty model for composite viscosity was extended to account for the effect of filler surface area to accurately model paste viscosity. The final conversion of the materials was linearly related to the logarithm of viscosity and thus the filler surface area, allowing accurate modeling of both composite viscosity and conversion with different loading levels and filler sizes. This work was submitted for publication on October 11, 2017 (Eric Habib, Ruili Wang, X.X. Zhu, Correlation of Resin Viscosity and Monomer Conversion to Filler Particle Size in Dental Composites, *Dental Materials*. Experimental design and performance as well as writing were done by Eric Habib, Ruili Wang provided some samples for testing and manuscript revision, revision was also done by X.X. Zhu).

Chapter 5 describes experimental work that explores the link between the size and loading of the filler particles, and the mechanical properties and transparency properties of the resulting composites. The results show that the size of the filler particles has little influence on the mechanical properties of the resulting composites, however, the loading is limited by the composites' increasing viscosity. Finally, smaller particles result in a higher transparency of composites. This work has been published as a research article (Eric Habib, Ruili Wang, X.X. Zhu, Monodisperse silica-filled composite restoratives mechanical and light transmission properties, *Dental Materials*, 33 (3), 2017, Pages 280-287. Experimental design and performance as well as writing were done by Eric Habib, Ruili Wang provided some samples for testing and manuscript revision, revision was also done by X.X. Zhu).

Chapter 6 is an overall summary of the work in this thesis and presents further work that could be performed in the same vein.

1.6 References

1. Canada, H. *Canadian Health Measures Survey (CHMS)*; 2010.
2. CDA *Dental care expenditures in Canada in 2013*; 2017.
3. Barras, C. How our ancestors drilled rotten teeth. http://www.bbc.com/earth/story/20160229-how-our-ancestors-drilled-rotten-teeth (accessed 2017-05-29).
4. Oxilia, G.; Peresani, M.; Romandini, M.; Matteucci, C.; Spiteri, C. D.; Henry, A. G.; Schulz, D.; Archer, W.; Crezzini, J.; Boschin, F.; Boscato, P.; Jaouen, K.; Dogandzic, T.; Broglio, A.; Moggi-Cecchi, J.; Fiorenza, L.; Hublin, J. J.; Kullmer, O.; Benazzi, S., Earliest evidence of dental caries manipulation in the Late Upper Palaeolithic. *Sci Rep* **2015,** *5*, 12150.
5. Gray, R. Did prehistoric humans use dentists? 14,000-year-old tooth decay found to have been scraped out with sharpened stone *Mail Online* [Online], 2015. http://www.dailymail.co.uk/sciencetech/article-3165079/Did-prehistoric-humans-use-DENTISTS-14-000-year-old-tooth-decay-scraped-sharpened-stone.html (accessed 2017-05-31).
6. Than, K. Yeeowww! Prehistoric dentists used stone drills *Live Science* [Online], 2006. http://www.livescience.com/4024-yeeowww-prehistoric-dentists-stone-drills.html (accessed May 31, 2017).
7. Bernardini, F.; Tuniz, C.; Coppa, A.; Mancini, L.; Dreossi, D.; Eichert, D.; Turco, G.; Biasotto, M.; Terrasi, F.; De Cesare, N.; Hua, Q.; Levchenko, V., Beeswax as dental filling on a neolithic human tooth. *PLoS One* **2012,** *7* (9), e44904.
8. Zylstra, F. The history of dental amalgam *caringtreechildrensdentistry.com* [Online], 2015. http://www.caringtreechildrensdentistry.com/the-history-of-dental-amalgams/.
9. ADA History of Dentistry Timeline. http://www.ada.org/en/about-the-ada/ada-history-and-presidents-of-the-ada/ada-history-of-dentistry-timeline (accessed May 31, 2017).
10. Miyazaki, T.; Hotta, Y.; Kunii, J.; Kuriyama, S.; Tamaki, Y., A review of dental CAD/CAM: current status and future perspectives from 20 years of experience. *Dent Mater J* **2009,** *28* (1), 44-56.

11. Brown, C. Which is the highly competent dental lab technology use today *WebDental Blog* [Online], 2015. http://www.webdental.com/profiles/blogs/which-is-the-highly-competent-dental-lab-technology-use-today.
12. Dentsply, Dispersalloy - Technical Product Guide. Caulk, D., Ed. 2015.
13. Antony, K.; Genser, D.; Hiebinger, C.; Windisch, F., Longevity of dental amalgam in comparison to composite materials. *GMS Health Technol Assess* **2008,** *4* (12).
14. Phinney, D. J.; Halstead, J. H., *Delmar's Dental Materials Guide, Spiral bound Version*. Cengage Learning: 2008.
15. ADA Statement on Dental Amalgam. (accessed Sept. 2017).
16. CDA CDA Position on Dental Amalgam. (accessed Sept 2017).
17. Sakaguchi, R. L.; Powers, J. M., *Craig's Restorative Dental Materials - E-Book*. Elsevier Health Sciences: 2012.
18. Bowen, R. L., Properties of a silica-reinforced polymer for dental restorations. *J Am Dent Assoc* **1963,** *66* (1), 57-64.
19. Lee, J. H.; Um, C. M.; Lee, I. B., Rheological properties of resin composites according to variations in monomer and filler composition. *Dent Mater* **2006,** *22* (6), 515-526.
20. Atai, M.; Ahmadi, M.; Babanzadeh, S.; Watts, D. C., Synthesis, characterization, shrinkage and curing kinetics of a new low-shrinkage urethane dimethacrylate monomer for dental applications. *Dent Mater* **2007,** *23* (8), 1030-1041.
21. Moszner, N.; Fischer, U. K.; Angermann, J.; Rheinberger, V., A partially aromatic urethane dimethacrylate as a new substitute for Bis-GMA in restorative composites. *Dent Mater* **2008,** *24* (5), 694-699.
22. Podgorski, M., Synthesis and characterization of novel dimethacrylates of different chain lengths as possible dental resins. *Dent Mater* **2010,** *26* (6), e188-94.
23. Fróes-Salgado, N. R. G.; Boaro, L. C.; Pick, B.; Pfeifer, C. S.; Francci, C. E.; Méier, M. M.; Braga, R. R., Influence of the base and diluent methacrylate monomers on the polymerization stress and its determinants. *J Appl Polym Sci* **2012,** *123* (5), 2985-2991.
24. Podgorski, M., Structure-property relationship in new photo-cured dimethacrylate-based dental resins. *Dent Mater* **2012,** *28* (4), 398-409.

25. Wang, R.; Zhu, M.; Bao, S.; Liu, F.; Jiang, X.; Zhu, M., Synthesis of Two Bis-GMA Derivates with Different Size Substituents as Potential Monomer to Reduce the Polymerization Shrinkage of Dental Restorative Composites. *J Mater Sci Res* **2013,** *2* (4), 12-22.

26. Sarrett, D. C., Clinical challenges and the relevance of materials testing for posterior composite restorations. *Dent Mater* **2005,** *21* (1), 9-20.

27. Braga, R. R.; Ballester, R. Y.; Ferracane, J. L., Factors involved in the development of polymerization shrinkage stress in resin-composites: a systematic review. *Dent Mater* **2005,** *21* (10), 962-970.

28. Emmler, J.; Seiss, M.; Kreppel, H.; Reichl, F. X.; Hickel, R.; Kehe, K., Cytotoxicity of the dental composite component TEGDMA and selected metabolic by-products in human pulmonary cells. *Dent Mater* **2008,** *24* (12), 1670-1675.

29. Durner, J.; Wellner, P.; Hickel, R.; Reichl, F. X., Synergistic interaction caused to human gingival fibroblasts from dental monomers. *Dent Mater* **2012,** *28* (8), 818-823.

30. Ansteinsson, V.; Kopperud, H. B.; Morisbak, E.; Samuelsen, J. T., Cell toxicity of methacrylate monomers-the role of glutathione adduct formation. *J Biomed Mater Res A* **2013,** *101* (12), 3504-3510.

31. Ferracane, J. L., Resin composite—State of the art. *Dent Mater* **2011,** *27* (1), 29-38.

32. Vazifehasl, Z.; Hemmati, S.; Zamanloo, M.; Jaymand, M., Synthesis and characterization of novel diglycidyl methacrylate-based macromonomers on isosorbide for dental composites. *Macromolecular Research* **2012,** *21* (4), 427-434.

33. Bogdal, D.; Pielichowski, J.; Boron, A., Application of diol dimethacrylates in dental composites and their influence on polymerization shrinkage. *J Appl Polym Sci* **1997,** *66* (12), 2333-2337.

34. Gauthier, M. A.; Zhang, Z.; Zhu, X. X., New dental composites containing multimethacrylate derivatives of bile acids: a comparative study with commercial monomers. *ACS Appl Mater Interfaces* **2009,** *1* (4), 824-832.

35. Gauthier, M. A.; Simard, P.; Zhang, Z.; Zhu, X. X., Bile acids as constituents for dental composites: in vitro cytotoxicity of (meth)acrylate and other ester derivatives of bile acids. *J R Soc Interface* **2007,** *4* (17), 1145-1150.

36. Hu, X.; Zhang, Z.; Zhang, X.; Li, Z.; Zhu, X. X., Selective acylation of cholic acid derivatives with multiple methacrylate groups. *Steroids* **2005,** *70* (8), 531-537.

37. Kuska, B. NIH funds six grants to build next generation dental composite. https://www.nih.gov/news-events/news-releases/nih-funds-six-grants-build-next-generation-dental-composite (accessed June 12, 2017).

38. Scott, T. F.; Kloxin, C. J.; Draughon, R. B.; Bowman, C. N., Nonclassical Dependence of Polymerization Rate on Initiation Rate Observed in Thiol−Ene Photopolymerizations. *Macromolecules* **2008,** *41* (9), 2987-2989.

39. Lu, H.; Carioscia, J. A.; Stansbury, J. W.; Bowman, C. N., Investigations of step-growth thiol-ene polymerizations for novel dental restoratives. *Dent Mater* **2005,** *21* (12), 1129-1136.

40. Carioscia, J. A.; Lu, H.; Stanbury, J. W.; Bowman, C. N., Thiol-ene oligomers as dental restorative materials. *Dent Mater* **2005,** *21* (12), 1137-1143.

41. Cramer, N. B.; Couch, C. L.; Schreck, K. M.; Carioscia, J. A.; Boulden, J. E.; Stansbury, J. W.; Bowman, C. N., Investigation of thiol-ene and thiol-ene-methacrylate based resins as dental restorative materials. *Dent Mater* **2010,** *26* (1), 21-28.

42. Cramer, N. B.; Couch, C. L.; Schreck, K. M.; Boulden, J. E.; Wydra, R.; Stansbury, J. W.; Bowman, C. N., Properties of methacrylate-thiol-ene formulations as dental restorative materials. *Dent Mater* **2010,** *26* (8), 799-806.

43. Xi, W.; Peng, H.; Aguirre-Soto, A.; Kloxin, C. J.; Stansbury, J. W.; Bowman, C. N., Spatial and Temporal Control of Thiol-Michael Addition via Photocaged Superbase in Photopatterning and Two-Stage Polymer Networks Formation. *Macromolecules* **2014,** *47* (18), 6159-6165.

44. Claudino, M.; Zhang, X.; Alim, M. D.; Podgórski, M.; Bowman, C. N., Mechanistic Kinetic Modeling of Thiol–Michael Addition Photopolymerizations via Photocaged "Superbase" Generators: An Analytical Approach. *Macromolecules* **2016,** *49* (21), 8061-8074.

45. Bowman, C. N.; Chatani, S.; Gong, T.; Nair, D. P.; Podogorski, M. Novel dental composites systems and methods of making the same and using same. US20150250687 A1, 2015.

46. Rawls, H. R.; Johnston, A. D.; Norling, B. K.; Whang, K. Restorative resin compositions and methods of use. US20170020789 A1, 2017.
47. Shin, D. H.; Rawls, H. R., Degree of conversion and color stability of the light curing resin with new photoinitiator systems. *Dent Mater* **2009,** *25* (8), 1030-1038.
48. Hoedebecke, B. L. A novel oxirane/acrylate restorative system with multifunctional acrylate. University of Texas Health Science Center at San Antonio, 2016.
49. Moszner, N.; Fischer, U. K.; Angermann, J.; Rheinberger, V., Bis-(acrylamide)s as new cross-linkers for resin-based composite restoratives. *Dent Mater* **2006,** *22* (12), 1157-1162.
50. Zhang, X.; Xi, W.; Wang, C.; Podgorski, M.; Bowman, C. N., Visible-Light-Initiated Thiol-Michael Addition Polymerizations with Coumarin-Based Photobase Generators: Another Photoclick Reaction Strategy. *ACS Macro Lett* **2016,** *5* (2), 229-233.
51. Wydra, J. W.; Fenoli, C. R.; Cramer, N. B.; Stansbury, J. W.; Bowman, C. N., Influence of small amounts of addition-fragmentation capable monomers on polymerization-induced shrinkage stress. *J Polym Sci A: Polym Chem* **2014,** *52* (9), 1315-1321.
52. Park, H. Y.; Kloxin, C. J.; Abuelyaman, A. S.; Oxman, J. D.; Bowman, C. N., Novel dental restorative materials having low polymerization shrinkage stress via stress relaxation by addition-fragmentation chain transfer. *Dent Mater* **2012,** *28* (11), 1113-1119.
53. Kloxin, C. J.; Scott, T. F.; Bowman, C. N., Stress relaxation via addition-fragmentation chain transfer in a thiol-ene photopolymerization. *Macromolecules* **2009,** *42* (7), 2551-2556.
54. Antonucci, J. M.; Zeiger, D. N.; Tang, K.; Lin-Gibson, S.; Fowler, B. O.; Lin, N. J., Synthesis and characterization of dimethacrylates containing quaternary ammonium functionalities for dental applications. *Dent Mater* **2012,** *28* (2), 219-228.
55. Oxman, J. D., Polymerizable ionic liquids with novel properties including minimal oxygen inhibition. In *AADR annual meeting*, 3M ESPE Dental Products: Los Angeles, CA, USA, 2016.

56. Kim, K.-H.; Ong, J. L.; Okuno, O., The effect of filler loading and morphology on the mechanical properties of contemporary composites. *J Prosth Dent* **2002,** *87* (6), 642-649.

57. Wang, R.; Habib, E.; Zhu, X. X., Application of close-packed structures in dental resin composites. *Dent Mater* **2017,** *33* (3), 288-293.

58. Wang, R.; Zhang, M.; Liu, F.; Bao, S.; Wu, T.; Jiang, X.; Zhang, Q.; Zhu, M., Investigation on the physical-mechanical properties of dental resin composites reinforced with novel bimodal silica nanostructures. *Mater Sci Eng C* **2015,** *50* (1), 266-273.

59. Ferracane, J. L.; Greener, E. H., The effect of resin formulation on the degree of conversion and mechanical properties of dental restorative resins. *J Biomed Mater Res* **1986,** *20* (1), 121-131.

60. Dailing, E. A.; Lewis, S. H.; Barros, M. D.; Stansbury, J. W., Construction of monomer-free, highly crosslinked, water-compatible polymers. *J Dent Res* **2014,** *93* (12), 1326-1331.

61. Moraes, R. R.; Garcia, J. W.; Barros, M. D.; Lewis, S. H.; Pfeifer, C. S.; Liu, J.; Stansbury, J. W., Control of polymerization shrinkage and stress in nanogel-modified monomer and composite materials. *Dent Mater* **2011,** *27* (6), 509-519.

62. Liu, J.; Howard, G. D.; Lewis, S. H.; Barros, M. D.; Stansbury, J. W., A Study of Shrinkage Stress Reduction and Mechanical Properties of Nanogel-Modified Resin Systems. *Eur Polym J* **2012,** *48* (11), 1819-1828.

63. Liu, J.; Rad, I. Y.; Sun, F.; Stansbury, J. W., Photo-Reactive Nanogel as a Means to Tune Properties during Polymer Network Formation. *Polym Chem* **2014,** *5* (1).

64. Chen, C.; Liu, J.; Sun, F.; Stansbury, J. W., Control of microstructure and gradient property of polymer network by photopolymerizable silicone-containing nanogel. *J Polym Sci A: Polym Chem* **2014,** *52* (19), 2830-2840.

65. Dailing, E.; Liu, J.; Lewis, S.; Stansbury, J., Nanogels as a Basis for Network Construction. *Macromol Symposia* **2013,** *329* (1), 113-117.

66. Stansbury, J. W. Nanogel materials and methods of use thereof. US9138383 B1, 2015.

Chapter 2 - **Inorganic Fillers for Dental Resin Composites - Present and Future***

Abstract

Dental resins represent an important family of biomaterials that have been evolving in response to the needs in biocompatibility and mechanical properties. They are composite materials consisting of mostly inorganic fillers and additives bound together with a polymer matrix. A large number of fillers in a variety of forms (spheroidal, fibrous, porous, etc.) along with other additives have been studied to enhance the performance of the composites. Silane derivatives are attached as coupling agents to the fillers to improve their interfacial properties. A review of the literature on dental composite fillers seems to suggest that each of the fillers tested presents its own strengths and weaknesses, and often combinations of these yield resin composites with the desired balance of properties. Additives such as nanotubes, whiskers, fibers, and nanoclusters have been shown to enhance the properties of these hybrid materials, and their use in small fractions may enhance the overall performance of the dental resin materials.

* Published as a review article: Eric Habib, Ruili Wang, Yazi Wang, Meifang Zhu, and X. X. Zhu, ACS Biomater Sci Eng, 2016, **2** (1), 1-11.

2.1 Introduction

Dental resin-based composites (RBCs) for both direct and indirect dental restorations have been in use for the last 50 years. Their advantageous aesthetic and biocompatibility properties have allowed them to gain prevalence, and gradually replace the mercury-containing dental amalgams that had previously been the standard of care for this type of restoration. While the toxicity of amalgam is still a topic of debate (*1-5*), many countries are reducing the use of mercury or even banning mercury-containing products outright (*6-7*), and so dental RBCs remain the main focus of current dental material research.

Dental RBCs are a mix of two major components: the resin matrix, which contains the monomers, photopolymerization initiators, accelerators, inhibitors, and tint compounds; and the inorganic filler particles that confer most of the mechanical properties observed in the final material in addition to the optical and radiopacity properties required for the composite. To enhance the binding of the filler particles, silane derivatives are covalently attached onto the inorganic fillers as coupling agents.

The monomers that have been used most frequently for this type of dental restorative have been bisphenol A glycerolate dimethacrylate (BisGMA), triethylene glycol dimethacrylate (TEGDMA), and urethane dimethacrylate (UDMA). Many derivatives of these monomers have been developed to improve upon specific properties (*8-10*). Several new classes of monomers are being explored to replace the bisphenol A-containing BisGMA, among which are oxiranes (*11-13*), bile acid derivatives (*14-15*), dendrimers (*16-17*), isosorbides (*18-19*), and more (*20-22*). In addition to these methacrylate monomers, alternate polymerization chemistries have been proposed, and in some cases commercialized (*23-24*). More thorough reviews concerning the resin monomers can be found in the literature (*25-27*).

While the commercially-used monomers have remained largely unchanged, the most significant changes in dental RBCs have been in the type, size, and distribution of the inorganic fillers. The effects of size, shape, and size distribution of different fillers have been investigated quite thoroughly, such that spherical particles in multimodal size distributions generally showed superior mechanical properties (*28-39*). This review will instead focus on the chemical composition of fillers in dental RBCs and how they affect the final RBC material. Many articles have covered the clinical performance of these composite restoratives

(*40-41*); this review focuses mainly on their material properties which are essential to determine their performance over time.

This review first describes the main filler types as classified by their chemical composition, followed by a section on filler additives, which are used in small fractions, including the surface silanization agents.

2.2 Filler Types

2.2.1 Silica

The first filler to be used for dental RBCs was silicon dioxide (Table 2.1), termed silica, or quartz when in its crystalline state. It can be considered the basis for many of the other types of fillers as the glass fillers are also silicates, but also include other elements. This material has been studied extensively including its syntheses and modifications, and is widely available at low cost (*42-52*).

Table 2.1 - Filler types and their elemental compositions

Filler Type	Examples	Chemical Composition
Oxides	Silica, alumina, titania, zirconia	M_xO_y
Alkaline silicate glass	Barium glass, strontium glass	$M_xO_ySiO_2$
Biomimetic filler	Hydroxyapatite	$Ca_5(PO_4)_3OH$
Organic-inorganic hybrids	ORMOCERs	SiO_2-polymer

M = metal or metalloid, x = 1-2, y = 2-3.

In its first iterations, silica fillers were made through a top-down approach by milling quartz, that resulted in coarse, irregularly-shaped particles (Figure 2.1A)(*53*). While this process produced good strength and modulus values, the size and shape of the particles caused problems of high roughness and low wear resistance in the final materials (*54*). Today, top-down synthesis has largely been replaced with bottom-up solution particle synthesis and pyrogenic particle synthesis (Figure 2.1B). The most commonly used solution synthesis method called the “Stöber process” produces monodisperse solid particles of well-

defined size and spherical shape (*55-56*). This method can produce particles from 5 nm up to several microns. The spherical particle shape also has lower surface roughness when compared to milled quartz, while retaining a high strength. Alternately, silica pyrogenesis involves superheating of silicon tetrachloride or quartz sand to generate nano-sized particles and particle aggregates. Pyrogenic or fumed silica gives easier access to very small-sized particles than solution synthesis, in the 5-50 nm range, but also leads to particle agglomeration, which may be considered as an inconvenience or an advantage (see section 3.2 Particle Clusters). In terms of optical properties, silica has a refractive index of 1.46 (*57*), which puts it slightly below that of the traditional BisGMA-TEGDMA resin mix, making it slightly more opaque than some of the other fillers described below in such a resin system. Regardless of the synthesis method, due to its advantageous properties and ease of use, silica has been widely used in dental composites and is still the subject of much research in composites for many applications.

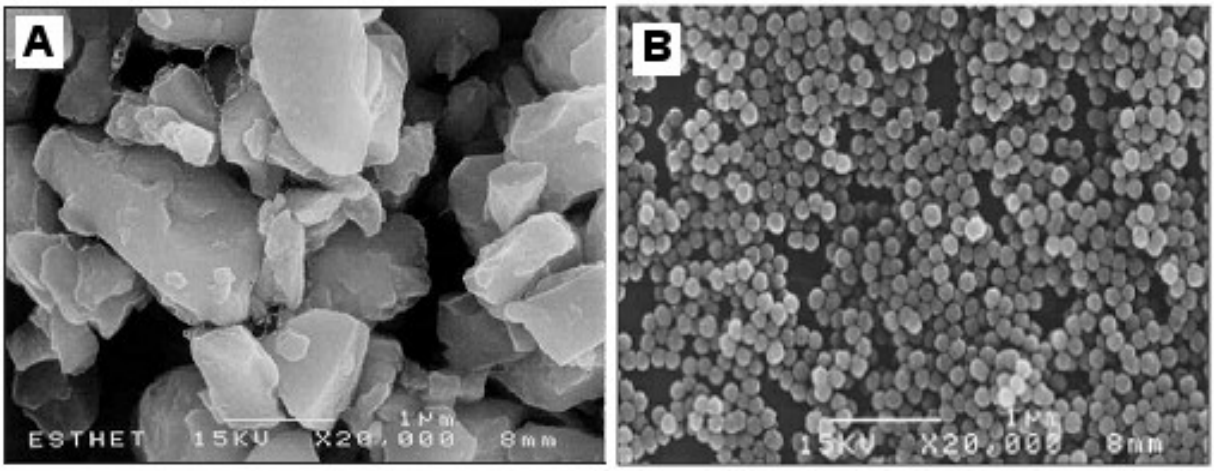

Figure 2.1 - SEM of (a) Irregular inorganic filler particles in microhybrid composite Esthet X, and (b) spherical filler in EsteliteΣ. Figure adapted from (*58*).

2.2.2 Alkaline glasses

Alkaline glasses are used in many of the currently available commercial composites including many of the leading products such as Tetric EvoCeram (Ivoclar Vivadent, Liechtenstein), Grandio (Voco, Germany), Esthet-X (Dentsply Caulk, USA), and Herculite

XRV (Kerr, USA) (see Table 2.2 for more examples). This class of fillers encompasses many different filler compositions. The material is composed primarily of silicon dioxide, but also includes a fraction of alkaline oxides such as barium oxide (BaO) and strontium oxide (SrO), which integrate into the silica network, disrupting the structure (Table 2.1). The resulting hardness of the material will be lower than that of pure silica, having a hardness of 5 on the Mohs scale, rather than 7 for silica (*59*). Due to this reduction in hardness, tests have shown that while the wear rate for this material is comparable to that of silica, for large particle sizes, it produces less wear on antagonist surfaces (*59-60*). In addition to the reduction in hardness, research has shown that over time, glass particles leach ions in aqueous solutions, losing their dopant salts in addition to the constituent silicic acid itself whose loss also occurs for silica (*60-62*). The main advantage of this material, however, is that due to the integration of heavier elements into the filler, the X-Ray radiopacity of the material is greatly increased, eliminating the need to add a separate radiopacity agent such as ytterbium or yttrium fluoride (*63*). Many types of alkaline glasses have been used including barium borosilicates, barium aluminosilicates, barium aluminum borosilicates, and strontium silicates. The refractive index of these materials can vary greatly due to the variation of dopant types and concentrations, but these glasses generally have higher refractive indices than silica, coming much closer to that of traditional resin matrix mixes, resulting in more transparent composites. Thus, while the particle hardness is lower and small amounts of the material may leech into aqueous solutions, the mechanical properties for wear, strength, and modulus are comparable to that of silica, and the optical properties are superior in most cases, as reflected by its widespread use in commercial materials.

2.2.3 Other Glasses

Other glasses have also been tested in dental materials, often integrating other oxides such as calcium, sodium, or phosphorus oxides. Some of the specific formulations attempted are termed bioactive glass. These were originally designed for bone replacement, but were also tested as fillers for RBCs. In bone repair, these are used to provide a temporary structure which adheres strongly to bone, and then dissolves, which in turn stimulates the re-growth of bone tissue (*64*). In the context of dental materials, their mechanical properties appear equal or worse than other types of fillers (*65-66*), though most papers about them focus on bioactivity and cytotoxicity rather than mechanical performance. Beyond bioactive glass, the

composition of glasses is extremely variable, and it is therefore possible to tune them for more advantageous properties, but due to the inclusion of ionic species into the matrix, the water-sorption and solubility of the resulting composites generally suffer when compared to ordinary silica, often leading to inferior mechanical properties. Such fillers may otherwise be of further use to regenerate the natural tooth structures rather than simply replacing damaged structures.

2.2.4 Other Metal Oxides

While silicon dioxide is the most extensively explored filler, many other metal oxides have also been studied for use as fillers including aluminum oxide (Al_2O_3) (*67*), titanium dioxide (TiO_2) (*68-70*), zinc oxide (ZnO), and zirconium oxide (ZrO_2). While alumina, titania, and zinc oxide have not seen very much use commercially (Table 2.2), many of the commercially available composites from 3M ESPE in particular contain significant amounts of zirconia filler and hybrid zirconia-silica fillers. There is little literature directly comparing zirconia with other filler types, but reports suggest that the high hardness of zirconia can lead to greater antagonist wear and fatigue wear (*71-72*). The synthesis of these materials is analogous to that of silica, in that metal alkoxides are hydrolyzed slowly to generate solid particles. In addition to the increased radiopacity of both ZnO and ZrO_2 due to their higher atomic numbers, similarly to glasses, they also exhibit different optical properties from other fillers, due to their higher refractive indices (2.00 and 2.16, respectively) (*73-76*). Silicate particles with varying fractions of Al_2O_3 or BaO have also been used to tune the refractive index of the particles from 1.46 to 1.55, to match that of the resin ($n \approx 1.5$) to obtain a more transparent composite (*77-78*).

In addition to the use of other pure or binary metal oxide mixtures, several mineral crystals have been attempted as reinforcements to conventional fillers including mica (*79-80*), feldspar, and leucite (*81-82*). These minerals were generally used in crystalline form and were shown to have higher wear and strength properties than traditional silica fillers. Despite their apparent superiority, concerns have been raised that particles made from less habitual compositions should be tested more extensively to ensure similar results to the known silica fillers, particularly with regards to the brittle nature of these materials, a property that is not regulated by the ISO standards (*83-84*). Thus particles of alternate compositions are still

being explored for various reasons, but thorough testing must be performed before any can be adopted as a true replacement.

2.2.5 Hydroxyapatite

Hydroxyapatite (HA, $Ca_5(PO_4)_3OH$), the main component of enamel and dentin, has also been explored as a dental filler. Its content in enamel is approximately 96% by weight (*85*), and 70% by weight in dentin (*86*). HA shows high bioactivity, which reduces the occurrence of secondary caries (*87-88*). Spheroidal particulate HA was studied as dental filler in RBCs. The size of HA particles had a significant effect on the mechanical properties of composites. RBCs containing only HA nanoparticles as filler were found to be unsuitable for practical application due to their extremely high solubility in water and poor mechanical properties (*89*). However, when mixed with HA microparticles, these nanoparticles can increase the total filler loading to yield improved mechanical properties (*89-91*). Other shapes of HA such as whiskers and nanofibers were of interest for composite development. The high aspect ratio filler reinforced dental RBCs showed better mechanical properties than those reinforced with spheroidal HA (*92-96*). Recently, a novel urchin-like hydroxyapatite (UHA, Figure 2.2a) was prepared through microwave irradiation and was applied as a dental filler. UHA was embedded in resin matrix, and displayed strong interfacial adhesion. Compared with unfilled resin matrix, the addition of silanized UHA significantly improved the flexural strength, flexural modulus, compressive strength, and Vickers microhardness. Furthermore, when used in combination with silica nanoparticles, UHA increased the flexural strength, flexural modulus, and compressive strength by 50, 40, and 13%, respectively (*97*). The main disadvantage of HA, however, remains its higher refractive index than resin matrix (n=1.65 versus 1.5 for the resin). The mismatch of refractive index could result in a decrease of monomer conversion and depth of cure (*89, 98*). Despite this shortcoming, dental RBCs containing HA filler are promising bioactive restoration materials.

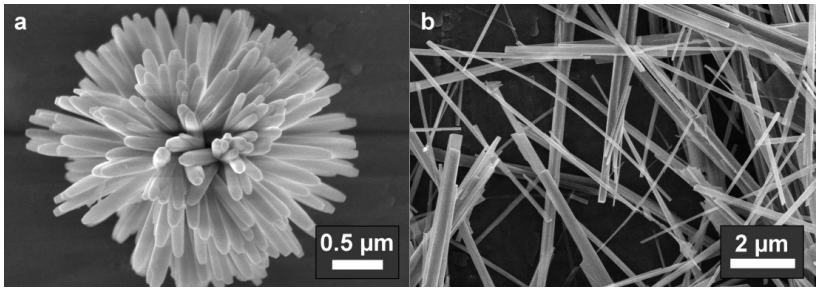

Figure 2.2 - SEM image of (a) urchin-like hydroxyapatite (UHA) particles, synthesized by microwave hydrothermal HA synthesis, and (b) hydroxyapatite whiskers (*99*).

2.2.6 Organic-Inorganic Hybrids

In order to improve overall composite properties, many research groups have tried attaching organic components to inorganic particles. One approach was using silane-modified polymers as seeds for the initial growth of silica particles. This type of filler was first developed and patented at Fraunhofer Silicate Research Institute and was later patented under the name ORMOCER™, for organically modified ceramics (*100*). These materials were shown to have improved surface wetting properties and compressive strength compared with ordinary surface-modified silica (*101*). Their adhesion to dentin and enamel was also found to be superior (*102*). In addition, materials containing these ORMOCERs were compared with a microhybrid composite and displayed increased surface roughness, but superior hardness (*103*). Moszner *et al* evaluated the flexural strength and modulus of these materials, and found that although these properties were equal to those of traditional fillers, their double bond conversion was lower (*36, 104*). Finally, work by Muh *et al* (*105*) made fillers using the same concept in combination with traditional BisGMA monomers. This composite mix yielded lower shrinkage (0.8-2.2%) than other commercially available composites (2-3%).

While traditional silane modification of particles only covers the surface, covalent core-shell type modifications have recently been made to increase the interfacial binding between the particles and the resin. Liu *et al* (*88*) used this approach to synthesize crosslinked brush-modified HA particles to examine its effect on mechanical properties, but saw no significant improvements.

2.2.7 Other Fillers

Over time many materials have been tested for use as fillers and it is beyond the scope of this review to cover them all. Most notably, in 2002, Jandt *et al* (*106*) tried novel compositions of filler, adding titanium nanoparticles as well as Ag-Sn-Cu particles to assess their effect on mechanical properties as well as radiodensity, citing the routine use of these metals in posterior restorations. They found that the addition of these particles increased diametral tensile strength, fracture toughness, as well as radiopacity. Due to its advantageous mechanical properties, but adverse aesthetic properties, they suggested the possibility of its use in core materials as an alternative to the currently used materials.

2.2.8 Prepolymerized Composite Particles

In order to minimize the overall shrinkage of the composites upon photopolymerization while maintaining the advantageous properties of both large and small particles, an alternate filler preconditioning method has also been used. This method involved the mixing and pre-polymerization of resin and filler before integration into the final composite. This type of preparation can be considered a sub-class of micro-filled composites. This treatment can be applied to any type of filler, making it a method rather than a filler type as described. With this pre-polymerization, the viscosity of the unpolymerized paste is lower than that of traditional microfilled composites, allowing higher filler loading and superior workability prior to polymerization. In terms of performance, this method has also been shown to reduce the tendency to stain (*107*), increase the fracture toughness (*108*), and reduce the shrinkage (*109*). In addition, since the resin matrix can be different for the pre-polymers and the final composite, by varying the composition of the resin matrix of the prepolymer, the mechanical properties can be tuned to obtain a superior final material (*110*). Despite the advantages of this technique, some of their properties remain inferior to some of the competing hybrid materials in terms of yield strength (*111*). Regardless, this type of material is the subject of many patents (*112-114*), and remains a very useful method in the arsenal of methods for reinforcing RBCs (Table 2.2).

2.2.9 Porous Fillers

Fillers are most frequently used as solid particles, but porous particles have also been explored. These are meant to improve the bonding between the filler and the resin matrix

through mechanical retention in the irregular pores of the filler. These fillers have been made from many of the previously mentioned types including silica (*115-116*), glasses (*82, 117*), alumina (*118-119*), as well as other minerals (*120*). Thus porous versions of many fillers are being explored for potential improvement of existing properties. While the work on this filler type is ongoing, literature has shown improvements in modulus (*82, 115*), strength (*82, 120*), and fracture toughness (*116*). In addition to the mechanical improvements, the porous structures have been proposed as a method of producing bioactivity, releasing compounds from the pores over time (*119*).

Table 2.2 - Examples of Commercial Products Using Specified Filler Types (*39*)

Type of Filler *	Example Products Using Filler **
Silica	Voco Admira, Bisco micronew, Ivoclar Vivadent Artemis,
Alkaline Glass	Ivoclar Vivadent Artemis, Kuraray Noritake Dental Clearfil Majesty
Other Glasses	Voco Admira, Shofu Beautifil II, Dentsply Ceram X
Other Metal Oxides	Tokuyama Estelite Σ, Shofu Beautifil II, 3M ESPE Filtek Supreme
Prepolymerized Filler	Kuraray Noritake Dental Clearfil Majesty, Kerr Premise

* Hydroxyapatite not included due to the lack of literature on its use in commercial composites

** Not an exhaustive list, and only representative examples are shown

2.3 Filler Additives

2.3.1 Fibers, Nanotubes, and Whiskers

Due to the wide use of fiber-reinforced polymers in many other industry-specific composites, this class of materials has also been explored for use in dental composites. While the chemical composition of this type of filler has varied widely, they are primarily distinguished by the differences in their morphology and aspect ratio. Fibers have a very high aspect ratio (20 to 500)(*121*) and are often flexible; nanotubes also have a high aspect ratio but have a hollow center; and whiskers have the lowest aspect ratio of the three and are

usually rigid. Addition of these higher aspect ratio fillers has been shown to improve the mechanical properties of the material. The mechanisms by which this occurs include whisker/fiber pinning and pullout, crack deflection, and bridging. Since more extensive reviews on the topic have been written recently (*122-123*), we present here a general description and previously explored use of some of these materials.

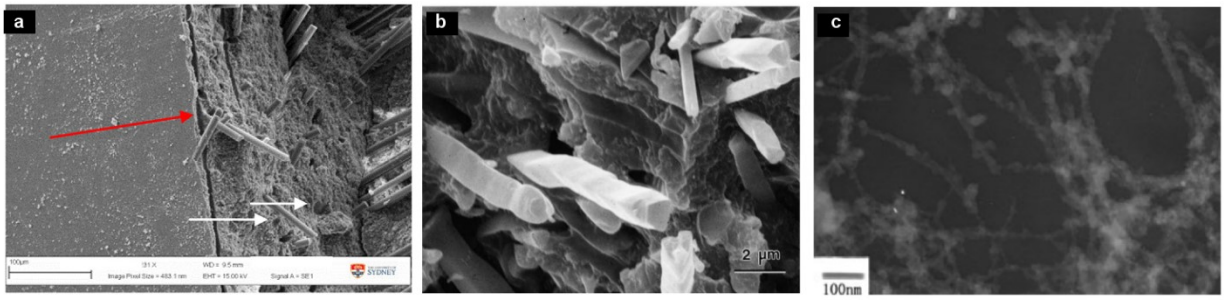

Figure 2.3 - Electron micrographs of different types of filler additives used to reinforce dental composites: (a) SEM of glass fiber-reinforced composite (*124*), (b) SEM of silicon carbide whisker-reinforced composite (*125*), and (c) TEM of single-walled carbon nanotube-reinforced composite (*126*).

The most widely used fibers in dental composites have been glass fibers. The choice of glass was logical, given the nearly identical chemical composition and refractive index to the existing silica filler, as well as its extensive use for many other applications in addition to its low cost. While micron-sized fibers were shown to decrease the material properties, nano-sized electrospun fibers were generally found to improve composite properties when used in small fractions with spheroidal silica particulate filler. Flexural strength, modulus, and work of fracture were increased by as much as 77%, 29%, and 66%, respectively (*124, 127*). An alternative to ordinary fibers was attempted by Ruddell (*128*), where they used resin-filled impregnated fused-fiber filler blocks as dental restorative fillers. When blended with a traditional particulate composite, these composites showed improvements in mechanical properties, though it was difficult to completely wet the fused-fiber blocks with the resin, leading to voids and heterogeneity in the final material.

Polymeric fibers of many different types were also tried to improve the overall properties of the composites. These were often made by electrospinning, and include

poly(vinyl acetate) fibers (*129*), polyethylene and aramid fibers (*130*), and nylon 6 fibers (*131*). The addition of fibers was generally beneficial to the mechanical properties of the composites, as long as they were only added in small fractions (< 5 wt%) due to problems with aggregation and void creation upon the addition of larger amounts.

Several different kinds of nanotubes have also been explored as reinforcements of dental RBCs. The best known of these were carbon nanotubes. Zhang *et al*(*126*) were able to oxidize single-walled carbon nanotubes, electrostatically bind silanized methacrylate groups onto their surface. When small fractions of these were blended into a commercial composite, the flexural strength was increased from 115 to 142 MPa, a 23% increase. There has also been work using random or aligned fibers made from electrospun nylon-6/multiwalled carbon nanotubes as reinforcement (*132*). They found that incorporating 0.5 wt% nanotubes into these nylon mats increased the strength performance of the composite. Finally, two-walled halloysite nanotubes were also used to reinforce unfilled and glass-filled dental composites. Chen *et al* (*133*) found that the addition 1-2.5 wt% of halloysite nanotubes yielded only a slightly higher flexural strength, but almost doubled the work of fracture of these composites. Therefore, nanotubes yielded very similar results as fibers, where a small percentage was generally favorable to the mechanical properties.

More rigid whiskers were also attempted. These whiskers ranged from metal oxides to ceramics and carbides. Some of these are mentioned above (see sections Other Metal , and Hydroxyapatite). Other types of whiskers include zinc oxide (*134*), zirconia/silica (*135*), silicon nitride (*136*), and silicon carbide (*137*). A series of papers was published by Xu *et al* examining the influence of different parameters using either plain whiskers, or whiskers fused with silica nanoparticles (*125, 136, 138-139*). These silica-fused whiskers showed 33% decrease in wear depth compared to the control. Furthermore, the evaluations of flexural strength also showed an almost two-fold improvement over the control composites. With the exception of hardness, these additives significantly improved the mechanical properties.

Many authors concluded that the optimal fraction of fiber loading is low (1-5 wt%), since at low concentrations, the number of fibers is sufficient to bridge cracks and prevent further damage, whereas at high concentrations, the difficulty in fully dispersing the additives and their agglomeration may cause defects in the materials.

2.3.2 Particle Clusters

The size of the silica particles has always been a point of concern: larger sizes allowed higher filler loading, while smaller particles produced superior wear properties (*140*). While the use of hybrids bridged this gap, an alternate strategy was developed to get the best of both worlds. With a similar objective as porous fillers (**2.2.9 Porous Fillers**), with the aim of developing RBCs with excellent strength and esthetics, a novel filler called "nanocluster" was first introduced in Filtek™ Supreme Universal Restorative (3M ESPE, St. Paul, MN, USA) in 2003. Nanoclusters can be defined as an association of individually dispersed nanoparticles such as SiO_2 and ZrO_2 and their agglomerations, which are be fabricated by self-assembly methods (*141*), spray-drying techniques (*142*), aerosol-assisted technology (*143*), calcination processes (*144*), and coupling reactions (*145-146*). Among all these synthetic routes, only the last two methods have been applied to dental RBCs, due to their ease and high yield of nanocluster fillers (*144-146*). Contrary to prepolymerized fillers, these clustering methods contain no resin to bind the particles together, but instead rely on direct bonding between them, resulting in a large, porous, but covalently bonded particle assembly.

The manufacturers of Filtek™ Supreme Universal Restorative have suggested that the employed nanoclusters were fabricated by the calcination using a bottom-up approach. The obtained nanofilled RBCs exhibited superior esthetics and polish retention similar to those of microfilled composite, while maintaining a physical-mechanical performance comparable to hybrid RBCs, which could be applied for both anterior and posterior restorations (*144*). Curtis *et al* assessed mechanical properties of commercial microhybrid (Filtek Z250), microfill (Filtek Z100 and Heliomolar), nanohybrid (Grandio and Grandio Flow), and nanofilled (Filtek™ Supreme in Body and Translucent shades, FSB and FST) composites, and found that composites reinforced with the nanocluster system showed distinctly superior performance. For cyclic pre-loading of 20 N, the Weibull modulus of both FSB and FST were increased by 42 and 182 %, respectively, over control samples without pre-cyclic load. This increase can be ascribed to the improved damage resistance due to the infiltration of silane coupling agents into the interstices of the nanoclusters, and subsequent reinforcement with the resin matrix (*147-149*). Instead of using aqueous colloidal SiO_2 sols to synthesize SiO_2 nanoparticles (*144*), Atai *et al* used amorphous fumed SiO_2 (~12 nm, Aerosil® 200) to

form porous clusters through the sintering process at 1300 °C. They prepared the corresponding composite named *Sintered nano*, and compared its mechanical properties and surface roughness with an experimental composite *Microfiller* reinforced with micron-sized glass fillers (average particle size: 2-5 μm) and commercial Filtek Supreme® Translucent (FST) mentioned above (*150*). It was found that the flexural modulus and fracture toughness of *Sintered nano* were statistically higher than the other two composites ($p<0.05$, ANOVA and Tukey HSD tests), which could be ascribed to the mechanical interlocking formed between the resin matrix and the sintered fillers (*115, 150*). The sintered nanocomposite and FST also exhibited a smoother surface finish after a toothbrush abrasion test compared to the microfilled composite, due to the introduction of nano-scale filler particles.

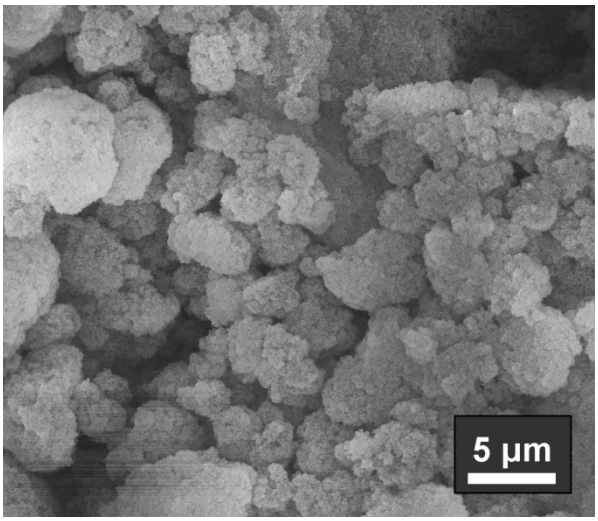

Figure 2.4 - Silica nanoclusters synthesized of 3-8 μm using chemical crosslinking reactions as in reference 1 with a primary particle size of approximately 70 nm.

Recently, Wang *et al* introduced SiO_2 nanoclusters through a coupling reaction between amine and epoxide functionalized silica nanoparticles at room temperature, and constructed bimodal silica nanostructures comprising of SiO_2 nanoparticles and nanoclusters. Among all RBCs, the maximum filler loading of SiO_2 nanoclusters alone was only 60 wt%, due to its wide size distribution (0.07~2.70 μm), but was increased to 70 wt% with the additional use of SiO_2 nanoparticles. When added at the optimal weight ratio at 70% loading, 20% of which were nanoclusters, the flexural strength, flexural modulus, compressive

strength, and wear volume were improved by 28, 48, 42 and 38%, respectively, when compared to nanoclusters alone, which was mainly due to the increased filler packing density and the reduced inter-particle spacing (*145-146*). Based on these results, it seems likely that the physical-mechanical properties of the optimized composite could be further increased by also utilizing smaller silica particles directly, or by including these as building blocks for nanoclusters. The introduction and further exploration of particle nanostructures might provide more insight into the design and fabrication of RBCs for clinical use.

2.3.3 POSS

An interesting offshoot of silica that has emerged recently is polyhedral oligomeric silsesquioxanes (POSS). POSS is made from a minimally sized, caged silicon dioxide functionalized with organic groups on the corners (Figure 2.5). Being a liquid, POSS can be used as a replacement for resin matrix rather than the solid filler. Fong *et al* (*151*) explored this use of POSS methacrylate as a partial or total replacement of the BisGMA monomer and showed that at the optimal ratio (10 wt% of the resin), it improved the flexural strength of the final composite by 20 %. Additional work with these compounds not only confirmed that a small fraction of POSS improved the mechanical properties, but also caused a significant decrease in polymerization shrinkage from 3.53 to 2.18% (*152*). Therefore this work showed that such a monomer is promising (*74*), but further studies are necessary to establish a more quantitative link between its inclusion and the improved material properties.

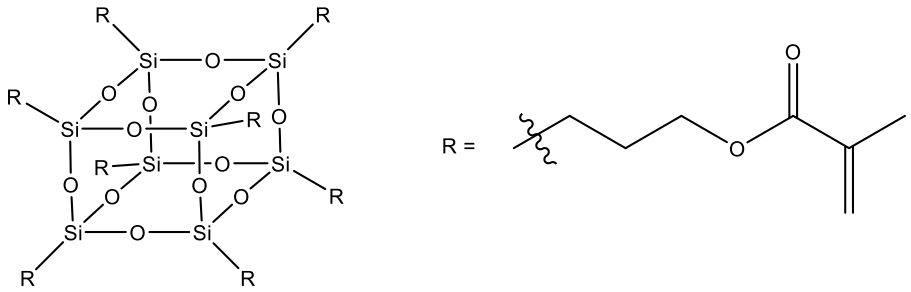

Figure 2.5 - Structure of POSS-Methacrylate, used as a partial replacement for the resin matrix monomer.

2.3.4 Silane Coupling Agents

The filler composition and morphology have a significant impact on the properties of the final composite, but the coupling agents determine the interfacial properties. A wide variety of silane coupling agents has been tested to enhance the interfacial interactions between the resin matrix and the filler particles. The original paper citing the advent of dental RBCs used vinyltrimethoxysilane (Figure 2.6a) (*53*). After further studies, γ-methacryloxypropyl trimethoxysilane (γ-MPS, Figure 2.6b) was adopted as the industry standard coupling agent. Many more studies have examined other parameters of silane coupling agents such as fraction functionalization (*153-154*), type of silanization agent (*155-156*), and hyperbranched methacrylate surface functionalization (Figure 2.6c) (*17*). These papers mostly examined the influence of all these variables on the mechanical properties of the final materials, but also thoroughly evaluated the effects on water sorption, solubility, and swelling. While there is some conflicting information as to the true influence of the coupling agent on the final properties of the materials (*157-158*), γ-MPS remains the most widely used. Wilson *et al* showed that decreasing methacrylate density while maintaining surface hydrophobicity marginally increased the flexural strength of the material, and more importantly reduced the viscosity of the unpolymerized material (*156*). In addition, Ye's work also showed that using a hyper-branched coupling agent significantly reduced the shrinkage stress (*17*), suggesting that new modifications of this type could further improve dental materials' properties for clinical use.

In addition to varying methacrylate surface density, using different types of alkenes, or even growing polymer brushes; the most promising recent trend has been the use of mixed polymerization chemistry, combining the traditional methacrylate free-radical polymerization with the so-called click chemistry using the radical-initiated thiol-ene reaction, though this approach has mostly been explored for the modification of monomers, rather than fillers (*23-24*). While there is still much work to do with this method, its advantageous properties may lead to their wider exploration as a promising alternative method for dental composite polymerization.

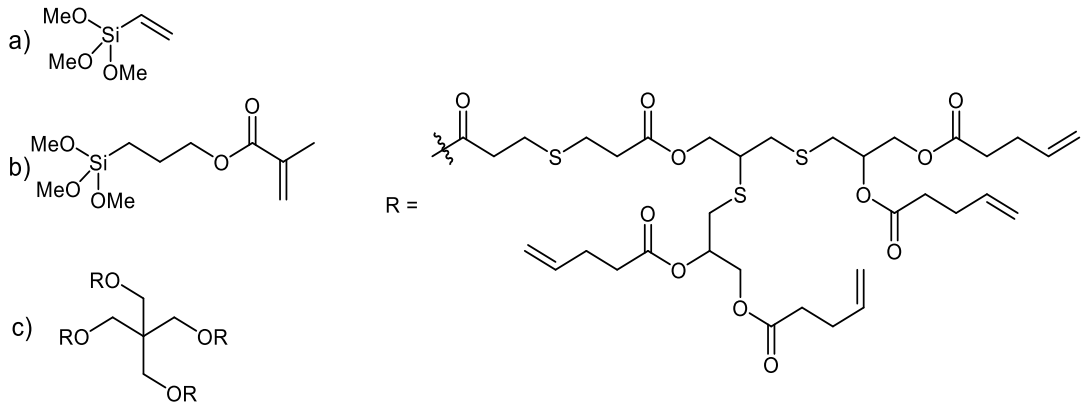

Figure 2.6 - Organic silanes to modify the inorganic particle surface: (a) the originally used trimethoxyvinyl silane, (b) the most commonly used γ-methacryloyl propyltrimethoxysilane (γ-MPS), and (c) a hyperbranched multimethacrylate ligand for reduced shrinkage stress (*17*).

2.4 Conclusions and Perspectives

The main challenges for fillers in RBCs remain the same as those for the composites themselves. The primary cause of failure is the development secondary caries, thought to be indirectly caused by polymerization shrinkage (*159*), and restoration breaks due to fracture; both of these remain the main issues to overcome (*160*). While the monomer can be said to be directly responsible for the volumetric shrinkage of the materials, some filler technologies such as POSS addition have been shown to decrease the volumetric shrinkage, and therefore could be used to aid in minimizing this problem.

The greatest obstacle in composites that is directly caused by the fillers, however, is the overall opacity of the material. Aside from purely esthetic considerations, the difficulty in perfectly matching the refractive indices of the resin and the filler prevents the curing light from fully penetrating the restoration, thus multiple increments are needed for a full cure (in addition to shrinkage concerns). In recent years, "bulk fill" restoratives have made great strides in the use of non-incremental curing (*161-164*). These composites allow non-incremental curing due to high transparency and low shrinkage. Therefore the main solution so far has been the reduction of filler particle size to reduce light scattering. Smaller particles, however, cause problems of their own. The most promising results for refractive index matching so far have been in the use of chemical hybrid fillers specifically designed for such a purpose (See 2.2.4 Other Metal Oxides).

The mechanical properties of many of the commercially available composites are already far superior to those required by the ISO standards for mechanical properties (*84*), but many of the additives discussed were shown to further improve these properties. Beyond the standards, many properties such as wear resistance and fracture toughness have a significant influence on the material performance that should be assigned a greater importance in order to produce materials that have better resistance and longer functional life spans.

The aim of dental RBCs is to restore teeth to their original working shape and shade. While the true regeneration of enamel under clinical conditions has not been achieved due to its highly complex structure, the ideal solution would be to simply rebuild it, or at least a framework that can be transformed into it. Some preliminary work by Fan (*165-166*) has shown promise for the eventual development of enamel regeneration. This may become an interesting research objective in this field, though still distant for now.

Despite a few key properties to improve upon, there is no clear unified direction of research for dental fillers (*167*). New types of reinforcements are being explored; new types of surface modifications are being attempted. The only clear trend is the use of increasingly small particles to favor advantageous optical and polishing properties. In addition, fillers are currently being developed with more sophisticated functionality such as antibacterial compound release and bioactivity such as remineralization and fluoride release (*168-169*). Composites with these functions will likely be commercialized in the near future.

A final consideration for dental RBCs is that due to the staggering number of possibilities for both filler and resin matrix, most investigations have focused on the effect of single components on these complex mixtures, assuming there was no change in the interaction between the two. The future of RBC fillers will likely continue as begun by ORMOCERs™ where the line between monomer and filler is no longer so stark, and specific interactions between the resin matrix and the filler are optimized for superior overall RBC properties. The drive for innovation will bring about a new generation of dental fillers and composites that will respond to the rapid and growing need for new biomaterials that are safe, strong, and easy to use.

Since their advent, a great variety of different fillers have been developed and tested. The difficulty in using these materials remains that it is impossible to directly compare all the

materials available simply due to the large number of possible compositions and combinations. Most of the fillers offer distinct advantages and inconveniences, and so can be used in specific applications that play to their strengths. Despite their current shortcomings, much of the research discussed above highlights ways in which one can improve the current commercially-used fillers. In concert with the development of more sophisticated monomers and resin systems, the lifespan of current dental products is expected to increase, and only by using optimized combination of all these available methods will one be able to achieve a truly great dental RBC.

2.5 References

1. Priya, E. L.; Ranganathan, K.; Rao, U. D.; Joshua, E.; Mathew, D. G.; Wilson, K., A study of sister chromatid exchange in patients with dental amalgam restorations. *Ind J Dent Res* **2014,** *25* (6), 772-776.
2. Miriam Varkey, I.; Shetty, R.; Hegde, A., Mercury exposure levels in children with dental amalgam fillings. *Int J Clin Pediatr Dent* **2014,** *7* (3), 180-185.
3. Kern, J. K.; Geier, D. A.; Bjørklund, G.; King, P. G.; Homme, K. G.; Haley, B. E.; Sykes, L. K.; Geier , M. R., Evidence supporting a link between dental amalgams and chronic illness, fatigue, depression, anxiety, and suicide. *Neuroendocrinol Lett* **2014,** *35* (7), 537-552.
4. Woods, J. S.; Heyer, N. J.; Russo, J. E.; Martin, M. D.; Farin, F. M., Genetic polymorphisms affecting susceptibility to mercury neurotoxicity in children: summary findings from the Casa Pia Children's Amalgam clinical trial. *Neurotoxicology* **2014,** *44*, 288-302.
5. Watson, G. E.; van Wijngaarden, E.; Love, T. M.; McSorley, E. M.; Bonham, M. P.; Mulhern, M. S.; Yeates, A. J.; Davidson, P. W.; Shamlaye, C. F.; Strain, J. J.; Thurston, S. W.; Harrington, D.; Zareba, G.; Wallace, J. M.; Myers, G. J., Neurodevelopmental outcomes at 5 years in children exposed prenatally to maternal dental amalgam: the Seychelles Child Development Nutrition Study. *Neurotoxicol Teratol* **2013,** *39*, 57-62.
6. Bartold, P. M., Is Amalgam Ready to be Buried? *Aust Dent J* **2014,** *59* (1), 1.
7. Mackey, T. K.; Contreras, J. T.; Liang, B. A., The Minamata Convention on Mercury: attempting to address the global controversy of dental amalgam use and mercury waste disposal. *Sci Total Environ* **2014,** *472*, 125-129.

8. Moszner, N.; Fischer, U. K.; Angermann, J.; Rheinberger, V., A partially aromatic urethane dimethacrylate as a new substitute for Bis-GMA in restorative composites. *Dent Mater* **2008,** *24* (5), 694-699.
9. Wang, R.; Zhu, M.; Bao, S.; Liu, F.; Jiang, X.; Zhu, M., Synthesis of Two Bis-GMA Derivates with Different Size Substituents as Potential Monomer to Reduce the Polymerization Shrinkage of Dental Restorative Composites. *J Mater Sci Res* **2013,** *2* (4), 12-22.
10. Sideridou, I. D.; Tserki, V.; Papanastasiou, G., Effect of chemical structure on degree of conversion in light-cured dimethacrylate-based dental resins. *Biomaterials* **2002,** *23*, 1819-1829.
11. Eick, J. D.; Kostoryz, E. L.; Rozzi, S. M.; Jacobs, D. W.; Oxman, J. D.; Chappelow, C. C.; Glaros, A. G.; Yourtee, D. M., In vitro biocompatibility of oxirane/polyol dental composites with promising physical properties. *Dent Mater* **2002,** *18*, 413-421.
12. Palin, W. M.; Fleming, G. J. P.; Trevor Burke, F. J.; Marquis, P. M.; Randall, R. C., Monomer conversion versus flexure strength of a novel dental composite. *J Dent* **2003,** *31* (5), 341-351.
13. Weinmann, W.; Thalacker, C.; Guggenberger, R., Siloranes in dental composites. *Dent Mater* **2005,** *21* (1), 68-74.
14. Gauthier, M. A.; Zhang, Z.; Zhu, X. X., New dental composites containing multimethacrylate derivatives of bile acids: a comparative study with commercial monomers. *ACS Appl Mater Interfaces* **2009,** *1* (4), 824-832.
15. Gauthier, M. A.; Simard, P.; Zhang, Z.; Zhu, X. X., Bile acids as constituents for dental composites: in vitro cytotoxicity of (meth)acrylate and other ester derivatives of bile acids. *J R Soc Interface* **2007,** *4* (17), 1145-1150.
16. Viljanen, E. K.; Skrifvars, M.; Vallittu, P. K., Dendritic copolymers and particulate filler composites for dental applications: degree of conversion and thermal properties. *Dent Mater* **2007,** *23* (11), 1420-1427.
17. Ye, S.; Azarnoush, S.; Smith, I. R.; Cramer, N. B.; Stansbury, J. W.; Bowman, C. N., Using hyperbranched oligomer functionalized glass fillers to reduce shrinkage stress. *Dent Mater* **2012,** *28* (9), 1004-1011.

18. Lukaszczyk, J.; Janicki, B.; Frick, A., Investigation on synthesis and properties of isosorbide based bis-GMA analogue. *J Mater Sci: Mater Med* **2012,** *23* (5), 1149-1155.
19. Vazifehasl, Z.; Hemmati, S.; Zamanloo, M.; Jaymand, M., Synthesis and characterization of novel diglycidyl methacrylate-based macromonomers on isosorbide for dental composites. *Macromol Res* **2012,** *21* (4), 427-434.
20. Podgorski, M., Synthesis and characterization of novel dimethacrylates of different chain lengths as possible dental resins. *Dent Mater* **2010,** *26* (6), e188-94.
21. Avci, D.; Mathias, L. J., Synthesis and photopolymerizations of new hydroxyl-containing dimethacrylate crosslinkers. *Polymer* **2004,** *45* (6), 1763-1769.
22. Lu, H.; Stansbury, J. W.; Nie, J.; Berchtold, K. A.; Bowman, C. N., Development of highly reactive mono-(meth)acrylates as reactive diluents for dimethacrylate-based dental resin systems. *Biomaterials* **2005,** *26* (12), 1329-1336.
23. Ye, S.; Cramer, N. B.; Smith, I. R.; Voigt, K. R.; Bowman, C. N., Reaction Kinetics and Reduced Shrinkage Stress of Thiol-Yne-Methacrylate and Thiol-Yne-Acrylate Ternary Systems. *Macromolecules* **2011,** *44* (23), 9084-9090.
24. Cramer, N. B.; Couch, C. L.; Schreck, K. M.; Carioscia, J. A.; Boulden, J. E.; Stansbury, J. W.; Bowman, C. N., Investigation of thiol-ene and thiol-ene-methacrylate based resins as dental restorative materials. *Dent Mater* **2010,** *26* (1), 21-28.
25. Ferracane, J. L., Resin composite--state of the art. *Dent Mater* **2011,** *27* (1), 29-38.
26. Leprince, J. G.; Palin, W. M.; Hadis, M. A.; Devaux, J.; Leloup, G., Progress in dimethacrylate-based dental composite technology and curing efficiency. *Dent. Mater.* **2013,** *29* (2), 139-56.
27. Lavigueur, C.; Zhu, X. X., Recent advances in the development of dental composite resins. *RSC Adv* **2012,** *2* (1), 59.
28. Kim, K.-H.; Ong, J. L.; Okuno, O., The effect of filler loading and morphology on the mechanical properties of contemporary composites. *J Prosth Dent* **2002,** *87* (6), 642-649.
29. Valente, L. L.; Peralta, S. L.; Ogliari, F. A.; Cavalcante, L. M.; Moraes, R. R., Comparative evaluation of dental resin composites based on micron- and submicron-sized monomodal glass filler particles. *Dent Mater* **2013,** *29* (11), 1182-1187.

30. Beun, S.; Glorieux, T.; Devaux, J.; Vreven, J.; Leloup, G., Characterization of nanofilled compared to universal and microfilled composites. *Dent Mater* **2007,** *23* (1), 51-59.

31. Robertson, C. G.; Lin, C. J.; Rackaitis, M.; Roland, C. M., Influence of Particle Size and Polymer-Filler Coupling on Viscoelastic Glass Transition of Particle-Reinforced Polymers. *Macromolecules* **2008,** *21*, 2727-2731.

32. Satterthwaite, J. D.; Vogel, K.; Watts, D. C., Effect of resin-composite filler particle size and shape on shrinkage-strain. *Dent Mater* **2009,** *25* (12), 1612-1615.

33. Karabela, M. M.; Sideridou, I. D., Synthesis and study of properties of dental resin composites with different nanosilica particles size. *Dent Mater* **2011,** *27* (8), 825-835.

34. Turssi, C. P.; Ferracane, J. L.; Vogel, K., Filler features and their effects on wear and degree of conversion of particulate dental resin composites. *Biomaterials* **2005,** *26* (24), 4932-4937.

35. Fu, S.-Y.; Feng, X.-Q.; Lauke, B.; Mai, Y.-W., Effects of particle size, particle/matrix interface adhesion and particle loading on mechanical properties of particulate–polymer composites. *Composites, Part B* **2008,** *39* (6), 933-961.

36. Klapdohr, S.; Moszner, N., New Inorganic Components for Dental Filling Composites. *Monatsh. Chem.* **2004,** *136* (1), 21-45.

37. Palaniappan, S.; Bharadwaj, D.; Mattar, D. L.; Peumans, M.; Van Meerbeek, B.; Lambrechts, P., Three-year randomized clinical trial to evaluate the clinical performance and wear of a nanocomposite versus a hybrid composite. *Dent Mater* **2009,** *25* (11), 1302-1314.

38. Ernst, C. P.; Brandenbusch, M.; Meyer, G.; Canbek, K.; Gottschalk, F.; Willershausen, B., Two-year clinical performance of a nanofiller vs a fine-particle hybrid resin composite. *Clin Oral Investig* **2006,** *10* (2), 119-125.

39. Kaizer, M. R.; de Oliveira-Ogliari, A.; Cenci, M. S.; Opdam, N. J.; Moraes, R. R., Do nanofill or submicron composites show improved smoothness and gloss? A systematic review of in vitro studies. *Dent Mater* **2014,** *30* (4), 41-78.

40. Demarco, F. F.; Collares, K.; Coelho-de-Souza, F. H.; Correa, M. B.; Cenci, M. S.; Moraes, R. R.; Opdam, N. J., Anterior composite restorations: A systematic review on long-term survival and reasons for failure. *Dent Mater* **2015,** *31* (10), 1214-1224.

41. Demarco, F. F.; Correa, M. B.; Cenci, M. S.; Moraes, R. R.; Opdam, N. J., Longevity of posterior composite restorations: not only a matter of materials. *Dent Mater* **2012,** *28* (1), 87-101.

42. Schlanbusch, R. D.; Jelle, B. P.; Christie Sandberg, L. I.; Fufa, S. M.; Gao, T., Integration of life cycle assessment in the design of hollow silica nanospheres for thermal insulation applications. *Building and Env* **2014,** *80*, 115-124.

43. Xu, T.; Davis, V. A., Liquid crystalline phase behavior of silica nanorods in dimethyl sulfoxide and water. *Langmuir* **2014,** *30* (16), 4806-4813.

44. Lazaro, A.; van de Griend, M. C.; Brouwers, H. J. H.; Geus, J. W., The influence of process conditions and Ostwald ripening on the specific surface area of olivine nano-silica. *Microporous Mesoporous Mater* **2013,** *181*, 254-261.

45. Ma, Y.; Han, L.; Miyasaka, K.; Oleynikov, P.; Che, S.; Terasaki, O., Structural Study of Hexagonal Close-Packed Silica Mesoporous Crystal. *Chem Mater* **2013,** *25* (10), 2184-2191.

46. Tang, L.; Cheng, J., Nonporous Silica Nanoparticles for Nanomedicine Application. *Nano Today* **2013,** *8* (3), 290-312.

47. Edrissi, M.; Soleymani, M.; Adinehnia, M., Synthesis of Silica Nanoparticles by Ultrasound-Assisted Sol-Gel Method: Optimized by Taguchi Robust Design. *Chem Eng Technol* **2011,** *34* (11), 1813-1819.

48. Banerjee, S.; Ghosh, H.; Datta, A., Lamellar Micelles as Templates for the Preparation of Silica Nanodisks. *J Phys Chem C* **2011,** *115* (39), 19023-19027.

49. Kuijk, A.; van Blaaderen, A.; Imhof, A., Synthesis of monodisperse, rodlike silica colloids with tunable aspect ratio. *J Am Chem Soc* **2011,** *133* (8), 2346-2349.

50. Manet, S.; Schmitt, J.; Imperor-Clerc, M.; Zholobenko, V.; Durand, D.; Oliveira, C. L.; Pedersen, J. S.; Gervais, C.; Baccile, N.; Babonneau, F.; Grillo, I.; Meneau, F.; Rochas, C., Kinetics of the formation of 2D-hexagonal silica nanostructured materials by nonionic block copolymer templating in solution. *J Phys Chem B* **2011,** *115* (39), 11330-11344.

51. Masalov, V. M.; Sukhinina, N. S.; Kudrenko, E. A.; Emelchenko, G. A., Mechanism of formation and nanostructure of Stober silica particles. *Nanotechnology* **2011,** *22* (27), 275718.

52. Rahman, I. A.; Padavettan, V., Synthesis of Silica Nanoparticles by Sol-Gel: Size-Dependent Properties, Surface Modification, and Applications in Silica-Polymer Nanocomposites—A Review. *J Nanomater* **2012,** *2012*, 1-15.

53. Bowen, R. L., Properties of a silica-reinforced polymer for dental restorations. *J Am Dent Assoc* **1963,** *66* (1), 57-64.

54. Lee, G. Y.; Dharan, C. K. H.; Ritchie, R. O., A physically-based abrasive wear model for composite materials. *Wear* **2002,** *2002*, 322-331.

55. Kim, J. W.; Kim, L. U.; Kim, C. K., Size control of silica nanoparticles and their surface treatment for the fabrication of dental nanocomposites. *Biomacromolecules* **2007,** *8*, 215-222.

56. Nozawa, K.; Gailhanou, H.; Raison, L.; Panizza, P.; Ushiki, H.; Sellier, E.; Delville, J. P.; MDelville, M. H., Smart control of monodisperse Stober silica nanoparticles: effect of reactant addition rate on growth process. *Langmuir* **2005,** *21*, 1516-1523.

57. Malitson, I. H., Interspecimen Comparison of the Refractive Index of Fused Silica*,†. *J Optical Soc Am* **1965,** *55* (10), 1205-1209.

58. Lu, H.; Lee, Y. K.; Oguri, M.; Powers, J. M., Properties of a dental resin composite with a spherical inorganic filler. *Oper Dent* **2006,** *31* (6), 734-740.

59. Osiewicz, M. A.; Werner, A.; Pytko-Polonczyk, J.; Roeters, F. J.; Kleverlaan, C. J., Contact- and contact-free wear between various resin composites. *Dent Mater* **2015,** *31* (2), 134-140.

60. Soderholm, K.-J. M.; Yang, M. C. K.; Garcea, I., Filler particle leachability of experimental dental composites. *Eur J Oral Sci* **2000,** *108*, 555-560.

61. Soderholm, K. J., Degradation of glass filler in experimental composites. *J Dent Res* **1981,** *60* (11), 1867-1875.

62. Soderholm, K.-J. M.; Mukherjee, R.; Longmate, J., Filler Leachability of Composites Stored in Distilled Water or Artificial Saliva. *J Dent Res* **1996,** *75* (9), 1692-1699.

63. Watts, D. C., Radiopacity vs. composition of some barium and strontium glass composites. *J Dent* **1987,** *15* (1), 38-43.

64. Jones, J. R., Review of bioactive glass: from Hench to hybrids. *Acta Biomater* **2013,** *9* (1), 4457-4486.

65. Chiari, M. D.; Rodrigues, M. C.; Xavier, T. A.; de Souza, E. M.; Arana-Chavez, V. E.; Braga, R. R., Mechanical properties and ion release from bioactive restorative composites containing glass fillers and calcium phosphate nano-structured particles. *Dent Mater* **2015,** *31* (6), 726-733.

66. Khvostenko, D.; Mitchell, J. C.; Hilton, T. J.; Ferracane, J. L.; Kruzic, J. J., Mechanical performance of novel bioactive glass containing dental restorative composites. *Dent Mater* **2013,** *29* (11), 1139-1148.

67. Thorat, S. B.; Diaspro, A.; Salerno, M., Effect of alumina reinforcing fillers in BisGMA-based resin composites for dental applications. *Adv Mater Lett* **2013,** *4* (1), 15.

68. Yoshida, K.; Tanagawa, M.; Atsuta, M., Effects of filler composition and surface treatment on the characteristics of opaque resin composites. *J Biomed Mater Res* **2001,** *58* (5), 525-530.

69. Yoshida, K.; Taira, Y.; Atsuta, M., Properties of Opaque Resin Composite Containing Coated and Silanized Titanium Dioxide. *J Dent Res* **2001,** *80* (3), 864-868.

70. Thorat, S. B.; Patra, N.; Ruffilli, R.; Diaspro, A.; Salerno, M., Preparation and characterization of a BisGMA-resin dental restorative composites with glass, silica and titania fillers. *Dent Mater J* **2012,** *31* (4), 635-644.

71. Yap, A. U. J.; Tan, C. H.; Chung, S. M., Wear Behavior of New Composite Restoratives. *Oper Dent* **2004,** *29* (3), 269-274.

72. Suzuki, S.; Suzuki, S. H.; Cox, C. F., Evaluating the Antagonistic Wear of Restorative Materials When Placed against Human Enamel. *J Am Dent Assoc* **1996,** *127* (1), 74-80.

73. Bond, W. L., Measurement of the Refractive Indices of Several Crystals. *J Appl Phys* **1965,** *36* (5), 1674-1677.

74. Soh, M. S.; Yap, A. U. J.; Sellinger, A., Methacrylate and epoxy functionalized nanocomposites based on silsesquioxane cores for use in dental applications. *Eur Polym J* **2007,** *43* (2), 315-327.

75. Toyooka, H.; Yaira, M.; Wakasa, K.; Yamaki, M.; Fujita, M.; Wada, T., Radiopacity of 12 visible-light-cured dental composites. *J Oral Rehabil* **1993,** *20* (6), 615-622.

76. Wood, D. L.; Nassau, K., Refractive index of cubic zirconia stabilized with yttria. *Appl Optics* **1982,** *21* (16), 2978-2981.

77. Bowen, R. L., Compatibility of Various Materials with Oral Tissues. I: The Components in Composite Restorations. *J Dent Res* **1979,** *58* (5), 1493-1503.

78. Suzuki, H.; Taira, M.; Wakasa, K.; Yamaki, M., Refractive-index-adjustable Fillers for Visible-light-cured Dental Resin Composites: Preparation of TiO2-SiO2 Glass powder by the Sol-gel Process. *J Dent Res* **1991,** *70* (5), 883-888.

79. Liu, Y.; Tan, Y.; Lei, T.; Xiang, Q.; Han, Y.; Huang, B., Effect of porous glass-ceramic fillers on mechanical properties of light-cured dental resin composites. *Dent. Mater.* **2009,** *25* (6), 709-15.

80. Tan, Y.; Liu, Y.; Grover, L. M.; Huang, B., Wear behavior of light-cured dental composites filled with porous glass-ceramic particles. *J Mech Behav Biomed Mater* **2010,** *3* (1), 77-84.

81. Atai, M.; Yassini, E.; Amini, M.; Watts, D. C., The effect of a leucite-containing ceramic filler on the abrasive wear of dental composites. *Dent Mater* **2007,** *23* (9), 1181-1187.

82. Zandinejad, A. A.; Atai, M.; Pahlevan, A., The effect of ceramic and porous fillers on the mechanical properties of experimental dental composites. *Dent Mater* **2006,** *22* (4), 382-387.

83. Sanon, C.; Chevalier, J.; Douillard, T.; Cattani-Lorente, M.; Scherrer, S. S.; Gremillard, L., A new testing protocol for zirconia dental implants. *Dent Mater* **2015,** *31* (1), 15-25.

84. In *Dentistry - Polymer-based restorative materials*, ISO: 4049-2009.

85. Palmer, L. C.; Newcomb, C. J.; Kaltz, S. R.; Spoerke, E. D.; Stupp, S. I., Biomimetic Systems for Hydroxyapatite Mineralization Inspired By Bone and Enamel. *Chemical Reviews* **2008,** *108* (11), 4754-4783.

86. Chun, K.; Choi, H.; Lee, J., Comparison of mechanical property and role between enamel and dentin in the human teeth. *Journal of Dental Biomechanics* **2014,** *5*.

87. Santos, C.; Luklinska, Z. B.; Clarke, R. L.; Davy, K. W. M., Hydroxyapatite as a filler for dental composite materials: mechanical properties and in vitro bioactivity of composites. *Journal of Materials Science-Materials in Medicine* **2001,** *12* (7), 565-573.

88. Liu, F.; Jiang, X.; Zhang, Q.; Zhu, M., Strong and bioactive dental resin composite containing poly(Bis-GMA) grafted hydroxyapatite whiskers and silica nanoparticles. *Compos Sci Technol* **2014,** *101*, 86-93.

89. Arcis, R. W.; Lopez-Macipe, A.; Toledano, M.; Osorio, E.; Rodriguez-Clemente, R.; Murtra, J.; Fanovich, M. A.; Pascual, C. D., Mechanical properties of visible light-cured resins reinforced with hydroxyapatite for dental restoration. *Dent Mater* **2002,** *18* (1), 49-57.

90. Domingo, C.; Arcís, R. W.; López-Macipe, A.; Osorio, R.; Rodríguez-Clemente, R.; Murtra, J.; Fanovich, M. A.; Toledano, M., Dental composites reinforced with hydroxyapatite: Mechanical behavior and absorption/elution characteristics. *J Biomed Mater Res* **2001,** *56* (2), 297-305.

91. Domingo, C.; Arcis, R. W.; Osorio, E.; Osorio, R.; Fanovich, M. A.; Rodriguez-Clemente, R.; Toledano, M., Hydrolytic stability of experimental hydroxyapatite-filled dental composite materials. *Dent Mater* **2003,** *19* (6), 478-486.

92. Chen, L.; Yu, Q.; Wang, Y.; Li, H., BisGMA/TEGDMA dental composite containing high aspect-ratio hydroxyapatite nanofibers. *Dental Materials* **2011,** *27* (11), 1187-1195.

93. Hongquan, Z.; Ming, Z., Effect of Surface Treatment of Hydroxyapatite Whiskers on the Mechanical Properties of Bis-gma-based Composites. *Biomed Mater* **2010,** *5* (5), 054106 (7 pp.)-054106 (7 pp.).

94. Liu, F.; Wang, R.; Cheng, Y.; Jiang, X.; Zhang, Q.; Zhu, M., Polymer grafted hydroxyapatite whisker as a filler for dental composite resin with enhanced physical and mechanical properties. *Materials Science and Engineering: C* **2013,** *33* (8), 4994-5000.

95. Zhang, H.; Darvell, B. W., Mechanical properties of hydroxyapatite whisker-reinforced bis-GMA-based resin composites. *Dent Mater* **2012,** *28* (8), 824-830.

96. Liu, F. W.; Bao, S.; Jin, Y.; Jiang, X. Z.; Zhu, M. F., Novel bionic dental resin composite reinforced by hydroxyapatite whisker. *Mater Res Innovations* **2014,** *18*, 854-858.

97. Liu, F.; Sun, B.; Jiang, X.; Aldeyab, S. S.; Zhang, Q.; Zhu, M., Mechanical properties of dental resin/composite containing urchin-like hydroxyapatite. *Dental Materials* **2014,** *30* (12), 1358-1368.

98. Ruyter, I. E.; Oysaed, H., Conversion in different depths of ultraviolet and visible light activated composite materials. *Acta Odontol Scand* **1982,** *40* (3), 179-192.

99. Liu, F.; Sun, B.; Jiang, X.; Aldeyab, S. S.; Zhang, Q.; Zhu, M., Mechanical properties of dental resin/composite containing urchin-like hydroxyapatite. *Dent Mater* **2014,** *30* (12), 1358-1368.

100. Albert, P.; Lohden, G.; Gall, C.; Borup, B. Ormocers, method for their production, and their use. US20010056197 A1, 2001.

101. Wei, Y.; Jin, D.; Wei, G.; Yang, D.; Xu, J., Novel Organic–Inorganic Chemical Hybrid Fillers for Dental Composite Materials. *J Appl Polym Sci* **1998,** *70*, 1689-1699.

102. Hamouda, I. M.; Shehata, S. H., Shear Bond Strength of Ormocer-Based Restorative Material Using Specific and Nonspecific Adhesive Systems. *ISRN Mater Sci* **2011,** *2011*, 1-4.

103. Tagtekin, D. A.; Yanikoglu, F. C.; Bozkurt, F. O.; Kologlu, B.; Sur, H., Selected characteristics of an Ormocer and a conventional hybrid resin composite. *Dent Mater* **2004,** *20* (5), 487-497.

104. Moszner, N.; Gianasmidis, A.; Klapdohr, S.; Fischer, U. K.; Rheinberger, V., Sol-gel materials 2. Light-curing dental composites based on ormocers of cross-linking alkoxysilane methacrylates and further nano-components. *Dent Mater* **2008,** *24* (6), 851-856.

105. Muh, E.; Marquardt, J.; Klee, J. E.; Frey, H.; Mulhaupt, R., Bismethacrylate-Based Hybrid Monomers via Michael-Addition Reactions. *Macromolecules* **2001,** *34*, 5778-5785.

106. Jandt, K. D.; Al-Jasser, A. M. O.; Al-Ateeq, K.; Vowles, R. W.; Allen, G. C., Mechanical properties and radiopacity of experimental glass-silica-metal hybrid composites. *Dent Mater* **2002,** *18*, 429-435.

107. Imamura, S.; Takahashi, H.; Hayakawa, I.; Loyaga-Rendon, P. G.; Minakuchi, S., Effect of filler type and polishing on the discoloration of composite resin artificial teeth. *Dent Mater* **2008,** *27* (6), 802-808.

108. Kim, K.-H.; Kim, Y.-B.; Okuno, O., Microfracture mechanisms of composite resins containing prepolymerized particle fillers. *Dent Mater* **2000,** *19* (1), 22-33.

109. Yukitani, W.; Hasegawa, T.; Itoh, K.; Hisamitsu, H.; Wakumoto, S., Marginal adaptation of dental composites containing prepolymerized filler. *Oper Dent* **1997,** (22), 242-248.

110. Suzuki, S.; Ori, T.; Saimi, Y., Effects of filler composition on flexibility of microfilled resin composite. *J Biomed Mater Res B* **2005,** *74* (1), 547-552.

111. Blackham, J. T.; Vandewalle, K. S.; Lien, W., Properties of hybrid resin composite systems containing prepolymerized filler particles. *Oper Dent* **2009,** *34* (6), 697-702.

112. Okada, K.; Omura, I., Dental restorative material. Google Patents: 1993.

113. Angeletakis, C.; Nguyen, M. D. S.; Kobashigawa, A. I., Prepolymerized filler in dental restorative composite. Google Patents: 2005.

114. Waknine, S., Dental restorative material. Google Patents: 1985.

115. Samuel, S. P.; Li, S.; Mukherjee, I.; Guo, Y.; Patel, A. C.; Baran, G.; Wei, Y., Mechanical properties of experimental dental composites containing a combination of mesoporous and nonporous spherical silica as fillers. *Dent Mater* **2009,** *25* (3), 296-301.

116. Atai, M.; Pahlavan, A.; Moin, N., Nano-porous thermally sintered nano silica as novel fillers for dental composites. *Dent Mater* **2012,** *28* (2), 133-145.

117. Bowen, R. L.; Reed, L. E., Semiporous Reinforcing Fillers for Composite Resins: I. Preparation of Provisional Glass Formulations. *J Dent Res* **1976,** *55* (5), 738-747.

118. Azevedo, C.; Tavernier, B.; Vignes, J.-L.; Cenedese, P.; Dubot, P., Structure and Surface Reactivity of Novel Nanoporous Alumina Fillers. *J Biomed Mater Res B Appl Biomater* **2008,** *88*, 174.

119. Thorat, S. B.; Diaspro, A.; Salerno, M., In vitro investigation of coupling-agent-free dental restorative composite based on nano-porous alumina fillers. *J Dent* **2014,** *42* (3), 279-286.

120. Liu, Y.; Tan, Y.; Lei, T.; Xiang, Q.; Han, Y.; Huang, B., Effect of porous glass-ceramic fillers on mechanical properties of light-cured dental resin composites. *Dent Mater* **2009,** *25* (6), 709-715.

121. *Handbook of Manufacturing Engineering and Technology*. Springer London: 2015; p 865.

122. Li, X.; Liu, W.; Sun, L.; Aifantis, K. E.; Yu, B.; Fan, Y.; Feng, Q.; Cui, F.; Watari, F., Resin composites reinforced by nanoscaled fibers or tubes for dental regeneration. *BioMed Res Int* **2014,** *2014*, 542958.

123. Khan, A. S.; Azam, M. T.; Khan, M.; Mian, S. A.; Rehman, I. U., An update on glass fiber dental restorative composites: A systematic review. *Mater Sci Eng C* **2015,** *47C*, 26-39.

124. Shouha, P.; Swain, M.; Ellakwa, A., The effect of fiber aspect ratio and volume loading on the flexural properties of flowable dental composite. *Dent Mater* **2014,** *30* (11), 1234-1244.

125. Xu, H. H. K.; Quinn, J. B.; Smith, D. T.; Giuseppetti, A. A.; Eichmiller, F. C., Effects of different whiskers on the reinforcement of dental resin composites. *Dent Mater* **2003,** *19*, 359-367.

126. Zhang, F.; Xia, Y.; Xu, L.; Gu, N., Surface modification and microstructure of single-walled carbon nanotubes for dental resin-based composites. *J Biomed Mater Res B* **2008,** *86* (1), 90-97.

127. Gao, Y.; Sagi, S.; Zhang, L.; Liao, Y.; Cowles, D. M.; Sun, Y.; Fong, H., Electrospun nano-scaled glass fiber reinforcement of bis-GMA/TEGDMA dental composites. *J Appl Polym Sci* **2008,** *110* (4), 2063-2070.

128. Ruddell, D. E.; Maloney, M. M.; Thompson, J. Y., Effect of novel filler particles on the mechanical and wear properties of dental composites. *Dent Mater* **2002,** *18*, 72-80.

129. Dodiuk-Kenig, H.; Lizenboim, K.; Roth, S.; Zalsman, B.; McHale, W. A.; Jaffe, M.; Griswold, K., Performance Enhancement of Dental Composites Using Electrospun Nanofibers. *J Nanomater* **2008,** *2008*, 1-6.

130. Bae, J. M.; Kim, K. N.; Hattori, M.; Hasegawa, K.; Yoshinari, M.; Kawada, E.; Oda, Y., The flexural properties of fiber-reinforced composite with light-polymerized polymer matrix. *Int J Prosthodont* **2001,** *14* (1), 33-39.

131. Tian, M.; Gao, Y.; Liu, Y.; Liao, Y.; Xu, R.; Hedin, N. E.; Fong, H., Bis-GMA/TEGDMA Dental Composites Reinforced with Electrospun Nylon 6 Nanocomposite Nanofibers Containing Highly Aligned Fibrillar Silicate Single Crystals. *Polymer* **2007,** *48* (9), 2720-2728.

132. Borges, A. L.; Munchow, E. A.; de Oliveira Souza, A. C.; Yoshida, T.; Vallittu, P. K.; Bottino, M. C., Effect of random/aligned nylon-6/MWCNT fibers on dental resin composite reinforcement. *J Mech Behav Biomed Mater* **2015,** *48*, 134-144.

133. Chen, Q.; Zhao, Y.; Wu, W.; Xu, T.; Fong, H., Fabrication and evaluation of Bis-GMA/TEGDMA dental resins/composites containing halloysite nanotubes. *Dent Mater* **2012,** *28* (10), 1071-1079.

134. Niu, L. N.; Fang, M.; Jiao, K.; Tang, L. H.; Xiao, Y. H.; Shen, L. J.; Chen, J. H., Tetrapod-like zinc oxide whisker enhancement of resin composite. *J Dent Res* **2010,** *89* (7), 746-750.

135. Guo, G.; Fan, Y.; Zhang, J. F.; Hagan, J. L.; Xu, X., Novel dental composites reinforced with zirconia-silica ceramic nanofibers. *Dent Mater* **2012,** *28* (4), 360-368.

136. Xu, H. H. K.; Quinn, J. B.; Giuseppetti, A. A., Wear and Mechanical Properties of Nano-silica-fused Whisker Composites. *J Dent Res* **2004,** *83* (12), 930-935.

137. Xu, H. H. K.; Quinn, J. B.; Smith, D. T.; Antonucci, J. M.; Schumacher, G. E.; Eichmiller, F. C., Dental resin composites containing silica-fused whiskers—effects of whisker-to-silica ratio on fracture toughness and indentation properties. *Biomaterials* **2002,** *23* (3), 735-742.

138. Xu, H. H. K., Dental Composite Resins Containing Silica-fused Ceramic Single-crystalline Whiskers with Various Filler Levels. *J Dent Res* **1999,** *78* (7), 1304-1311.

139. Xu, H. H. K.; Martin, T. A.; Antonucci, J. M.; Eichmiller, E., Ceramic Whisker Reinforcement of Dental Resin Composites. *J Dent Res* **1999,** *78* (2), 706-712.

140. Darvell, B. W., *Material Science for Dentistry*. 9th ed.; Woodhead Publishing: 2009; p 688.

141. Kraft, D. J.; Vlug, W. S.; van Kats, C. M.; van Blaaderen, A.; Imhof, A.; Kegel, W. K., Self-assembly of colloids with liquid protrusions. *J Am Chem Soc* **2009,** *131* (3), 1182-1186.

142. Lee, S. Y.; Gradon, L.; Janeczko, S.; Iskandar, F.; Okuyama, K., Formation of highly ordered nanostructures by drying micrometer colloidal droplets. *ACS Nano* **2010,** *4* (8), 4717-4724.

143. Cho, Y. S.; Yi, G. R.; Chung, Y. S.; Park, S. B.; Yang, S. M., Complex colloidal microclusters from aerosol droplets. *Langmuir* **2007,** *23* (24), 12079-12085.

144. Mitra, S. B.; Wu, D.; Holmes, B. N., An application of nanotechnology in advanced dental materials. *J Am Dent Assoc* **2003,** *134* (10), 1382-1390.

145. Wang, R.; Bao, S.; Liu, F.; Jiang, X.; Zhang, Q.; Sun, B.; Zhu, M., Wear behavior of light-cured resin composites with bimodal silica nanostructures as fillers. *Mater Sci Eng C* **2013,** *33* (8), 4759-4766.

146. Wang, R.; Zhang, M.; Liu, F.; Bao, S.; Wu, T.; Jiang, X.; Zhang, Q.; Zhu, M., Investigation on the physical-mechanical properties of dental resin composites reinforced with novel bimodal silica nanostructures. *Mater Sci Eng C* **2015,** *50* (1), 266-273.

147. Kumar, N.; Khoso, N. A.; Sangi, L.; Bhangar, F.; Kalhoro, F. A., Dental resin-based composites: A transition from macrofilled to nanofilled. *J Pak Dent Assoc* **2012,** *21* (1), 39-44.

148. Curtis, A. R.; Palin, W. M.; Fleming, G. J.; Shortall, A. C.; Marquis, P. M., The mechanical properties of nanofilled resin-based composites: characterizing discrete filler particles and agglomerates using a micromanipulation technique. *Dent Mater* **2009,** *25* (2), 180-187.

149. Curtis, A. R.; Palin, W. M.; Fleming, G. J.; Shortall, A. C.; Marquis, P. M., The mechanical properties of nanofilled resin-based composites: the impact of dry and wet cyclic pre-loading on bi-axial flexure strength. *Dent Mater* **2009,** *25* (2), 188-197.

150. Atai, M.; Pahlavan, A.; Moin, N., Nano-porous thermally sintered nano silica as novel fillers for dental composites. *Dent. Mater.* **2012,** *28* (2), 133-145.

151. Fong, H.; Dickens, S. H.; Flaim, G. M., Evaluation of dental restorative composites containing polyhedral oligomeric silsesquioxane methacrylate. *Dent Mater* **2005,** *21* (6), 520-529.

152. Wu, X.; Sun, Y.; Xie, W.; Liu, Y.; Song, X., Development of novel dental nanocomposites reinforced with polyhedral oligomeric silsesquioxane (POSS). *Dent Mater* **2010,** *26* (5), 456-462.

153. Sideridou, I. D.; Karabela, M. M., Effect of the amount of 3-methacyloxypropyltrimethoxysilane coupling agent on physical properties of dental resin nanocomposites. *Dent Mater* **2009,** *25* (11), 1315-1324.

154. Debnath, S.; Ranade, R.; Wunder, S. L.; McCool, J.; Boberick, K.; Baran, G., Interface effects on mechanical properties of particle-reinforced composites. *Dent Mater* **2004,** *20* (7), 677-686.

155. Karabela, M. M.; Sideridou, I. D., Synthesis and study of physical properties of dental light-cured nanocomposites using different amounts of a urethane dimethacrylate trialkoxysilane coupling agent. *Dent Mater* **2011,** *27* (11), 1144-1152.

156. Wilson, K. S.; Zhang, K.; Antonucci, J. M., Systematic variation of interfacial phase reactivity in dental nanocomposites. *Biomaterials* **2005,** *26* (25), 5095-5103.

157. Rodriguez, H. A.; Giraldo, L. F.; Casanova, H., Formation of functionalized nanoclusters by solvent evaporation and their effect on the physicochemical properties of dental composite resins. *Dent Mater* **2015,** *31* (7), 789-798.

158. Xavier, T. A.; Froes-Salgado, N. R. D.; Meier, M. M.; Braga, R. R., Influence of silane content and filler distribution on chemical-mechanical properties of resin composites. *Brazil Oral Res* **2015,** *29* (1), 1-8.

159. Ferracane, J. L.; Hilton, T. J., Polymerization stress - Is it clinically meaningful? *Dent Mater* **2015**.

160. Lempel, E.; Toth, A.; Fabian, T.; Krajczar, K.; Szalma, J., Retrospective evaluation of posterior direct composite restorations: 10-year findings. *Dent Mater* **2015,** *31* (2), 115-122.

161. Zorzin, J.; Maier, E.; Harre, S.; Fey, T.; Belli, R.; Lohbauer, U.; Petschelt, A.; Taschner, M., Bulk-fill resin composites: polymerization properties and extended light curing. *Dent Mater* **2015,** *31* (3), 293-301.

162. Kantürk Figen, A.; Yilmaz Atali, P.; Pişkin, M. B., Thermal properties and kinetics of new-generation posterior bulk fill composite cured light-emitting diodes. *J Therm Anal Calorim* **2014,** *118* (1), 31-42.

163. Bucuta, S.; Ilie, N., Light transmittance and micro-mechanical properties of bulk fill vs. conventional resin based composites. *Clin Oral Investig* **2014,** *18* (8), 1991-2000.

164. Flury, S.; Hayoz, S.; Peutzfeldt, A.; Husler, J.; Lussi, A., Depth of cure of resin composites: is the ISO 4049 method suitable for bulk fill materials? *Dent Mater* **2012,** *28* (5), 521-528.

165. Fan, Y.; Sun, Z.; Moradian-Oldak, J., Controlled remineralization of enamel in the presence of amelogenin and fluoride. *Biomaterials* **2009,** *30* (4), 478-483.

166. Fan, Y.; Sun, Z.; Wang, R.; Abbott, C.; Moradian-Oldak, J., Enamel inspired nanocomposite fabrication through amelogenin supramolecular assembly. *Biomaterials* **2007,** *28* (19), 3034-3042.

167. Seemann, R.; Flury, S.; Pfefferkorn, F.; Lussi, A.; Noack, M. J., Restorative dentistry and restorative materials over the next 20 years: a Delphi survey. *Dent Mater* **2014,** *30* (4), 442-448.

168. Xu, H. H.; Weir, M. D.; Sun, L.; Moreau, J. L.; Takagi, S.; Chow, L. C.; Antonucci, J. M., Strong nanocomposites with Ca, PO(4), and F release for caries inhibition. *J Dent Res* **2010,** *89* (1), 19-28.

169. Wiegand, A.; Buchalla, W.; Attin, T., Review on fluoride-releasing restorative materials--fluoride release and uptake characteristics, antibacterial activity and influence on caries formation. *Dent Mater* **2007,** *23* (3), 343-362.

Chapter 3 - **Photocalorimetry Method Optimization for the Study of Light-initiated Radical Polymerizations***

Abstract

The properties of the dental resin composites have been studied extensively with several different methods including infrared and Raman spectroscopy, volume dilatometry, and mechanical analyses. Photo-calorimetry has also been used to measure the kinetics and extent of polymerization, but many of the variables associated with this technique remain to be fully defined and tested to enable quick and reproducible measurements under clinically relevant conditions. We have systematically varied the sample mass, light intensity, temperature, nitrogen purge time, and examined their effects on the monomer conversion and polymerization kinetics with the aim to optimize and standardize the photo-DSC method for the study of dental resins. A post-cure isothermal baseline at 37 °C yielded reproducible results. This systematic study detailing the effects of several variables of photo-calorimetry allows its direct use as a standard method to study polymerization kinetics and monomer conversion of dental resins and other photo-curable materials.

---

*Eric Habib and X. X. Zhu. *Polymer*, accepted Dec. 2017.

3.1 Introduction

In the last decades, progress in polymer research has led to a variety of products that are used in advanced technology as well as daily life. A sub-category of medically related polymers is resins that can be cured by light *in situ*. Of particular interest are dental resin composites for which their bulk polymerization is photo-initiated in the mouth and must take place quickly. These materials have been studied extensively on a case-by-case basis, particularly for commercially available composites, but the fundamental understanding of these materials and their properties remains lacking. The challenge in this area of research is to make the experimental conditions for the measurements relevant to dental clinical practice, making the results obtained pertinent to the comparison of existing materials and the formulation of new and improved dental composites. The optimization and standardization of the characterization methods by a systematic examination of the variables involved will facilitate the development of new materials and the comparison of their performance.

The degree of conversion during the polymerization of these resins is considered to be an important indicator for these materials due to its correlation to several other important characteristics [1, 2] such as mechanical performance [3-5], shrinkage [6], and post-cure monomer leaching [7]. In dental resin composites, the degree of conversion is typically measured by the use of FTIR, near IR or Raman spectroscopy to follow the band of the methacrylate carbon-carbon double bonds. While these methods boast a high spatial resolution, they have limited temporal resolution due to the longer acquisition time necessary to obtain a sufficiently high signal-to-noise ratio. Conversely, calorimetry has very low spatial resolution, but very high temporal resolution, which permits users to follow reaction progress with very high time accuracy. Furthermore, spectroscopic measurements always follow band intensities relative to the starting sample (monomers), whereas the study of the polymerization process and of the product formed may provide more pertinent and/or complimentary information of the dental resins.

Differential scanning calorimetry (DSC) is a common technique used in the study of polymer materials and polymerization processes. DSC equipped with additional light irradiation (photo-DSC or pDSC) operates on similar principles as conventional DSC to measure the enthalpy of reaction, relying on accurate measurements of the polymerization reaction exotherms. Dental resins are photo-polymerized *in situ* in clinical procedures, which

makes pDSC an ideal technique to directly study the polymerization process of such materials. The polymerization conditions can be varied and the heat of reaction can be determined easily and accurately. While a number of reports appeared in the literature on the use of this technique for the study of dental resins, there has been a lack of details on the experimental design and the choice of suitable measurement parameters of pDSC to obtain useful and reproducible results. The experimental procedure and data processing need to be optimized to monitor photo-activated reactions such as the photo-polymerization of the dental resins, which generally proceed rapidly at ambient temperatures and ideally to completion with conditions mimicking the constrained oral environment. It is essential to systematically assess the parameters involved in such measurements to produce reliable, reproducible, and comparable results.

The objective of this investigation is to optimize the parameters for the pDSC measurement of the photo-polymerization of dental composites. This was done by establishing a link between the analysis sequence, sample mass, temperature, light intensity, nitrogen purge time; and the double bond conversion and kinetics of the resin polymerization. These parameters were studied and optimized to obtain accurate and clinically relevant data on the kinetics and conversion for the polymerization of dental resins and composites.

3.2 Experimental

3.2.1 Materials

Bisphenol A glycerolate dimethacrylate (Bis-GMA), triethylene glycol dimethacrylate (TEGDMA), and camphorquinone (CQ) were purchased from Sigma-Aldrich. Ethyl 4-N,N-dimethylaminobenzoate (EDMAB) was purchased from Alfa Aesar (Tewksbury, MA, USA). TEGDMA contains 80-120 ppm 4-methoxyphenol as an inhibitor, as purchased.

3.2.2 Resin Blending

The resins were left to warm to room temperature. CQ (50 mg) and EDMAB (50 mg) were dissolved in TEGDMA (3 g) with magnetic stirring at 30 °C for 10 minutes. BisGMA (7 g) was added into this solution and mixed by spatula, then mixed with a magnetic stirrer

until homogeneous (about 30 minutes) at 30 °C. The blended resin was stored in aluminium foil-covered vials at 4 °C.

3.2.3 Composite Formulation and Blending

Composites were formulated using the resin above, and filled with 60 wt% spherical silica nanoparticles with a size of 980 nm, whose synthesis and characterization were previously described (*8*). They were homogeneously blended using a three roll mill (Exact 50i TRM, Norderstedt, Germany).

3.2.4 Calorimetry

A Q2000 differential scanning calorimeter with a modified photo-calorimetry accessory (TA Instruments, New Castle, DE, USA) was used with an Omnicure s2000 light source with a 200 W mercury lamp (Excelitas Technologies Corp, Waltham, MA, USA) and a 400-500 nm band pass filter. The photo-calorimetry accessory had to be modified (Figure S 3.1) due to its unstable baseline from inadequate light guide positioning and fixation. Several set screws and adjustment mechanisms were added in the upper and lower light guide brackets to ensure the stability of the light guide's position. Furthermore, the light guides themselves were modified to allow them to be placed closer to the samples cells for higher light intensity.

Fig. 3.1 describes the detailed protocol used with the instrument. Each measurement was repeated in quadruplicate. The conversion (%) was calculated with the following equation:

$$Conversion = \frac{\Delta H}{DB * E} \times 100\% \quad (3.1)$$

where ΔH is the area under the curve measured by photo-calorimetry (J/g), DB is the number of moles of double bonds per gram of composite (mol/g), and E is the standard enthalpy change for the polymerization of methacrylate groups (56,902.4 J/mol) (*9*). All calorimetry figures are shown with exotherms up (positive).

To assess the effect of oxygen inhibition on the pDSC measurements, a second protocol was used (Fig. 3.1 dashed boxes) where air was purged over the sample for 5 minutes first. The sample was then purged with nitrogen for different durations (0 to 15 minutes) to assess the effect of the oxygen content of the atmosphere on the resin polymerization.

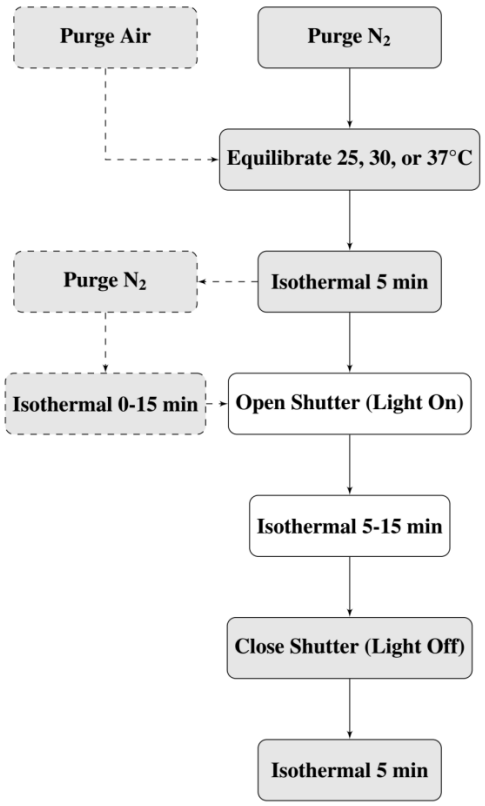

Fig. 3.1. pDSC protocols used for standardized measurements (solid boxes), and for oxygen inhibition tests (dashed boxes).

3.2.5 Light Intensity Measurements

The light intensity was measured using the DSC calorimeter. The nominal light intensity was as measured from the DSC cells with aluminum pans containing 5 mg of carbon black completely coating the surface, which was considered an ideal black body. The light intensity in the calorimeter was measured at different levels, as set from the light source in percentage points of full capacity. The maximum intensity of radiance with the 400-500 nm filter (Figure S 3.2) was measured to be 980 mW/cm^2, and the source percentage power indeed corresponded to a linear change in energy density (Figure S 3.2). This method of light intensity measurement has the advantage of measuring the precise luminal output that the sample is exposed to, as opposed to a radiometer reading that measures the lamp's output under conditions different from that of the polymerization reaction. This eliminates variations in distance from the light source, since the distance becomes fixed, to sub-millimeter precision. This is much more precise than freehand curing protocols where changing the

surface distance from 2 to 4 mm can result in a four-fold decrease in light flux, since luminance follows an inverse-squares law (*10*).

3.2.6 Statistical Analysis

Statistical significance was established using one-sided student t-test. Error bars represent standard deviations.

3.3 Results and Discussion

Accurate pDSC conversion measurements rely on measurements of polymerization enthalpy. Antonucci et al. (*9*) previously examined the reaction enthalpies for the polymerization of several methacrylates and obtained a consistent value of 56,902 J/mol methacrylate, regardless of the substitution groups. Using the integral of the heat flow obtained by pDSC, the degree of conversion can then be calculated using the known methacrylate density of the material.

Several parameters were altered systematically in pDSC measurements of kinetics and conversion to evaluate their influence on the measured values, baseline quality, and overall accuracy.

3.3.1 Analysis Sequence

The sequence used in photo-calorimetry analysis has a strong influence on the measured value, mainly in due to the quality and stability of the baseline. DSC measurements typically involve quantifying the difference in heat flow between the sample and reference cells, knowing that the mass of the pans is effectively identical; the exotherm of empty pan serves as a baseline for the measurement, which is then subtracted from the sample pan's exotherm. In photo-calorimetry, however, since the resin-filled and empty pans absorb different amounts of light, this leads to significant differences in heat flow even with equal irradiance. This problem was previously solved by recording a second post-cure exotherm with the same sample. This 'asynchronous baseline' can then be subtracted from the initial run, resulting in an exotherm that shows only the contributions from the heat of polymerization (*8, 11-12*). Although asynchronous baselines seem to be the norm for the most accurate results, two types of calculated baselines are also compared: a flat baseline, where the light intensity is assumed to be constant in time once on, and an exponential decay

baseline that accounts for the lamp's onset time. As shown in Fig. 3.2, the flat calculated baseline results in similar values to the asynchronous one, but has larger errors. The exponential decay baseline results in a closer fit to the measured asynchronous baseline, but also has a large inter-sample variability. Therefore, the calculated baselines yield similar values to the measured asynchronous baseline, but yielded lower accuracy for the results. Calculated baselines may be used as a time-saving measure, but in the end, asynchronously measured baselines provide the most reproducible and accurate measurements, and were used in this work.

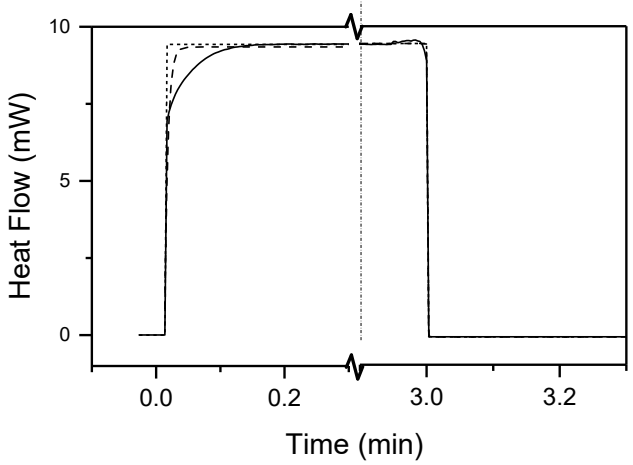

Fig. 3.2. Baseline exotherms, after polymerization was already completed, showing the measured asynchronous baseline (solid) and calculated flat baseline (dots), and calculated exponential decay baselines (dashes).

In terms of measurement protocols, while clinical conditions for composite polymerization have no active temperature control, the surrounding tooth tissue and saliva act to dissipate some of the heat released upon polymerization. This typically results in increases of 3-8 °C in the surrounding pulp tissue upon polymerization (*13-14*), which also affects polymerization kinetics and the degree of polymerization. To reflect this heat dissipation effect, the default measurement protocol used isothermal measurements, where the temperature was set to remained constant throughout the experiments. Other procedures were attempted to regulate the temperature to the desired set point, but led to unstable and unrepeatable baselines with large errors (Figure S 3.3). The isothermal protocol (Fig. 3.1) was thus used to obtain the most reproducible measurements.

3.3.2 Temperature Variations

In free radical polymerizations, individual chain growth occurs very rapidly once initiated (*15*). The increasing molecular weight causes a commensurate increase in viscosity, resulting in the gel effect (or Trommsdorff effect); the termination rate decreases due to lower chain mobility and results in an increase in the polymerization rate as the reaction progresses. Due to the exothermic nature of the polymerization reaction, the increase in temperature also leads to an increased rate of polymerization which will itself lead to more a more rapid heat release. This phenomenon is referred as rate auto-acceleration, which is sometimes confounded with the gel effect. These two effects (gel and auto-acceleration) interact: the increase in temperature decreases the viscosity of the solution, which delays the gel point to higher conversion values (*1*).

The most clinically significant temperature for photo-calorimetric analysis of curing in the context of dental materials is 37 °C. Aside from the effects noted above, the temperature is expected to affect the rate of reaction as described by the Arrhenius equation, resulting in theoretical differences of up to 48% in the rate constants for reactions at 25 °C and 37 °C (see Supporting Information calculations). Furthermore, analogously to the effect of light intensity (see Section 3.4), a higher rate of reaction is expected to result in increased conversion values.

To measure the effect of the initial temperature on the extent and kinetics of polymerization, the photo-polymerization experiments were performed at initial temperatures of 25, 30 or 37 °C. These changes led to variations of the peak and equilibrium temperatures reached while the lamp was turned on, but the change was constant with respect to the initial temperature (Figure S 3.4A).

The maximum rate of polymerization exhibited a small increase with temperature from 25 to 30 °C, but not from 30 to 37 °C (Figure S 3.4B). The Arrhenius equation, however, predicted larger differences (See Supporting Information Calculations); the smaller changes were most likely due to the interference of the other factors affecting the reaction rate, such as network formation and changes in the properties of the medium. Previous work by Calheiros (*16*) suggests that the differences are more pronounced if the photo-polymerization is done for shorter time periods, rather than going to completion. Kinetics of bulk

polymerizations have been extensively studied, but still lack a definitive model (*17*). In the end, small temperature changes had little effect on the kinetics or the degree of conversion.

The final conversion of the materials was slightly lower at 25 °C (62 ± 2%) than at either 30 ℃ (68 ± 5%) or 37 °C (67 ± 3%); the difference between the latter two was not statistically significant ($p = 0.77$). While such differences in temperature (5-12 ℃ increase) were expected to cause larger changes in conversion as reported by Cook et al. (*18*), the measured changes were quite small (Fig. 3.3A), likely due to the small size of the differences relative to the error in the measurement.

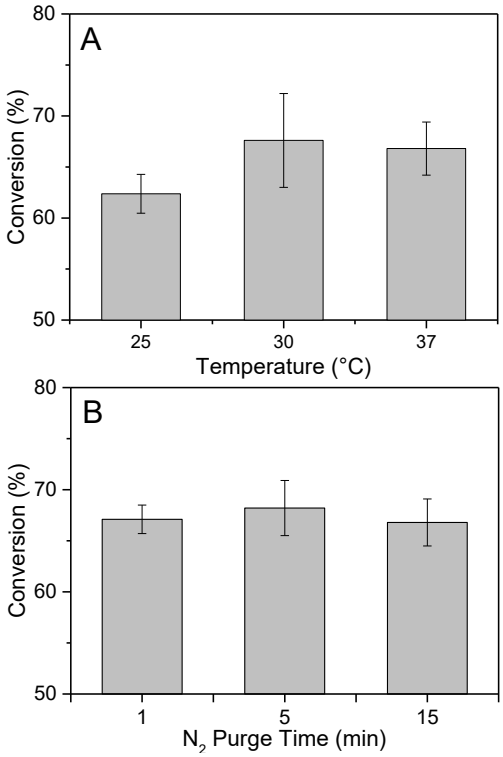

Fig. 3.3. Monomer conversion variations with (A) changes in equilibrium temperature, and (B) changes in nitrogen gas purge time for a 10 mg sample.

3.3.3 Mass Variations

The mass of the sample can also have a significant effect on the pDSC measurements. Larger masses should yield more precise conversion values, minimizing instrumental and weighing errors. However, large masses may also cause heat transfer delays resulting in significant heat flow signal distortion. Additionally, since the sample pan must remain open to allow light exposure, heat dissipation from the top may become a significant problem,

reducing the apparent enthalpy. Large masses can cause light intensity gradients due to sample thickness. Calculations show that even if the DSC pan is filled to the top, only 11.8% of the light is absorbed by the sample, including light reflected from the bottom of the pan (see Supporting Information, calculations). Therefore, for the masses observed, we can approximate that the light exposure on the sample is uniform. These combined factors suggest that for the best DSC measurement precision, small sample masses are optimal, with recommended masses for conventional DSC of 2-5 mg (*19*). In typical fillings for caried teeth, however, restorations have much larger masses (50-100 mg) (*20-21*). Therefore, larger masses would better reflect the clinical reality, while smaller masses would yield more accurate results with this measuring method.

Masses of 1 to 50 mg were used to evaluate their influence on the temperature increase, the conversion, kinetics, and baseline stability. While the system theoretically maintained a temperature of 37 °C, the temperature increased to a peak due to the light exposure and polymerization reaction, and then tapered off. The measured equilibrium temperature varied little with sample mass, but the peak temperature was significantly higher ($p < 0.01$) for the two largest samples (25 and 50 mg) than for the smaller ones (1 and 5 mg, Fig. 3.4A). Both the peak temperature and equilibrium temperature eventually leveled off with increasing sample mass. This is most likely due to competition between larger total exotherm in the sample due to a larger mass, and more efficient heat transfer due to a steeper temperature gradient. Furthermore, since the polymerization process is exothermic, a sample containing 60 wt% inorganic fillers would release 60% less heat than the pure resin without fillers, resulting in a smaller increment in temperature. For example, the polymerization of 70:30 wt% BisGMA:TEGDMA resin results in a 199 J/g exotherm at 73% conversion, but the same resin loaded with 60 wt% silica filler results in 83 J/g exotherm at 76% conversion, or 42% that of the resin alone. Therefore, the heat release is proportional to the mass of the monomers in the composites.

In terms of the polymerization kinetics, the apparent maximum polymerization rate varied linearly with sample mass with strong correlation (Fig. 3.4B), and the time at which this maximum is reached (maximum polymerization time) varies exponentially with the sample mass. Both were modeled with high correlation coefficient values. Examination of the polymerization exotherms (Fig. 3.4D) suggests that the changes in the apparent maximum

polymerization rate and time may be measurement artifacts caused by the longer average distance to the measurement cell with samples of larger mass and volume. The heat transfer rate to the cell and to the surrounding air is a function of surface area, which itself increases more slowly than mass (area/volume $\propto l^{-1}$, where l is a length dimension), therefore apparent decreases in energy are expected with larger samples masses.

Despite significant changes in the polymerization kinetics, the variation of final measured conversion for 5, 10, and 25 mg samples was very small, within error, but the 50 mg sample had a significantly lower apparent conversion value (Fig. 3.4C), most likely due to heat loss from the top of the sample. Fig. 3.4D inset shows that up to 10 mg sample size, the baseline distortion is minimal; 25 and 50 mg samples show significant distortion since larger sample mass leads to smaller surface/volume ratios (surface area/volume $\propto l^{-1}$, where l is a length dimension). This confirms that masses of less than 25 mg are required for the most accurate conversion measurements.

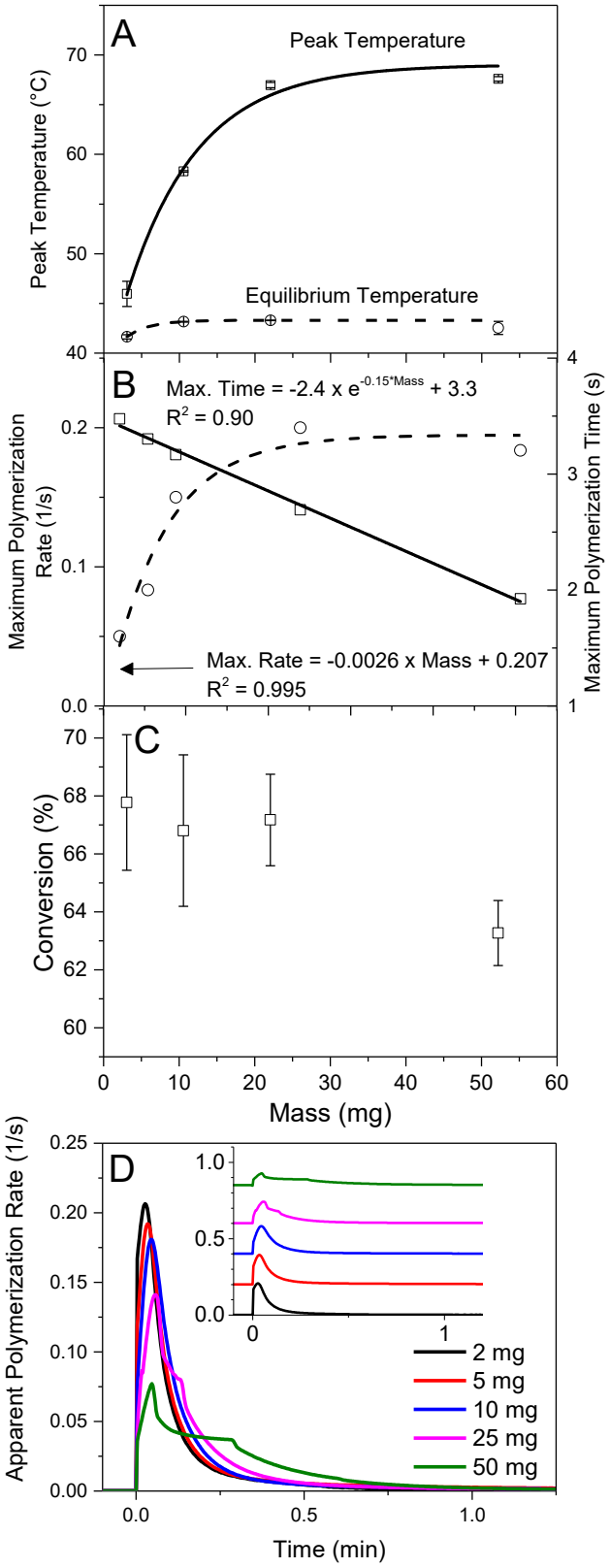

Fig. 3.4. Photo-polymerizations of 70:30 wt% ratio BisGMA:TEGDMA resin at 37 ℃ with a light intensity of 740 mW/cm^2. The effect of sample mass on (A) temperature upon polymerization, (B) maximum polymerization rate and the time to reach this rate, (C) apparent overall conversion, and (D) signal intensity and (inset) overall peak distortion that is observed with increasing mass.

3.3.4 Light Intensity Variations

According to previous studies, the light intensity (I_L) of the polymerization lamp determines the initiation rate, which then affects the rate of polymerization (R_p) proportionally to the square root of the light intensity (*22-23*):

$$R_p = k_p\,[M]\sqrt{\frac{I_L * \phi[I]}{2k_t}} \tag{3.2}$$

where k_p and k_t are the propagation and termination rate constants, [M] and [I] are the monomer and initiators concentrations, respectively, ϕ is the photo-initiator efficiency, and I_L is the light intensity. Therefore, at constant [M] and [I],

$$R_p = a\sqrt{I_L} \tag{3.3}$$

$$a = \frac{k_p[M]\sqrt{\phi[I]}}{\sqrt{2k_t}} \tag{3.4}$$

Literature in dental materials has shown that increased light intensity leads to higher double bond conversions (*10, 23-26*). Leprince (*27*) explained this behaviour with the initiation kinetics: a higher light intensity leads to a higher concentration of active radicals, leading to an increased termination rate. This results in localized polymer growth centers, which more slowly increase the solution viscosity than polymers synthesized at lower initiation rates where an extended network forms throughout the resin (*25*). This lower viscosity leads to lower auto-acceleration resulting in a higher overall conversion. Lu et al. (*28*) had a similar explanation, suggesting it was due to a temporary increase in the apparent free volume during the polymerization with a speed spike in the initial reaction that allowed the reaction to progress further, similarly to supercooling before freezing upon a rapid temperature drop.

Light intensity in clinical situations usually varies between 400 and 1200 mW/cm^2 for wavelengths of 390-520 nm (*29*). A stable baseline is critical to obtain accurate results in pDSC. The Omnicure lamp is equipped with ‘closed feedback loop’ technology that monitors the light level and maintains stable levels. While this light source produces a very stable output in the long term, it tends to slightly overshoot when being turned on, proportionally to the light intensity. Otherwise, the heat flow from the lamp can be regarded as a constant intensity function.

To evaluate the effect of different light intensities, a test series was performed with order of magnitude variations in light intensity within the limits of the lamp used. The samples were illuminated until the sample was fully cured (5-15 minutes, depending on light intensity, to insure a complete reaction despite clinical relevance). At lower light intensities (1-5%), the background subtraction was much more accurate, leading to higher reproducibility; but these are less representative of clinical conditions for dental resins.

The sudden temperature increase (jump) upon light exposure was much smaller at lower intensities, following a square root relationship (Fig. 3.5A); the equilibrium temperature followed the same type of function. There were significant changes in the polymerization kinetics, consistent with changes in the rate of initiation due to changes in light intensity (Fig. 3.5B). The polymerization rate followed the theoretical relationship (*22-23*), in proportion to the square root of light intensity (Eqs. 3.2 and 3.3). The values obtained allow us to calculate the ratio of the propagation and termination rates of the reaction ($k_p/\sqrt{k_t}$), yielding 0.43, which allows the prediction of maximum reaction rate at any light intensity, monomer and initiator concentration. The time of maximum polymerization (Fig. 3.5B) was modeled as a log function of light intensity. The overall curve shape remains similar (Fig. 3.5D) regardless of the light intensity, indicating that any intensity should provide accurate data.

Finally, there were large variations in the overall degree of polymerization (Fig. 3.5C) measured at different I_L: lower I_L resulted in lower conversion values. Lower starting light intensities for curing have been suggested for reducing shrinkage stress in dental resins, but were also previously shown to concurrently reduce overall conversion (*30*). Although there has been a large body of research examining alternate curing protocols to reduce shrinkage (*24-25, 30*), the standard protocol remains high intensity light for short periods (400-1200 mW/cm^2, 15-30 s), and so despite a somewhat lower accuracy, high light intensity for a short period of time remains the most representative clinically relevant measurement for dental resins, and results in the highest conversion values.

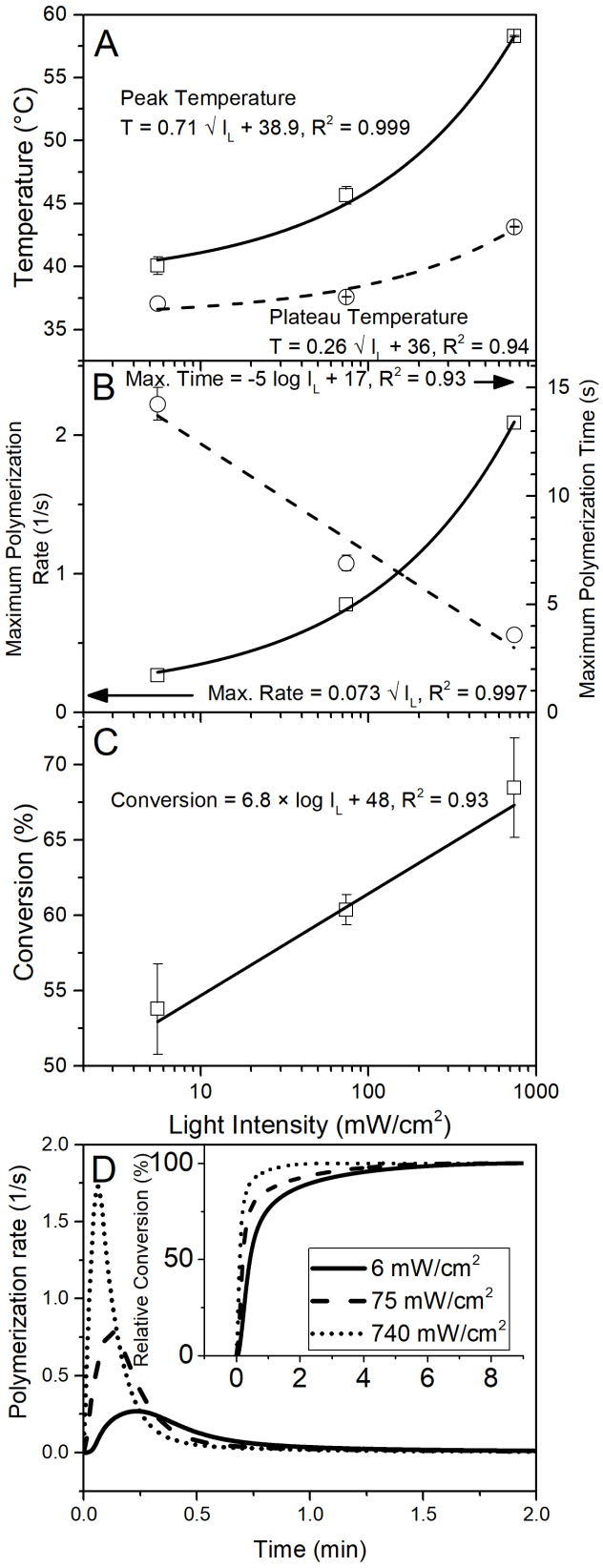

Fig. 3.5. The effect of light intensity on (A) temperature upon polymerization, (B) polymerization rate and the time to the peak rate, (C) apparent overall conversion, and (D) rate of polymerization and (inset) conversion kinetics, shown as a percentage of final conversion for each sample to better compare the curve shape at different light intensities.

The amount of photo-initiator added in the composite may have a similar effect as the light intensity on polymerization kinetics and overall conversion. Since numerous previous studies have examined the effect of changes in the type and concentrations of the initiators (*31-41*), their effects are not evaluated in this study.

3.3.5 Nitrogen Purge Time Variations

Finally, the oxygen inhibition that occurs at the interface with the atmosphere can also affect conversion measurements. Oxygen diffuses into the resin and interferes with polymerization by reacting with the propagating chains, effectively terminating the reaction. With common resins, these layers will be around 25 μm thickness (*42*). Most measurements should not be affected by this layer since the inhibited layer volume accounts for less than 3% of the total sample volume (considering the sample size and layer thickness).

To evaluate this effect experimentally, air was flowed over the sample, and subsequently nitrogen gas purge time was varied, to reduce atmospheric oxygen concentration during polymerization, since most of the inhibition was shown to be due to active gas diffusion upon polymerization (*42*). No significant difference was observed at different nitrogen purge times for a 10 mg resin sample (Fig. 3.3B); the changes are small and within the error of the measurements. If there is a need to observe these differences by photo-calorimetry, smaller samples should lead to an increase in sensitivity, as a larger fraction of the resin would be inhibited. We conclude that oxygen inhibition had little effect on these measurements.

3.4 Conclusion

We have optimized of the parameters of pDSC for the reliable measurement of the degree of conversion and polymerization kinetics of dental resins. The protocol developed can also be applied in general to photo-polymerizations and other photo-reactions involving enthalpy changes that can be measured. The most reliable pDSC measurements were done using a post-cure isothermal baseline at 37 °C, close to the conditions during curing in the mouth in clinical situations. The optimal sample size was found to be 10 mg, which was the largest size without signal distortion. The light intensity should be set close to the clinical

level, since all the light intensities tested yielded consistent results with different conversion values. Finally, for a 10 mg sample, the nitrogen purge time had no effect on the conversion measurements. This systematic study optimized the use of pDSC for conversion measurements for dental resin composite applications, allowing the direct application of this method in further studies to examine the effects of size and loading of micro- and nano-particles of inorganic fillers. The standardized use of this method will allow comparisons between different studies that may otherwise have been incomparable due to differences in the measurement parameters used.

3.5 Supplementary Information

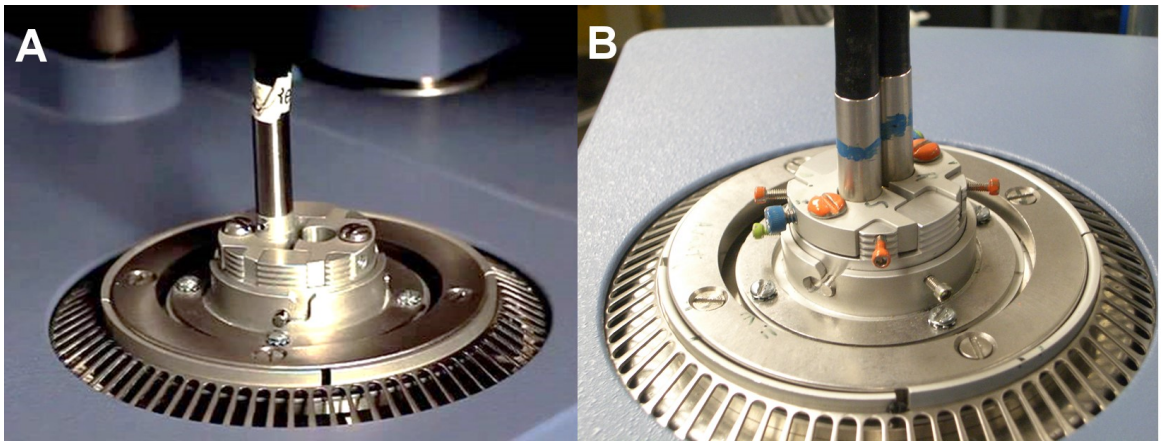

Figure S 3.1 - Photocalorimetry accessory modifications. A) – Original accessory as purchased. B) – Modified accessory: 4 set screws (small, orange) were added to stabilize the light guide brackets, 2 for each one; the Grub screws holding the light guides to the brackets were changed for normal screws (blue); 3 screws were added to hold the entire light guide assembly to the base. The light guides themselves were also modified to allow lower positioning.

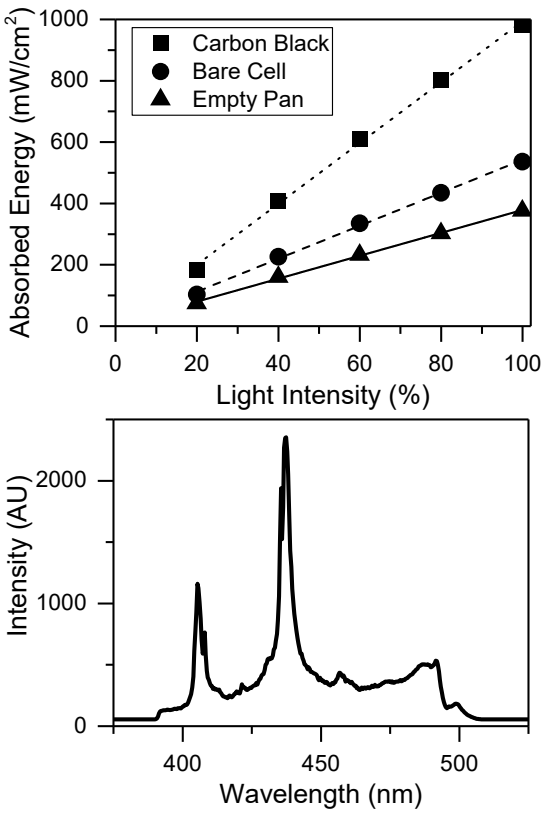

Figure S 3.2 - A) Heat flow measured from light irradiation only. Carbon black values were obtained by solvent evaporation of 5 mg of carbon black suspended in acetone, bare cell measurements were from the photocalorimetry cell with nothing more, empty pan measurements were performed with an empty aluminium DSC pan. B) Emission spectrum of the lamp used with 400-500 nm filter.

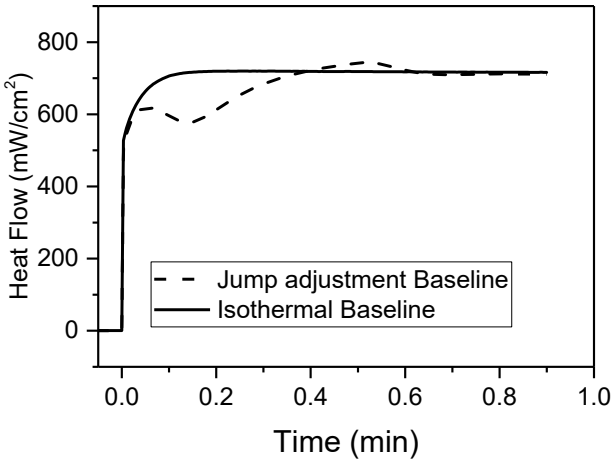

Figure S 3.3 - Exotherms measured with different measurement procedures. (dashed) The exotherm using a 'jump' step showed significant distortion, undershooting and subsequently overshooting the more stable (solid) 'isothermal' measurement.

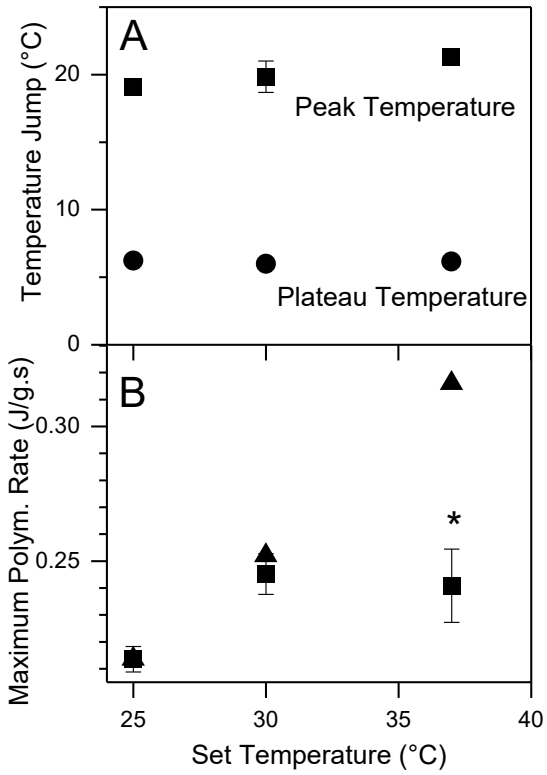

Figure S 3.4 - A) Temperature jump upon polymerization at different set temperatures. B) Variations of maximum rate as a function of the set temperature as measured (squares). While a rise occurred from 25-30 °C, no change occurred from 30-37 °C, contrary to the behaviour predicted by the Arrhenius equation (triangles). * indicates a statistically significant difference.

3.5.1 Calculations

3.5.1a Calculations for the predicted change in reaction rate with temperature

According to Arrhenius equation:

$$k = A \cdot e^{\frac{-E_A}{RT}}$$

where k is the rate constant, E_A is the reaction activation energy ($J.mol^{-1}$), R is the gas constant 8.314 $J\ K^{-1}\ mol^{-1}$, and T is the absolute temperature, therefore:

$$\frac{k_2}{k_1} = e^{-\frac{E_A}{R}\left(\frac{1}{T_1}-\frac{1}{T_2}\right)}$$

E_A for this reaction can be approximated to 25.1×10^3 J.mol^{-1}, which is the value for methyl methacrylate (*18*). The calculated rate constant increase is 18% from 25 to 30 °C is, 25% from 30 to 37 °C, and 48% from 25 to 37 °C.

3.5.1b Absorbed light calculations for resin in DSC pans

Pan depth = 1.6 mm

Path length with reflection = 3.2 mm

Camphorquinone extinction coefficient: $\varepsilon_{468\ nm}$ = 46 cm^{-1}.L.mol^{-1} (*31*)

Camphorquinone concentration: 0.5 % = 3.5×10^{-3} mol.L^{-1}

According to the Beer-Lambert law:

$$A = \varepsilon \cdot c \cdot l$$

where ε is the extinction coefficient (L.mol^{-1}cm^{-1}), c is the concentration (mol.L^{-1}) and l is the path length (cm), therefore absorbance is 0.0515, transmittance is = 88.8% , and the fraction of light absorbed is 11.2%.

3.6 References

1. Leprince, J. G.; Palin, W. M.; Hadis, M. A.; Devaux, J.; Leloup, G., Progress in dimethacrylate-based dental composite technology and curing efficiency. *Dent Mater* **2013,** *29* (2), 139-156.
2. Ferracane, J. L., Resin-based composite performance: are there some things we can't predict? *Dent Mater* **2013,** *29* (1), 51-58.
3. Ferracane, J. L.; Greener, E. H., The effect of resin formulation on the degree of conversion and mechanical properties of dental restorative resins. *J Biomed Mater Res* **1986,** *20* (1), 121-131.
4. Li, J.; Li, H.; Fok, A. S.; Watts, D. C., Multiple correlations of material parameters of light-cured dental composites. *Dent Mater* **2009,** *25* (7), 829-836.
5. Ferracane, J. L.; Mitchem, J. C.; Condon, J. R.; Todd, R., Wear and marginal breakdown of composites with various degrees of cure. *J Dent Res* **1997,** *76* (8), 1508-1516.

6. Dewaele, M.; Truffier-Boutry, D.; Devaux, J.; Leloup, G., Volume contraction in photocured dental resins: the shrinkage-conversion relationship revisited. *Dent Mater* **2006,** *22* (4), 359-365.
7. Ferracane, J. L., Elution of leachable components from composites. *J Oral Rehabil* **1994,** *21* (4), 441-452.
8. Habib, E.; Wang, R.; Zhu, X. X., Monodisperse silica-filled composite restoratives mechanical and light transmission properties. *Dent Mater* **2017,** *33* (3), 280-287.
9. Antonucci, J. M.; Toth, E. E., Extent of Polymerization of Dental Resins by Differential Scanning Calorimetry. *J Dent Res* **1983,** *62* (2), 121-125.
10. Froes-Salgado, N. R.; Pfeifer, C. S.; Francci, C. E.; Kawano, Y., Influence of photoactivation protocol and light guide distance on conversion and microleakage of composite restorations. *Oper Dent* **2009,** *34* (4), 408-414.
11. Cadenaro, M.; Antoniolli, F.; Sauro, S.; Tay, F. R.; Di Lenarda, R.; Prati, C.; Biasotto, M.; Contardo, L.; Breschi, L., Degree of conversion and permeability of dental adhesives. *Eur J Oral Sci* **2005,** *113* (6), 525-530.
12. Photo-DSC 204 F1 Phoenix. https://www.netzsch-thermal-analysis.com/en/products-solutions/differential-scanning-calorimetry/photo-dsc-204-f1-phoenix/ (accessed 2017/05/16).
13. Hannig, M.; Bott, B., In-vitro pulp chamber temperature rise during composite resin polymerization with various light-curing sources. *Dent Mater* **1999,** *15* (4), 275-281.
14. Daronch, M.; Rueggeberg, F. A.; Hall, G.; De Goes, M. F., Effect of composite temperature on in vitro intrapulpal temperature rise. *Dent Mater* **2007,** *23* (10), 1283-1288.
15. Odian, G., Radical Chain Polymerization. In *Principles of Polymerization*, John Wiley & Sons, Inc.: 2004; pp 198-349.
16. Calheiros, F. C.; S. Costa Pfeifer, C.; Brandão, L. L.; Agra, C. M.; Ballester, R. Y., Flexural properties of resin composites: Influence of specimen dimensions and storage conditions. *Dent Mat* **2013,** *32* (2), 228-232.
17. Andrzejewska, E., Photopolymerization kinetics of multifunctional monomers. *Prog in Polym Sci* **2001,** *26* (4), 605-665.

18. Cook, W. D., Kinetics and properties of a photopolymerized dimethacrylate oligomer. *J Appl Polym Sci* **1991,** *42* (8), 2209-2222.
19. Riesen, R., Effect of Sample Mass on Tg Results. *TA Usercom* **1000,** *2*, 17.
20. Souza, E. J., Jr.; Borges, B. C.; Oliveira, D. C.; Brandt, W. C.; Hirata, R.; Silva, E. J.; Sinhoreti, M. A., Influence of the curing mode on the degree of conversion of a dual-cured self-adhesive resin luting cement beneath ceramic. *Acta Odontol Scand* **2013,** *71* (3-4), 444-448.
21. Watts, D. C.; Satterthwaite, J. D., Axial shrinkage-stress depends upon both C-factor and composite mass. *Dent Mater* **2008,** *24* (1), 1-8.
22. Bowman, C. N.; Kloxin, C. J., Toward an enhanced understanding and implementation of photopolymerization reactions. *AIChE Journal* **2008,** *54* (11), 2775-2795.
23. Wydra, J. W.; Cramer, N. B.; Stansbury, J. W.; Bowman, C. N., The reciprocity law concerning light dose relationships applied to BisGMA/TEGDMA photopolymers: theoretical analysis and experimental characterization. *Dent Mater* **2014,** *30* (6), 605-612.
24. Pfeifer, C. S.; Ferracane, J. L.; Sakaguchi, R. L.; Braga, R. R., Factors Affecting Photopolymerization Stress in Dental Composites. *J Dent Res* **2008,** *87* (11), 1043-1047.
25. Dewaele, M.; Asmussen, E.; Peutzfeldt, A.; Munksgaard, E. C.; Benetti, A. R.; Finne, G.; Leloup, G.; Devaux, J., Influence of curing protocol on selected properties of light-curing polymers: degree of conversion, volume contraction, elastic modulus, and glass transition temperature. *Dent Mater* **2009,** *25* (12), 1576-1584.
26. Abu-elenain, D. A.; Lewis, S. H.; Stansbury, J. W., Property evolution during vitrification of dimethacrylate photopolymer networks. *Dent Mater* **2013,** *29* (11), 1173-1181.
27. Leprince, J. G.; Palin, W. M.; Hadis, M. A.; Devaux, J.; Leloup, G., Progress in dimethacrylate-based dental composite technology and curing efficiency. *Dent. Mater.* **2013,** *29* (2), 139-56.
28. Lu, H.; Stansbury, J. W.; Nie, J.; Berchtold, K. A.; Bowman, C. N., Development of highly reactive mono-(meth)acrylates as reactive diluents for dimethacrylate-based dental resin systems. *Biomaterials* **2005,** *26* (12), 1329-1336.

29. Al Shaafi, M.; Maawadh, A.; Al Qahtani, M., Evaluation of light intensity output of QTH and LED curing devices in various governmental health institutions. *Oper Dent* **2011,** *36* (4), 356-361.

30. Lu, H.; Stansbury, J. W.; Bowman, C. N., Impact of Curing Protocol on Conversion and Shrinkage Stress. *J Dent Res* **2005,** *84* (9), 822-826.

31. Chen, Y. C.; Ferracane, J. L.; Prahl, S. A., Quantum yield of conversion of the photoinitiator camphorquinone. *Dent Mater* **2007,** *23* (6), 655-664.

32. Moszner, N.; Fischer, U. K.; Ganster, B.; Liska, R.; Rheinberger, V., Benzoyl germanium derivatives as novel visible light photoinitiators for dental materials. *Dent Mater* **2008,** *24* (7), 901-7.

33. Neshchadin, D.; Rosspeintner, A.; Griesser, M.; Lang, B.; Mosquera-Vazquez, S.; Vauthey, E.; Gorelik, V.; Liska, R.; Hametner, C.; Ganster, B.; Saf, R.; Moszner, N.; Gescheidt, G., Acylgermanes: photoinitiators and sources for Ge-centered radicals. insights into their reactivity. *J Am Chem Soc* **2013,** *135* (46), 17314-21.

34. Neumann, M. G.; Miranda, W. G., Jr.; Schmitt, C. C.; Rueggeberg, F. A.; Correa, I. C., Molar extinction coefficients and the photon absorption efficiency of dental photoinitiators and light curing units. *J Dent* **2005,** *33* (6), 525-32.

35. Neumann, M. G.; Schmitt, C. C.; Ferreira, G. C.; Correa, I. C., The initiating radical yields and the efficiency of polymerization for various dental photoinitiators excited by different light curing units. *Dent Mater* **2006,** *22* (6), 576-84.

36. Salgado, V. E.; Albuquerque, P. P.; Cavalcante, L. M.; Pfeifer, C. S.; Moraes, R. R.; Schneider, L. F., Influence of photoinitiator system and nanofiller size on the optical properties and cure efficiency of model composites. *Dent Mater* **2014,** *30* (10), e264-71.

37. Schneider, L. F.; Cavalcante, L. M.; Consani, S.; Ferracane, J. L., Effect of co-initiator ratio on the polymer properties of experimental resin composites formulated with camphorquinone and phenyl-propanedione. *Dent Mater* **2009,** *25* (3), 369-75.

38. Schneider, L. F.; Pfeifer, C. S.; Consani, S.; Prahl, S. A.; Ferracane, J. L., Influence of photoinitiator type on the rate of polymerization, degree of conversion, hardness and yellowing of dental resin composites. *Dent Mater* **2008,** *24* (9), 1169-77.

39. Schroeder, W. F.; Cook, W. D.; Vallo, C. I., Photopolymerization of N,N-dimethylaminobenzyl alcohol as amine co-initiator for light-cured dental resins. *Dent Mater* **2008,** *24* (5), 686-93.
40. Schroeder, W. F.; Vallo, C. I., Effect of different photoinitiator systems on conversion profiles of a model unfilled light-cured resin. *Dent Mater* **2007,** *23* (10), 1313-21.
41. Taira, M.; Urabe, H.; Hirose, T.; Wakasa, K.; Yamaki, M., Analysis of Photo-initiators in Visible-light-cured Dental Composite Resins. *J Dent Res* **1988,** *67* (1), 24-28.
42. Gauthier, M. A.; Stangel, I.; Ellis, T. H.; Zhu, X. X., Oxygen Inhibition in Dental Resins. *J Dent Res* **2005,** *84* (8), 725-729.

Chapter 4 - **Correlation of Resin Viscosity and Monomer Conversion to Filler Particle Size in Dental Composites**

Abstract

Objective. The viscosity of dental resin composites is important in their formulation and clinical use; it depends on the filler particle size and loading. We intend to study the viscosity and conversion of composites made of low dispersity spherical silica fillers.

Methods. Experimental dental resin composites were formulated using low dispersity spherical silica particles of graded sizes (75, 150, 500, 350, 500, 1000 nm) at several loading levels with resins based on Bis-GMA and UDMA. Their rheological properties and double bond conversion were measured with a rheometer and differential scanning calorimeter, respectively.

Results. The complex viscosity of the unpolymerized pastes can be fit to an extended Krieger-Dougherty equation that includes an adjustment factor to account for filler particle surface area. This relationship is also extended to estimate the degree of conversion, where the calculated or experimental viscosity is used to predict the resulting conversion.

Significance. The enhanced understanding of the relationship of filler size, composite viscosity, and monomer conversion will allow improved accuracy in the prediction of the properties of dental resin composite formulations to obtain ideal viscosity for their clinical use and a high degree of conversion.

---

*Submitted as a research article: Eric Habib, Ruili Wang, X. X. Zhu. *Dent. Mat.*, Oct. 2017.

4.1 Introduction

Dental resin composites have experienced a significant rise in usage since their advent in the 1960s. These composites are made from a photopolymerizable resin matrix (including initiator, co-initiator and inhibitors) mixed with surface-modified inorganic fillers. Most of the organic resin monomers in these products are based on the commercially available bisphenol A glycerolate dimethacrylate (BisGMA), diurethane dimethacrylate (UDMA), and triethylene glycol dimethacrylate (TEGDMA). The inorganic fillers used in commercial dental restoratives are generally silicates, most commonly silica or alkaline glasses (*1*). Many companies produce composites, and a large body of literature exists studying their mechanical properties and conversion values (*2-3*). The rheological properties and ease of polymerization are significant factors affecting the clinical use of these materials, but very few studies have systematically examined the effect of filler particles on composite viscosity, and its relationship to the dental monomer conversion.

The viscosity of these materials is important for commercial formulations since it determines their ease of use for repairing caries, which is a weak point of resin composite materials (*4*). The viscosity is also well known to affect the degree of polymerization and reaction kinetics in free radical polymerizations due to the reduced chain mobility and lower termination rate at higher viscosities (*5*). The effect of resin monomer composition on viscosity has been explored exhaustively (*6-7*). While the viscosity if suspensions at low loading is described by the Krieger-Dougherty model (*8*), viscosity increases due to the addition of filler particles in dental composites is not as well characterized, particularly for the high loading levels where particle-particle interactions become more important. To the best of our knowledge, no previous work has explored narrow dispersity fillers of different sizes with the same morphology to clearly define this thickening effect.

The degree of conversion in dental composites is related to their mechanical properties such as diametral tensile strength and flexural strength (*9-10*). Most of the work so far has examined the conversion of resin matrix alone (*7, 11*), and the effect of different monomer compositions on the conversion and viscosity. Turssi et al (*12*) found that filler size and morphology did not affect conversion except when the size corresponded to the photopolymerization wavelength, where lower conversion values were observed. Otherwise, the filler loading has been shown to decrease polymerization shrinkage and increase

mechanical properties after polymerization (*13-14*). Others have examined the degree of conversion of different commercial formulations for which the complete composition was not known (*15-16*), providing limited assistance in establishing fundamental rules for composite design.

The detailed formulations of commercial dental composites remain proprietary to the manufacturers, therefore the full effect of filler particles on composite properties before and after polymerization has not yet been established under controlled conditions. There remains a lack of fundamental understanding of the factors influencing the mechanical, chemical, and optical properties of the composites. We intend to establish a relationship between the size of the filler particles and the viscosity of dental composites, and in turn, the effect on the monomer conversion during photopolymerization.

4.2 Experimental

4.2.1 Materials

Tetraethyl orthosilicate (TEOS) was purchased from Alfa Aesar (Ward Hill, MA, USA). Anhydrous ethanol and ammonium hydroxide (35%) were purchased from Fisher Scientific (Waltham, MA, USA), 3-methacryloyltrimethoxypropylsilane (3-MPS), BisGMA, UDMA, and TEGDMA were purchased from VWR (Mont-Royal, QC, Canada); camphorquinone (CQ) and ethyldimethylaminobenzoate (EDMAB) were purchased from Sigma-Aldrich (Oakville, ON, Canada). All reagents were used without further purification. Room temperature is defined as 23 °C in this work.

4.2.2 Methods

4.2.2a Synthesis of monodisperse silica particles and characterisation

The silica particles with sizes of 75, 150, 350, 500, 1000 nm were synthesized by using the Stöber method (*17*) as described in our previous work (*18*). The sizes indicated in figures and tables refer to the particle diameters measured by laser diffraction (Horiba LA960, Japan), and scanning electron microscopy (JEOL FE-SEM, JSM-7400F, Japan) for the specific batches of particles that were used and not the nominal sizes.

Thermogravimetric analysis (TGA 2950 from TA Instruments, DE, USA) was used to measure the extent of silane surface modification. The temperature was increased to 120 °C

for 10 minutes to eliminate adsorbed water, and then a 20 °C.min^{-1} ramp until 800°C was then used to obtain the extent of silane modification.

The surface area of the particles was calculated from first principles using sphere area and volume equations, and confirmed with previous BET measurements (*19*), adjusted for the particle size. The equation is derived from the ratio of surface area in relation to volume and density:

$$S = \frac{A_{sphere}\Phi}{V_{sphere}\rho} = \frac{\pi d^2 \Phi}{\frac{1}{6}\pi d^3 \rho} = \frac{6\Phi}{d\rho} \tag{4.1}$$

where S is the specific surface area (m^2.g^{-1}) of the fillers, A_{sphere} and V_{sphere} are the surface area and volume of a sphere, Φ is the mass fraction of the fillers, ρ is the density of fused silica (2.2×10^6 g.m^{-3} (*20*)), and d is the particle diameter (m).

4.2.2b Resin and Composite Preparation

70:30 weight ratio BisGMA-TEGDMA (7B3T) and UDMA-TEGDMA (7U3T) resins were each blended by first dissolving 0.5 wt% CQ and 0.5 wt% EDMAB in TEGDMA (as a fraction of total resin weight) at room temperature, then adding the main monomer (either BisGMA or UDMA), mixing manually and then with a magnetic stirrer at 35°C (approx. 30 min) to obtain a homogeneous mixture. The resulting resin was then mixed with the indicated amount of filler particles (30, 50, 60, or 70 wt%) by spatula, and then homogenized using a three-roll mill (Exact 50i TRM, Norderstedt, Germany). Only the composites used for conversion measurements contained initiator (CQ) and co-initiator (EDMAB).

4.2.2c Rheological Studies

The rheology measurements were performed using an AR-2000 shear rheometer (TA Instruments) with 20 mm parallel steel disk and plate geometry with a gap size of 200 μm for 60 wt% loading and 1000 μm for 70 wt% loading. The composite pastes were put in place and trimmed using a spatula. The measurements were performed with a dynamic oscillatory shear test, at a constant frequency of 1 Hz, and time series at constant stress (10 Pa) where thixotropic behavior was observed. Each measurement was repeated three times, with a recovery period between each run to allow full recovery (<1 %/h change). The complex viscosity defines the internal friction of a material under oscillatory shearing stresses; the

values shown are the magnitude of the complex viscosity vector (|η*|), hereby referred to simply as 'complex viscosity':

$$\eta' = \frac{\sigma}{\dot{\gamma}} \cos\theta \tag{4.2}$$

$$\eta'' = \frac{\sigma}{\dot{\gamma}} \sin\theta \tag{4.3}$$

$$\eta^* = \eta' + i\eta'' \tag{4.4}$$

$$|\eta^*| = \sqrt{(\eta')^2 + (\eta'')^2} \tag{4.5}$$

where σ is the oscillatory stress, $\dot{\gamma}$ is the shear rate, and θ is the phase angle. The values were those obtained at minimum stable measured stress values (10-50 Pa). The temperature was regulated using an attached water recirculator with a thermoelectric cooler set to 23.0 or 32.5 °C.

4.2.2d Determination of Monomer Conversion and Polymerization Rates

The extent of monomer polymerization was evaluated by photocalorimetry (pDSC), on a TA Q2000 differential scanning calorimeter equipped with a modified photocalorimetry accessory (*21*), with an Omnicure S2000 light source with a 400-500 nm filter, under a nitrogen purge flow. The light intensity was adjusted to 885 mW/cm^2 using a cell containing carbon black. The method began with equilibration at 37 °C, and a one-minute isothermal segment to establish a baseline. The lamp was then turned on for three minutes, such that the temperature was kept constant during the exposure, and a final one minute isothermal segment for an end baseline. A second run was then immediately performed with the polymerized sample to obtain a flat baseline. The conversion was calculated with the following equation:

$$Conv = \frac{\Delta H}{n_{MA} \cdot \Delta H_{MA}} \tag{4.6}$$

$$n_{MA} = \frac{m_{filler} f_{silane}}{M_{silane}} + \sum \frac{2m_{mono}}{M_{mono}} \tag{4.7}$$

where *Conv* is the conversion, ΔH and ΔH_{MA} are the area under the curve measured by photocalorimetry (J/g) and the standard methacrylate polymerization enthalpy (56,902.4 J/mol) (*22*), respectively, n_{MA} is the number of moles per gram of methacrylate double bonds in the composite sample (mol/g), m_{filler} and m_{mono} are the masses of filler and monomer, respectively, f_{silane} is the mass fraction of silane (as measured by TGA), M_{silane} and M_{mono} are the molecular weights of 3-MPS (127.16 g/mol), and of the monomer, respectively. The sum is taken for all the resin monomers included in the blend.

The maximum rates were measured as the point with the largest heat flow of the polymerization exotherm, and converted to molar values with **Equation 4.6**; the gel point was the time at the inflection point, taken as the maximum of the derivative of heat flow with respect to time.

4.2.2e Statistical Analyses

Statistical significance was determined with pairwise comparisons using student's t-test with a 95% confidence interval.

4.3 Results and Discussion

Spherical silica particles of different sizes were synthesized by the use of the Stöber method. Their sizes were measured to be 70 to 980 nm by laser diffraction and scanning electron microscopy, and had dispersity values of 1.02 or less. Composites were then prepared with these particles and used to measure the pre-polymerization viscosity at different shear stress values and temperatures, and then to measure their polymerization kinetics and monomer conversions through the previously established photocalorimetry method (*21*).

4.3.1 Viscosity

4.3.1a Unfilled Resins

The viscosity of filled composites is important since it affects the ease of use in dental clinics, and the overall performance of the material, mainly due to the maximum filler loading. The complex viscosity of a material represents its resistance to flow under oscillatory shearing conditions and is obtained from both elastic and loss moduli (**Equations 4.2-4.5**). This value was measured for the monomers separately and for the resin blends (**Table 4.3**). Our results are consistent with previous studies, with Bis-GMA reportedly

having a viscosity of 100-1000 Pa.s, UDMA having a viscosity of 10-50 Pa.s, and TEGDMA having a viscosity just below 0.1 Pa.s (*6*). UDMA also displayed limited shear thinning (**Figure 4.1A**). When blended with TEGDMA in a 7:3 ratio, both BisGMA and UDMA blends have similar viscosities, with the UDMA blend being slightly more fluid; they had similar values to previously reported results: 0.76 Pa.s for 2:1 Bis-GMA:TEGDMA (*7*), and 0.27 Pa.s for 6U4T (*23*).

Table 4.3 - Viscosity of pure monomers and blends

	Complex Viscosity (Pa.s)	
Monomer(s)	**25°C**	**37°C**
Bis-GMA	206.50	22.43
UDMA	12.58	6.47
TEGDMA	0.10	0.10
7B3T	0.83	0.32
7U3T	0.29	0.18

4.3.1b Viscosity of Composites with Fillers

Studies in the literature are rare on the rheology of filled composites. Results on commercial composites were sometimes contradictory. For example, one study found that there was a correlation between filler loading and viscosity (*3*), and another study did not (*24*), likely due to the lack of complete composition information for these commercial formulations as well as the complex nature of the formulations. Previous rheology work with well-defined experimental composites with variations in filler size qualitatively showed exponential increases in viscosity with loading; and that this increase was more pronounced for smaller particles (*25-27*) without further quantitative descriptions.

As expected, the composites exhibited varying shear thinning, thickening, and thixotropic behaviours (**Figure 4.1**). The change in viscosity as well as the recovery time varied according to filler size and loading, such that the relaxation time was related to the suspension viscosity. This behaviour is complex, and requires further studies to define more clearly. For this reason, the values indicated were taken after the samples were allowed to relax (**Figure 4.1B**), resulting in higher viscosity values. Due to the shearing during syringe

extrusion and short application time, the clinically-observed viscosity may be lower than that reported here. More generally, thinning and thickening behaviours are thought to be caused by the breakup of particle clusters as the shear stress becomes greater than the capillary and attractive forces that hold them together (*8, 25, 28-29*).

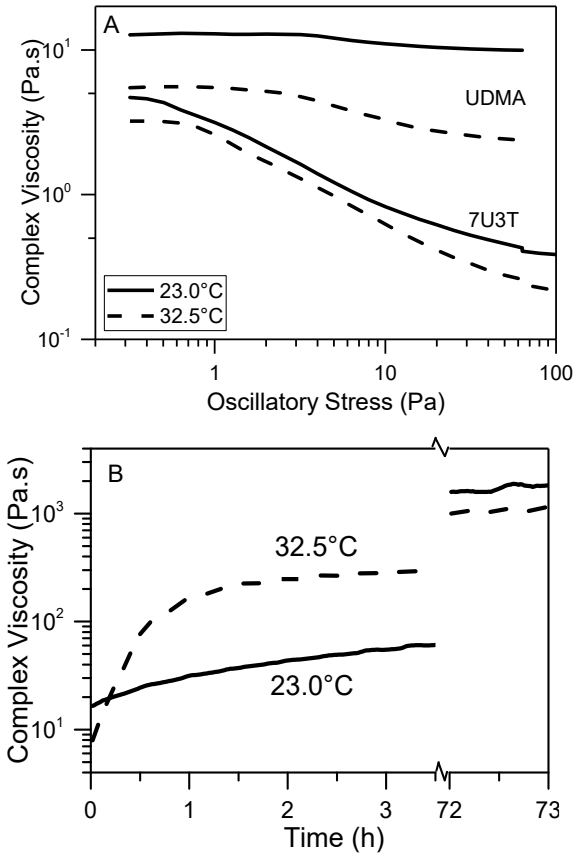

Figure 4.1 – (A) Variation of complex viscosity as a function of oscillatory stress, showing the shear thinning behavior of unfilled UDMA and 7U3T resins, and (B) variation of complex viscosity over time for 7B3T resin loaded with 60 wt% 185 nm filler particles. At constant low stress, the composites relax back to their maximum viscosity. Smaller filler particles and lower temperatures exhibited longer relaxation times.

Rheology tests with composites filled with spherical silica particles of graded sizes show that the complex viscosity of the materials at minimal stress has a strong dependence on the filler size (**Figure 4.2**). This effect has been qualitatively (but not quantitatively) described previously (*25-26, 30-31*). The 75 nm particle-filled composites at 60 wt% loading

had viscosity values of 31,000 to 44,000 Pa.s, larger filler sizes had exponentially lower viscosity values, following the filler size. The values obtained for the 70 wt% loaded composites were 102,000 Pa.s. for the 360 nm fillers, which was higher than those of the 60 wt% composites with 75 nm particles; again, an exponential decrease was observed for the larger particles. Therefore, both loading and surface area had a significant effect on composite viscosity.

4.3.1c Extended Krieger-Dougherty Model

For suspensions of hard spheres, the Krieger-Dougherty (KD) model relates the viscosity of suspensions to their loading and 'intrinsic viscosity', a variable related to a particle's contribution to solution viscosity from its shape (*32-33*). The KD model is derived from first principles, examining the mechanics of particle-particle interactions and clustering under shearing stresses, with particle-cluster equilibria (*8, 34*):

$$\frac{\eta}{\eta_c} = \left(1 - \frac{\varphi}{\varphi_M}\right)^{-[\eta]\varphi_M} \tag{4.8}$$

where η and η_c are the viscosities of the composite and the continuous (resin) phase, respectively; φ and φ_M are the actual and maximum volume loading fractions, respectively, and $[\eta]$ is the intrinsic viscosity (2.5 for spherical particles, and larger values for higher aspect ratios (*8, 33-35*)). This model considers the viscosity to be independent of particle size, and to only be dependent on the filler loading and the continuous phase viscosity. As stated above, studies with dental composites have shown, however, that the viscosity of these materials does indeed have a dependence on particle size. The viscosity of composites with smaller fillers was shown to be higher, regardless of their morphology (*25-26, 30-31*).

Modeling the above data with the KD equation with the known loading, maximum loading (72 wt% (*18*)), and resin viscosity as constants, yields constant viscosity values (dotted lines in **Figure 4.2**), but back calculations show that the exponential factor may be adjusted to obtain more accurate predictions. This adjustment factor is found to be linearly dependent on the filler surface area, most likely due to the influence of surface-resin interactions in the macroscopic viscosity. Thus, we have added a correction factor to the KD model leading to an extended KD model:

$$\frac{\eta}{\eta_c} = \left(1 - \frac{\varphi}{\varphi_M}\right)^{-[\eta]\cdot\varphi_M + C\cdot\varphi\cdot S} \tag{4.9}$$

where C is a constant (g.m^{-2}), specific for a given resin-filler system, and S is the specific surface area (m^2.g^{-1}) of the filler particles as defined in **Equation 4.1**. The value of C may depend on the interactions between the continuous phase and the fillers surface, such that stronger interactions would result in larger values, and consequently larger viscosity differences with larger filler surface area. For the composites tested, a global fit using measurements at both temperatures (23.0 and 32.5°C) and two loading levels (60 and 70 wt%) resulted in a general C value of 0.55 g.m^{-2} for the 7B3T resin and 3-MPS surface functionalization.

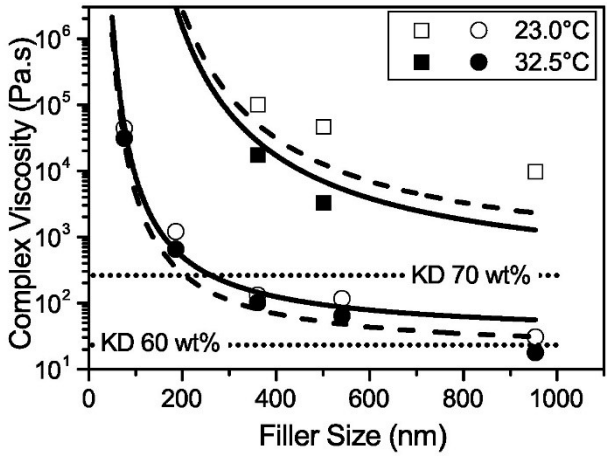

Figure 4.2 – Variation of complex viscosity with filler particle size for 7B3T-based composites at 60 wt% filler loading (43 vol%, circles) and 70 wt% (54 vol%, squares) and their extended KD equation fitting (dashed lines 32.5°C, solid lines 23°C). The fits yield C values of 0.55 for both temperatures, with the main difference being the continuous phase viscosity (fit to 2.3 and 4.1 Pa.s. for 23 and 32.5°C, respectively). The standard KD equation with the same parameters predicts equal viscosity for all filler sizes (KD, dotted lines).

The extended KD model developed here yielded accurate estimates for both loading values tested. Non-linear regressions of the viscosity data also obtained a maximum filler loading value of 72 wt%, confirming the previously measured value (*18*). Using the C values obtained from the fits, the extended model now allows more precise calculations than the standard KD model, even when approaching the situation of maximum loading.

4.3.1d Effect of Temperature on Viscosity

The effect of temperature on the viscosity of the composites is described by the Arrhenius equation (*36-38*), and has already been observed with some commercial composites (*3*):

$$\eta = A \cdot e^{-\frac{E_A}{RT}} \tag{4.10}$$

where η is the liquid viscosity, A is a constant, E_A is the activations energy, R is the gas constant (8.314 $JK^{-1}mol^{-1}$), and T is the absolute temperature. **Figure 4.3** shows that the composites exhibit thinning with increasing temperature. Although there are differences, the changes in A and E_A values in this temperature range are not statistically significant. Therefore, no clear conclusion can be drawn regarding the effect of temperature.

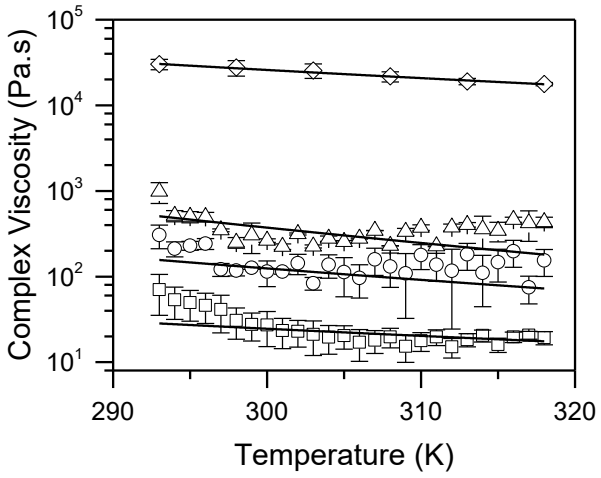

Figure 4.3 –The variation of complex viscosity with temperature for dental composites (7B3T, 60 wt% loading) with different filler sizes (diamonds, 75 nm; triangles, 150 nm; circles, 500 nm; squares, 1000 nm). There was no clear trend for different filler particles.

Despite the large difference in composite paste viscosity, previous work has shown that at identical loading, particle sizehas no effect on the mechanical properties of the composites after polymerization (*2, 14, 18*). In combination with the present work, this reinforces the conventional wisdom that larger particles produce better composites, not because of their superior mechanical performance at identical loading, but due to superior user-friendliness of lower viscosity pastes, particularly with hybrid fillers (*19*).

4.3.2 Polymerization Kinetics

In free radical polymerizations without added fillers, increasing viscosity during a polymerization slows polymer chain movement, lowers the termination rate, and increases the rate of the polymerization; this is known as the gel effect or Trommsdorf effect (*5*). This phenomenon is amplified in the case of bulk polymerizations where no solvent is present to allow chain mobility. The implication is that, for a given system, higher viscosity monomers polymerize faster, generally leading to an earlier gel point, and lower overall conversion (partially explaining higher conversion values for TEGDMA resins). Dental resin composites are heterogeneous systems where the viscosity increases are due to surface interactions with a solid phase in addition to monomer viscosity. Therefore, it is not known if the changes in polymerization kinetics due to monomer viscosity observed in solution polymerizations extend to viscosity increases caused by filler particles in a heterogeneous mixture.

The maximum polymerization rates of the monomers were measured with pDSC from the maximum value of the polymerization exotherm. The rate was adversely affected by the resin viscosity, such that higher viscosity (Table 4.1) led to slower kinetics (**Figure 4.4A**). TEGDMA shows a two-step rate change, where the beginning of the exotherm appears as a typical solution polymerization, but auto-acceleration eventually takes over, leading to a second, higher maximum rate (**Figure 4.5**). For the blended resins, 7B3T had a lower polymerization rate than 7U3T (**Figure 4.4A**), which is consistent with the viscosity trend of the individual monomers.

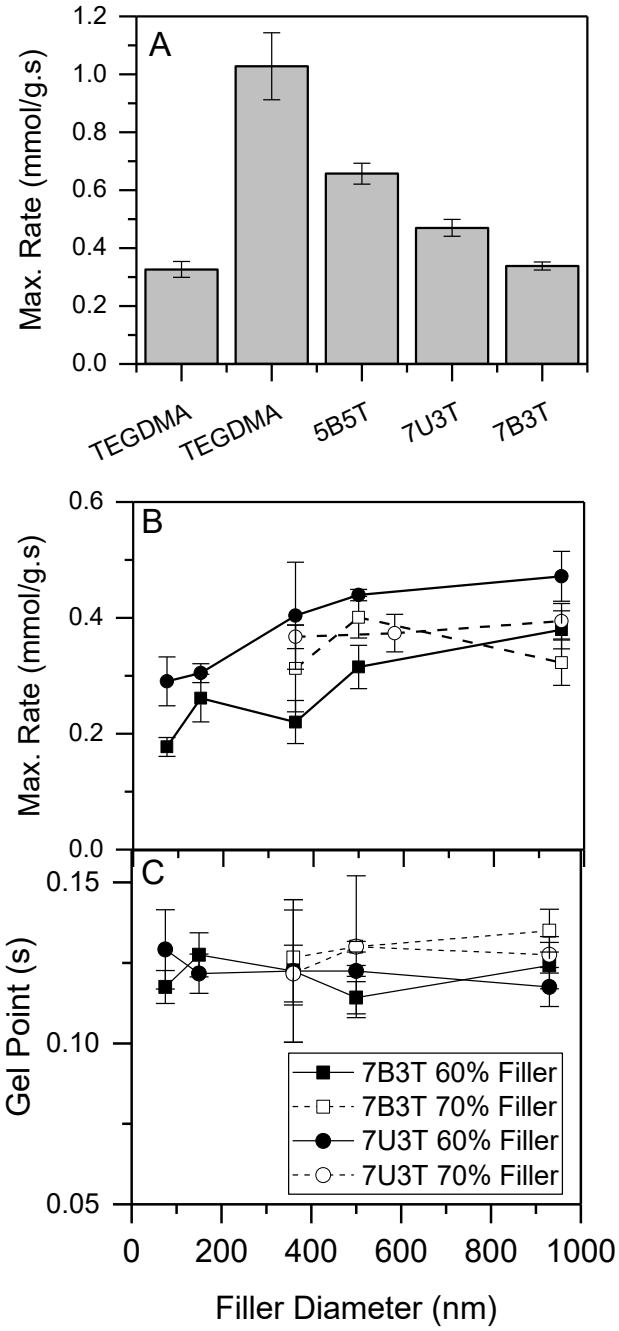

Figure 4.4 - Maximum polymerization rate measured by pDSC for (A) unfilled resins with increasing viscosity from left to right, and (B) for composites-loaded 60 and 70 wt% fillers of different sizes, and (C) the gel point for the same composites.

The polymerization kinetics of the composites were expected to exhibit an effect similar to auto-acceleration due to the viscosity increase caused by the filler particles. However, the pDSC polymerization rate measurements showed that the opposite occurred, where the smaller particle-filled composites with higher viscosity resulted in lower polymerization rates (**Figure 4.4B**). This is more akin to the effect observed with the monomer viscosity, and

suggests that the auto-acceleration is not a factor in the polymerization of these heterogeneous composite systems. Despite an almost two-fold rate increase between the smallest and largest particles, however, the measured gel point was not significantly changed (**Figure 4.4C**). Therefore, the viscosity increase due to filler slows the polymerization rate, but the gel point is reached simultaneously for all composites, regardless of their viscosity.

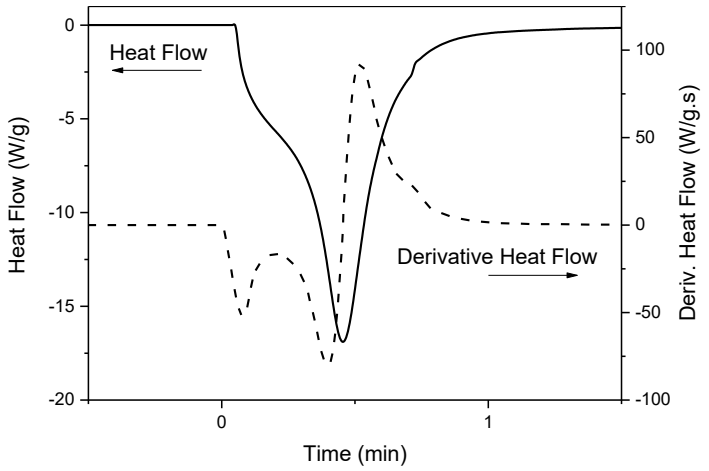

Figure 4.5 - Polymerization exotherm for TEGDMA at 37°C. A two-peak polymerization shows the typical slowing first, then autoacceleration due to the gel effect.

4.3.3 Monomer Conversion

The polymerization conversion was evaluated with pDSC to assess the effect of paste viscosity on extent of monomer conversion. Double bond conversion has been investigated quite thoroughly in the past for different resin matrices (*7, 11, 13*). The values obtained in this study (**Figure 4.6A**) agree with previous results for the commonly used resin matrices: The value obtained for TEGDMA was 88.5±2.6% compared to 83.6±3.1% previously (*39*), 77.3±1.7% for 7U3T is within error of 79±1% (*23*), as is the value of 72.6±0.5% for 7B3T compared to 72±1% (*23*). **Figure 4.6A** shows that the more liquid resins resulted in higher conversion values.

The double bond conversion of the filled composites showed a significant variation with the size of the filler used, as well as the filler loading (**Figure 4.6B-D**). The conversion values obtained showed a linear trend with respect to the log of viscosity:

$$Conv = Conv_0 - B\log|\eta^*| \tag{4.11}$$

where *Conv* and $Conv_0$ are the conversion for the final composite material and for resin alone, respectively, B is an empirical 'resin constant', and $|\eta^*|$ is the complex viscosity (**Equation 4.5**), either calculated with **Equation 4.9** or measured. This empirical equation allows the conversion to be fit either from the measured viscosity, or from the surface area of the particles, though higher loading tends to yield less accurate results (**Figure 4.6D**). The two resins tested have similar B constants for the conversion ($B = 6.9 \pm 0.5$), but at 70 wt% filler loading, the B constant has a higher value ($B = 11.7 \pm 0.8$) for both resins, indicating deviations near maximum loading. These errors at higher loading are further amplified due to the conversion value calculation (**Equation 4.7**) that uses the measured amount of silane modification, where multilayers can skew the results since only the outermost layer is available for polymerization. All samples in **Figure 4.6D** show a sharp decrease in the conversion at higher loading. The extended KD model allows a more accurate calculation of the conversion of the composites at all the loading levels tested.

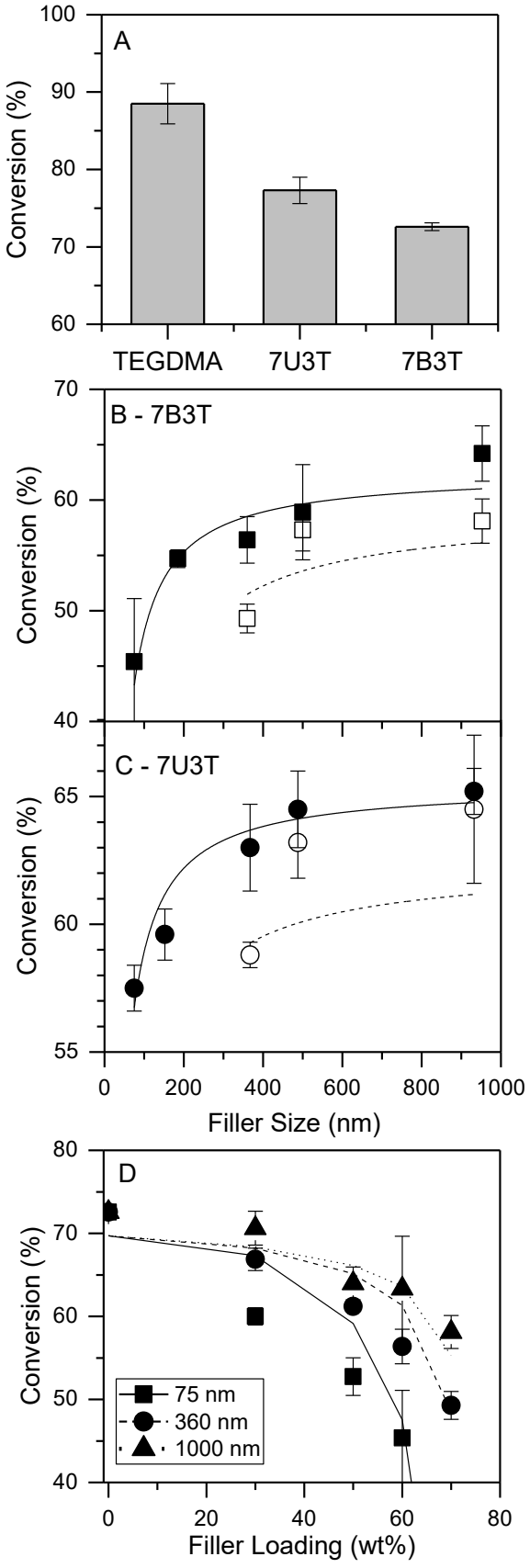

Figure 4.6 - Variation of double bond conversion for (A) unfilled resins, and according to filler size for (B) 7B3T-based composites, and (C) 7U3T-based composites, and (D) 7B3T composites at different filler loading levels. All composites yield a *B* value of 6.7.

Photopolymerizations at high light intensity and high initiation rates are known to form localized nanogel particles before complete crosslinking, which is thought to be the reason for higher conversion values with higher light intensities (*6, 21, 40*). We hypothesize that composites filled with smaller particles have lower polymerization rates and conversion values because of their smaller interparticle spacing, which limits the size of the nanogel particles (**Figure 4.4.7**). This constriction leads to a lower local monomer concentration, resulting in a lower polymerization rate and conversion. Since the propagation reaction occurs very rapidly, the observed gel point remains the same.

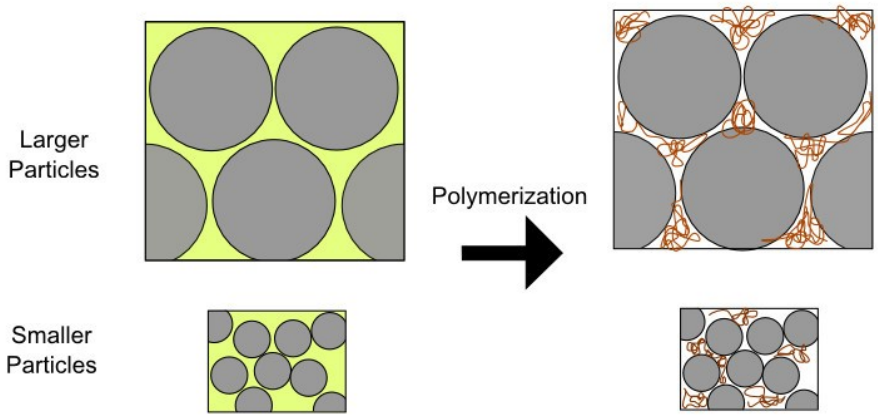

Figure 4.4.7 – Model for nanogel formation during composite polymerization. The larger gaps between the larger particles allow larger nanogel particles to form, whereas the smaller particles may constrict the growth of the nanogels, lowering the maximum polymerization rate and conversion.

The shrinkage stress data previously obtained by Satterthwaite et al (*41*) can be re-examined by the use of the equations developed here, considering the composition of these composites. The loading and size of their fillers, and the C value found here were used to establish a linear relationship between their measured shrinkage stress and the predicted conversion of those composites (**Figure 4.8**). Though further studies would be necessary to confirm this relationship, this suggests that filler size, composite viscosity, conversion, and shrinkage stress are all related.

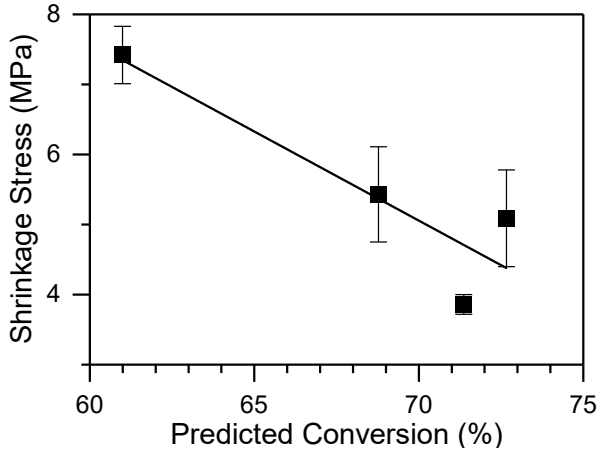

Figure 4.8 - The shrinkage stress measured by Satterthwaite et al (*41*) is linearly correlated to the conversion predicted by equation 4.9 and 4.11 extended KD ($R^2 = 0.811$). While there is a correlation between shrinkage stress and particle size, the change is mainly due to changes in conversion.

4.4 Conclusions

This work demonstrates that the viscosity of the composites and their double bond conversion can be estimated or even predicted, knowing the surface area of the filler particles used in the formulation. We have extended the KD model to allow accurate calculations of both viscosity and conversion with variations of filler loading, size, and resin matrix. This extended KD equation allows the optimization of composite properties and provides precise guidelines for the composition of the dental composites to obtain the desired characteristics. Moreover, the kinetics of polymerization are slowed with higher viscosity resins and composites. Coupled with our previous study examining the mechanical properties of the cured composites (*18*), the results of this work will allow users to optimize the viscosity properties of the composite pastes, as well as the mechanical properties of the resulting cured materials. Further studies may examine the validity of this relationship for irregular and multimodal fillers.

4.5 References

1. Habib, E.; Wang, R.; Wang, Y.; Zhu, M.; Zhu, X. X., Inorganic Fillers for Dental Resin Composites: Present and Future. *ACS Biomater Sci Eng* **2016,** *2* (1), 1-11.

2. Leprince, J.; Palin, W. M.; Mullier, T.; Devaux, J.; Vreven, J.; Leloup, G., Investigating filler morphology and mechanical properties of new low-shrinkage resin composite types. *J Oral Rehabil* **2010,** *37* (5), 364-376.
3. Al-Ahdal, K.; Silikas, N.; Watts, D. C., Rheological properties of resin composites according to variations in composition and temperature. *Dent Mater* **2014,** *30* (5), 517-524.
4. Seemann, R.; Flury, S.; Pfefferkorn, F.; Lussi, A.; Noack, M. J., Restorative dentistry and restorative materials over the next 20 years: a Delphi survey. *Dent Mater* **2014,** *30* (4), 442-448.
5. Odian, G., Radical Chain Polymerization. In *Principles of Polymerization*, John Wiley & Sons, Inc.: 2004; pp 198-349.
6. Stansbury, J. W., Dimethacrylate network formation and polymer property evolution as determined by the selection of monomers and curing conditions. *Dent Mater* **2012,** *28* (1), 13-22.
7. Gonçalves, F.; Kawano, Y.; Pfeifer, C.; Stansbury, J. W.; Braga, R. R., Influence of BisGMA, TEGDMA, and BisEMA content on viscosity, conversion, and flexural strength of experimental resins and composites. *Eur J Oral Sci* **2009,** *117*, 442-446.
8. Krieger, I. M.; Dougherty, T. J., A Mechanism for Non‐Newtonian Flow in Suspensions of Rigid Spheres. *Trans Soc Rheol* **1959,** *3* (1), 137-152.
9. Ferracane, J. L.; Greener, E. H., The effect of resin formulation on the degree of conversion and mechanical properties of dental restorative resins. *J Biomed Mater Res* **1986,** *20* (1), 121-131.
10. Ferracane, J. L., Resin-based composite performance: are there some things we can't predict? *Dent Mater* **2013,** *29* (1), 51-58.
11. Petrovic, L. M.; Zorica, D. M.; Stojanac, I.; Krstonosic, V. S.; Hadnadjev, M. S.; Janev, M. B.; Premovic, M. T.; Atanackovic, T. M., Viscoelastic properties of uncured resin composites: Dynamic oscillatory shear test and fractional derivative model. *Dent Mater* **2015,** *31* (8), 1003-1009.
12. Turssi, C. P.; Ferracane, J. L.; Vogel, K., Filler features and their effects on wear and degree of conversion of particulate dental resin composites. *Biomaterials* **2005,** *26* (24), 4932-4937.

13. Goncalves, F.; Azevedo, C. L.; Ferracane, J. L.; Braga, R. R., BisGMA/TEGDMA ratio and filler content effects on shrinkage stress. *Dent Mater* **2011,** *27* (6), 520-526.
14. Masouras, K.; Silikas, N.; Watts, D. C., Correlation of filler content and elastic properties of resin-composites. *Dent Mater* **2008,** *24* (7), 932-939.
15. Galvão, M. R.; Caldas, S. G. F. R.; Bagnato, V. S.; Rastelli, A. N. d. S.; Andrade, M. F. d., Evaluation of degree of conversion and hardness of dental composites photoactivated with different light guide tips. *Eur J Dent* **2013,** *7*, 86-93.
16. Zorzin, J.; Maier, E.; Harre, S.; Fey, T.; Belli, R.; Lohbauer, U.; Petschelt, A.; Taschner, M., Bulk-fill resin composites: polymerization properties and extended light curing. *Dent Mater* **2015,** *31* (3), 293-301.
17. Stöber, E.; Fink, A., Controlled Growth of Monodisperse Silica Spheres in the Micron Range. *J Coll Int Sci* **1968,** (26), 62-9.
18. Habib, E.; Wang, R.; Zhu, X. X., Monodisperse silica-filled composite restoratives mechanical and light transmission properties. *Dent Mater* **2017,** *33* (3), 280-287.
19. Wang, R.; Habib, E.; Zhu, X. X., Synthesis of wrinkled mesoporous silica and its reinforcing effect for dental resin composites. *Dent Mat* **2017**.
20. De Jong, B. H. W. S.; Beerkens, R. G. C.; van Nijnatten, P. A., Glass, Fundamentals. In *Ullmann's Encyclopedia of Industrial Chemistry*, Wiley: 2000.
21. Habib, E.; Zhu, X. X., Method for Photocalorimetric Determination of Free Radical Polymerization. *Polymer* **Submitted 2017**.
22. Antonucci, J. M.; Toth, E. E., Extent of Polymerization of Dental Resins by Differential Scanning Calorimetry. *Journal of Dental Research* **1983,** *62* (2), 121-125.
23. Gauthier, M. A.; Zhang, Z.; Zhu, X. X., New dental composites containing multimethacrylate derivatives of bile acids: a comparative study with commercial monomers. *ACS Appl Mater Interfaces* **2009,** *1* (4), 824-832.
24. Lee, I.-B.; Son, H.-H.; Um, C.-M., Rheologic properties of flowable, conventional hybrid, and condensable composite resins. *Dent Mater* **2003,** *19* (4), 298-307.
25. Genovese, D. B., Shear rheology of hard-sphere, dispersed, and aggregated suspensions, and filler-matrix composites. *Adv Colloid Interface Sci* **2012,** *171-172*, 1-16.

26. Lee, J. H.; Um, C. M.; Lee, I. B., Rheological properties of resin composites according to variations in monomer and filler composition. *Dent Mater* **2006,** *22* (6), 515-526.
27. Elbishari, H.; Satterthwaite, J. D.; Silikas, N., Effect of Filler Size and Temperature on Packing Stress and Viscosity of Resin-Composites. *Int J Mol Sci* **2011,** *12*, 5330-5338.
28. Bender, J.; Wagner, N. J., Reversible shear thickening in monodisperse and bidisperse colloidal dispersions. *J Rheology* **1996,** *40* (5), 899-916.
29. Watanabe, H.; Yao, M.-L.; Osaki, K.; Shikata, T.; Niwa, H.; Morishima, Y.; Balsara, N. P.; Wang, H., Nonlinear rheology and flow-induced structure in a concentrated spherical silica suspension. *Rheologica acta* **1998,** *37* (1), 1-6.
30. Halvorson, R. H.; Erickson, R. L.; Davidson, C. L., The effect of filler and silane content on conversion of resin-based composite. *Dent Mat* **2003,** *19* (4), 327-333.
31. Darvell, B. W., *Material Science for Dentistry*. 9th ed.; Woodhead Publishing: 2009; p 688.
32. Scheraga, H. A., Non‐Newtonian Viscosity of Solutions of Ellipsoidal Particles. *J Chem Phys* **1955,** *23* (8), 1526-1532.
33. Encyclopedia of Biophysics. 1 ed.; Roberts, G. C. K., Ed. Springer-Verlag Berlin Heidelberg: 2013; Vol. 1, p 2807.
34. Struble, L.; Sun, G.-K., Viscosity of Portland cement paste as a function of concentration. *Adv Cement Based Mat* **1995,** *2* (2), 62-69.
35. Douglas, J. F.; Garboczi, E. J., Intrinsic viscosity and the polarizability of particles having a wide range of shapes. *Adv chem phys* **1995,** *91*, 85-154.
36. Back, M. H., *Selected readings in chemical kinetics*. Pergamon Press: Oxford, 1967.
37. Laidler, K. J., The development of the Arrhenius equation. *J Chem Edu* **1984,** *61* (6), 494.
38. Logan, S. R., The origin and status of the Arrhenius equation. *J Chem Edu* **1982,** *59* (4), 279.
39. Emami, N.; Soderholm, K. J., Young's modulus and degree of conversion of different combination of light-cure dental resins. *Open Dentist J* **2009,** *3*, 202-207.

40. Leprince, J. G.; Palin, W. M.; Hadis, M. A.; Devaux, J.; Leloup, G., Progress in dimethacrylate-based dental composite technology and curing efficiency. *Dent Mater* **2013,** *29* (2), 139-156.

41. Satterthwaite, J. D.; Maisuria, A.; Vogel, K.; Watts, D. C., Effect of resin-composite filler particle size and shape on shrinkage-stress. *Dent Mater* **2012,** *28* (6), 609-614.

Chapter 5 - **Monodisperse silica-filled composite restoratives mechanical and light transmission properties***

Abstract

Objectives. The aim of this study was to formulate resin-based composites using spherical silica particulate fillers with graded size (75, 150, 350, 500, and 1000 nm), and to evaluate the influence of their size and loading on the mechanical and light transmission properties of the resulting material.

Methods. A series of five spherical silica fillers were synthesized, and then formulated with BisGMA/TEGDMA or UDMA/TEGDMA resins. These were then tested for maximum filler loading, flexural strength and modulus, as well as transparency and depth of cure.

Results. Low dispersity spherical silica particles of 75, 150, 350, 500, and 1000 nm were synthesized. Maximum loading was 70 wt% for the three largest filler particles, and decreased for the smaller sizes, where UDMA-based resins allowed slightly higher loading. When maximally loaded, the largest particle sizes produced the highest flexural properties. However, when using the same loading (60 wt%), all filler sized produced similar flexural strengths and moduli. The transparency and depth of cure were increased as the filler size decreased.

Significance. While hybrid filler particles are the norm in commercial materials, by studying and understanding the influence of individual components on the material properties, we can finely tune the properties of the materials as desired.

---

* Published as a research article: Eric Habib, Ruili Wang, X.X. Zhu, Dental Materials, 33 (3), 2017, 280-287.

5.1 Introduction

Dental resin composites have been slowly replacing the mercury containing dental amalgams since 1960s, due mainly to their superior aesthetic properties (*1*). Since their advent, a large body of research coming from both academia and industry has explored a variety of resin monomers as well as inorganic fillers. However, much of this research has remained proprietary.

The fillers used for dental composites have historically mostly been silicates, ranging from silicon dioxide to bioactive glass. Other types have also been used, such as hydroxyapatite, and polymer nanogels (*2-4*); recent reviews have described these fillers in great detail (*5-6*). Rather than examining the effect of different chemical compositions, this work strives to describe the effect of filler loading, size, and morphology on the mechanical and optical properties of the final composites.

The most commonly seen morphologies of filler particles are spheroidal and irregular, though a few others have also been explored (*7-8*). Spheroidal filler particles are synthesized by solution synthesis in a bottom-up approach, such that small particles are seeded and grow slowly to the desired size, as seen in the oft-used Stöber process, resulting in very low dispersity (*9-10*). Irregular particles are often made using a top-down approach, by milling the desired material, and passing it through sieves to obtain the desired size. These usually exhibit a high dispersity as well as a large variability in the particle shape.

With regards to the properties conferred by these fillers, there have been mixed results in the literature. Most of the work that has been done evaluating these properties used commercial composites whose compositions are variable, and often not fully known, making it difficult to derive meaningful trends. Nonetheless, some work with commercial composites has shown that spheroidal fillers can accommodate higher loading, leading to superior mechanical properties (*11*). Furthermore, while spherical fillers exhibit similar wear performance as irregular ones, they maintain superior gloss and smoothness in the process (*12*).

Few articles have examined the effect of filler morphologies on composite properties while keeping other parameters constant. Satterthwaite *et al* examined the effect of spheroidal and irregular fillers on shrinkage stress and strain, and found that spheroidal fillers had lower values for both, hypothesizing that the difference was due to the higher surface

area of irregular particles (*13-14*). The same group found that larger filler particles led to increased void volumes within the composites (*15*). Furthermore, Marghalani found that surface roughness was significantly lower for monodisperse spheroidal fillers than for irregular or multimodal fillers (*16*). Finally, Turssi *et al* examined the wear resistance and conversion, where their findings revealed that smaller particulate fillers result in lower wear volume, but also lower conversion values (*17*).

In terms of the optical characteristics of materials, a few papers examined commercial composites (*18-19*), while others examined the optical properties resulting from experimental composite formulations (*20-23*). Many of these examined samples of differing thickness, obtaining exponential decay with thickness as predicted by the Beer-Lambert law for translucency. Furthermore, for the tested silica filler, Azzopardi found a direct correlation between BisGMA content and translucency (*20*). The chemical composition of the filler (*21*) as well as the loading and size (*22-23*) were also shown to play a role in the final translucency.

The objective of this work is to establish the relationship between the size and loading of low dispersity silica filler and the mechanical and optical properties of the resulting composites. The hypothesis is that larger filler particles produce superior mechanical properties at the detriment of translucency, and in turn, depth of cure.

5.2 Materials and Methods

Tetraethyl orthosilicate (TEOS) was purchased from Alfa Aesar (Haverhill, MA, USA), 3-methacryloyltrimethoxypropylsilane (γ-MPS), bisphenol A glycerolate dimethacrylate (BisGMA), and triethylene glycol dimethacrylate (TEGDMA) were purchased from VWR (Radnor, PA, USA); camphorquinone (CQ) and ethyldimethylaminobenzoate (EDMAB) were obtained from Sigma-Aldrich (St. Louis, MO, USA); ammonium hydroxide (35%) and anhydrous ethanol were obtained from Fisher Scientific (Waltham, MA, USA). All reagents were used without further purification. The dental lamp used was a Kerr Demetron Optilux 500; its intensity was measured at 740 mW/cm^2 with the lamp's integrated radiometer. Room temperature is defined as 23 °C.

5.2.1 Synthesis of Monodisperse Silica Particles

Silica particles with graded size were synthesized using the Stöber method. Ethanol, water, and ammonium hydroxide were mixed together and equilibrated to the desired temperature. TEOS was then added either in one portion, or at the rate specified in **Table 5.1**. Once the reaction was complete (8 hours after last addition), surface modification (silanization) was done with 1.0 mL γ-MPS per 10 mL TEOS that was added directly to the solution with magnetic agitation for 16 h. Centrifugation was then performed at 12,000 × G for 20 minutes, followed by resuspension in ethanol. This process was repeated 3 times. After the final centrifugation step, the residual solvent was evaporated at 80 °C, and the particles were dried under vacuum at 115 °C for 24 h.

Table 5.1- Reaction conditions for monodisperse silica particles of varying size.

Target Size (nm)	Ethanol (ml)	NH_4OH (ml)	Water (ml)	TEOS (ml)	Additional TEOS (ml)	Addition Rate (ml/h)	Yield (g)	Average Size (nm)
75	250	16.5	0	40			13.7	77
150	250	5	25	15			4.2	148
350*	250	5	25	15			4.3	360
500	250	25	40	45	33**	8.3	32.0	488
1000	250	25	40	15.5	31	1	13.4	932

* Solution was cooled in an ice bath to 3 °C for the initial addition of TEOS and warmed naturally to room temperature

** TEOS was dissolved in 383 ml of anhydrous ethanol

5.2.2 Particle Characterization

The size of silica particles was characterized using laser diffraction (Horiba Laser Particle Sizer LA-950) in water or dynamic light scattering (Malvern Zetasizer) in ethanol, using an aliquot taken from the solution before centrifugation. In addition, scanning electron microscopy (JEOL JSM-7400F FE-SEM, Japan) was used to confirm the particle size, dispersity, and morphology, using a 5 kV accelerating voltage and 20 μA.

Thermogravimetric (TA TGA 2950 thermogravimetric analyzer, DE, USA) analysis was used, under an air atmosphere, at 20 °C/min to measure the extent of silane surface modification.

5.2.3 Composite Blending

The resins were prepared by first dissolving CQ and EDMAB (final concentration of 0.5 wt% of the final resin each) in the TEGDMA resin by mechanical stirring. BisGMA or UDMA was then added to the mix, stirred by hand, and then stirred mechanically at 35 °C for 30 min. The final ratio of BisGMA or UDMA to TEGDMA was 70:30 by weight.

The composites were then blended by coarsely mixing the filler and resin by hand, and then completing the mix with the three roll mill (Exakt 50i TRM, Norderstedt, Germany) until a homogenous material was obtained.

5.2.4 Mechanical Properties

To evaluate the maximum loading of the composites, the dry filler was slowly added to the liquid resin and mixed by hand, before blending with a three roll mill. There were two criteria that were used to measure the maximum loading: 1) when the composite was no longer cohesive and broke apart, it was considered to be overloaded, and the value before the last addition was used as the maximum filler loading, or 2) when the viscosity became so high that the samples could no longer be processed, they were also considered to be overloaded for all functional purposes. This test was done in duplicate. In the case of high viscosity, it is not the true maximum loading for the particles, so all references to 'maximum loading' refer to the functional maximum loading found here.

Composite bars were made using split stainless steel bar molds of 2 mm x 2 mm x 25 mm sandwiched between two 0.5 mm thick glass slides. They were polymerized with the lamp mentioned above for 20 s (3 times to cover the whole bar) and then 7 s from the other side (3 times again). The flexural strength and modulus of these specimens were measured in quadruplicate on a universal mechanical analyzer (Instron 5565, USA), according to ISO-4049.

5.2.5 Optical Properties

Composite disks were added into a stainless steel disk molds of 5 mm diameter and 0.5 mm thickness covered by 0.5 mm glass slides, and polymerized for 30 s using a dental

lamp. The transmission of light through the disks was measured on a UV/Vis spectrometer (Flame USB 2000, LS-1 tungsten halogen lamp, Ocean Optics Inc., USA) by transmission with a custom-machined brass holder for the glass fiber light guides. Each sample was measured three times at random points and then averaged.

The refractive indices of the resins were measured with a handheld digital refractometer (Reichert AR200, NY, USA)

5.2.6 Polymerization Conversion and Depth of Cure Measurements

The extent of monomer polymerization was evaluated by Raman spectroscopy (Renishaw Invia confocal microscope, 785 nm laser, 600 line/mm grating, Gloucestershire, UK). For general conversion measurements, 10-20 mg of composite paste was placed on aluminum foil and measured (spectrum centered at 1500 cm^{-1}), then polymerized under a dental lamp for 20 s, and measured again. The extent of polymerization was calculated with the following equations (*24*):

$$Conversion = 1 - \frac{C1638 \times U1608}{C1608 \times U1638} \quad (5.1)$$

where C1638 and C1608 are the areas under the curve for the cured sample for the bands centered at 1638 cm^{-1} and 1608 cm^{-1}, respectively, and U1638 and U1608 the analogous measurements before curing. These bands were used for BisGMA-containing composites with an aromatic C=C band at 1608 cm^{-1}, and

$$Conversion = 1 - \frac{C1638 \times U1725}{C1725 \times U1638} \quad (5.2)$$

for the UDMA-based composites without the aromatic band, using the C=O band at 1725 cm^{-1} (*25*).

For depth of cure measurements, the composite paste was put into a split cylindrical mold (diameter of 4 mm, depth of 10 mm or 30 mm, where necessary), and polymerized for 20 s. The sample was then de-molded, and excess paste was allowed to leak off (if applicable). The sample was then placed horizontally on the Raman spectrometer and a conversion map was made to evaluate the degree of cure by depth (1 point per 0.1 mm depth, 2 × 5 s scan). A separate sample of uncured resin was used as a reference. Subsequently, all of the soft paste from these samples was removed by gentle scraping, and the sample depth was measured with a micrometer (*26*). The depth of cure as measured by Raman

spectroscopy was the average of two measurements. Mechanical depth of cure measurements was the average of three samples.

5.2.7 Statistical Analysis

The statistical significance was compared using one-way ANOVA analysis with the Tukey method within a 95% confidence interval.

5.3 Results

The low dispersity spheroidal silica fillers were obtained using the Stöber method and were tuned to have sizes of 75, 150, 360, 500, and 1000 nm. These were silanized *in situ* with an excess of γ-methacryloyl propoxysilane to allow covalent bonding between filler and resin, and then centrifuged and rinsed before the degree of substitution was evaluated by thermogravimetric analysis. The particles showed low overall size dispersity, as measured by both laser light diffraction and scanning electron microscopy (Figure 5.1, Figure S 5.1).

These particles were then used to formulate dental composites using two commonly used resins: BisGMA/TEGDMA (7B3T) and UDMA/TEGDMA (7U3T). Several experimental series were performed, with varying filler size, and filler loading.

The smallest particles (75 and 150 nm) had the lowest maximum filler loads (Figure 5.2A) for both resins due to a high viscosity that prevented the mixer from blending in higher amounts of filler. The 360, 500, and 1000 nm particles all had a maximum loading of 70 wt%, but showed decreasing viscosity with increasing size (data not shown). Despite the lower viscosity, attempts to load the 1000 nm filler an additional 2% (to 72 wt%) proved too much, and resulted in the paste turning into a coarse powder. The 7U3T resin allowed more filler to be incorporated when using the two smallest fillers due to its inherently lower viscosity compared to the 7B3T resin, but displayed the same plateau for the larger particles.

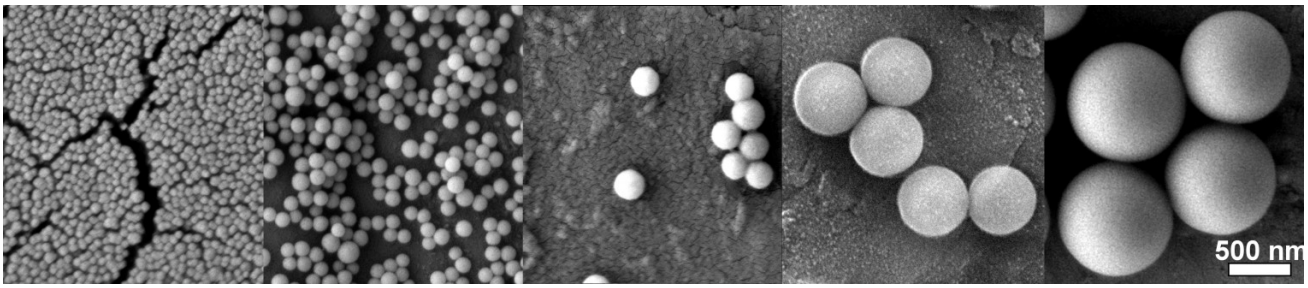

Nominal Particle Size (nm)	Mean Size ± SD (nm)[a]	Median (nm)[a]
75	77 ± 10	76
150	152 ± 30	151
360	367 ± 51	368
500	488 ± 53	485
1000	930 ± 66	932

[a] Values obtained by laser light diffraction

Figure 5.1 – FE-SEM images (left to right, 75, 150, 360, 500, 1000 nm particles) and size measurements of the silica particles prepared by the Stöber method.

The composites were blended and formed into bars to measure the flexural properties of these materials. Mechanical tests were performed in two groups: Group 1: The composites were all loaded equally at 60 wt%; and Group 2: the composites were maximally loaded, as indicated in Figure 5.2A. For Group 1, when loading was held constant at 60 wt%, there was no statistically significant difference in the flexural strength between the different filler sizes (Figure 5.2B). While there were some differences between the measured moduli, there was no clear trend. For Group 2, as expected, there is an increasing trend in both strength and modulus with increasing filler size (Figure 5.3A, C), though the increases in strength are not significant beyond the jump observed from 75 nm to 150 nm filler.

Furthermore, when grouping all of the composites with similar loading (Figure 5.3B, D), there is a significant increase in the mechanical properties with loading. This confirms the notion that larger filler fractions impart superior mechanical properties to the resulting material.

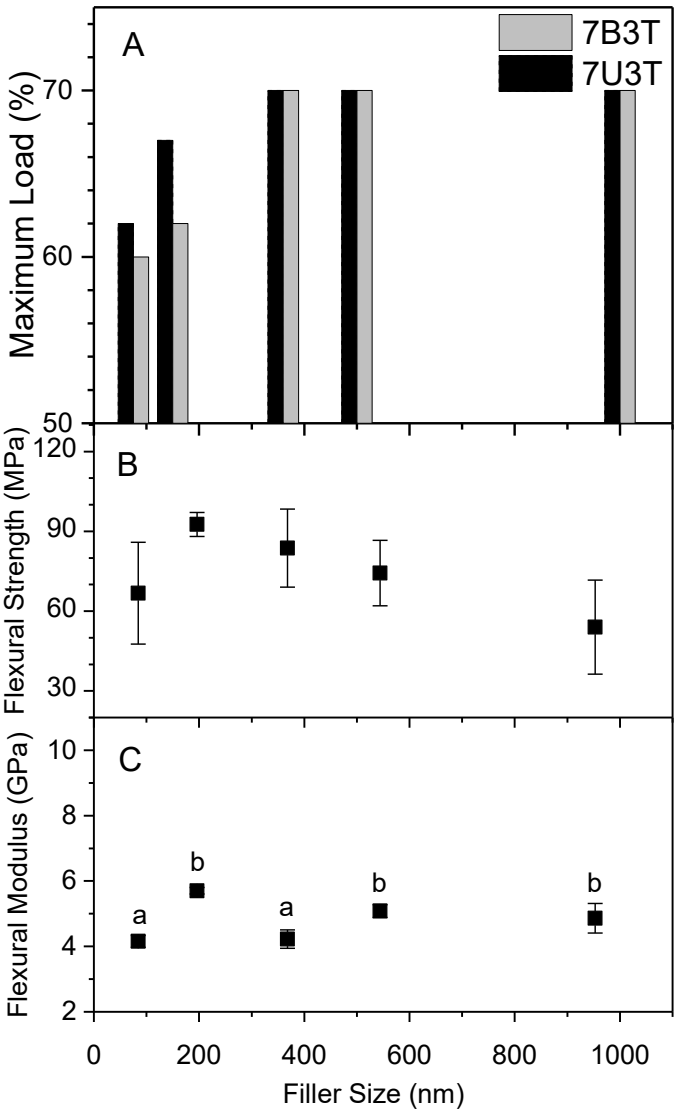

Figure 5.2 - A) Maximum filler loading of 7B3T (square, dashed line) and 7U3T (circle, solid line) based composites with different filler sizes, based on duplicate tests, B) Flexural strength and C) Flexural modulus at constant 60 wt% loading using 7B3T resin. Each test was performed in quadruplicate. Letters indicate statistically similar groups.

In terms of the influence of the resin matrix, the 7B3T composites showed marginally higher flexural strength values in comparison with 7U3T composites, but the difference was not statistically significant. The flexural moduli of these composites, however, were markedly higher with the 7B3T resin (CI: 0.95) for filler sizes of 360, 500, and 1000 nm.

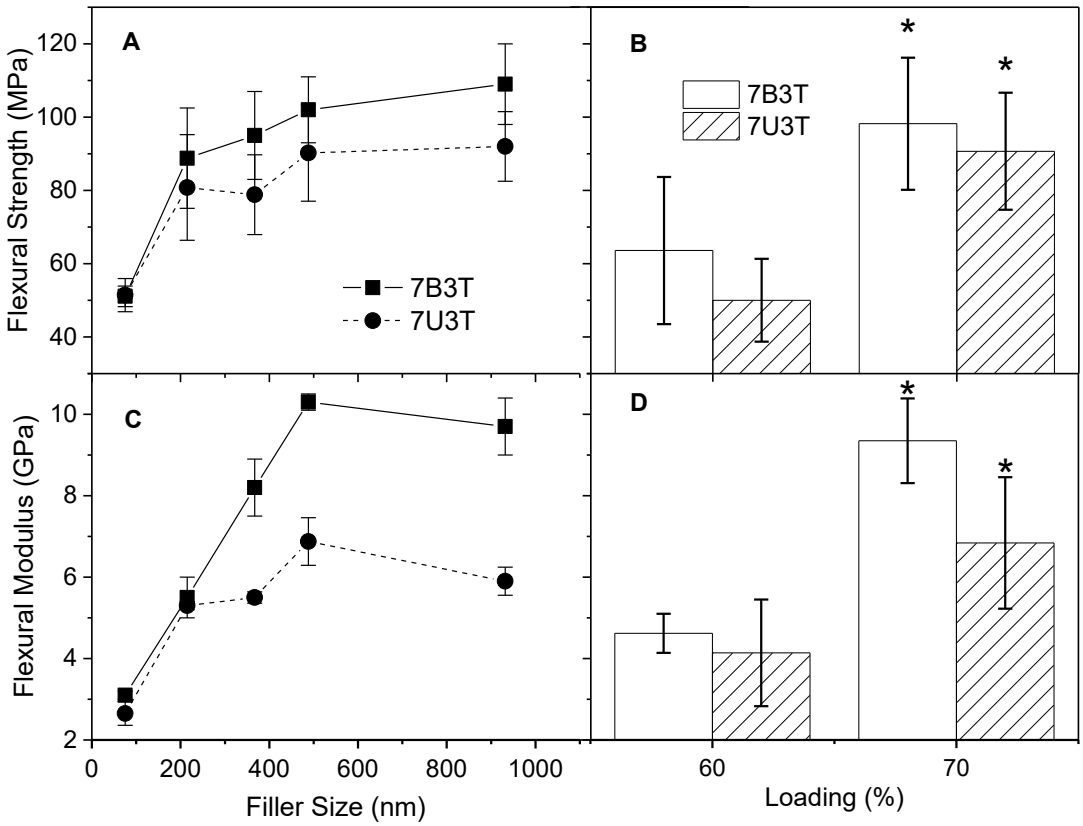

Figure 5.3 - Flexural properties of BisGMA-based (solid line, squares; empty bars) and UDMA-based (dashed line, circles; hatched line bars) composites by particle size at maximum loading (A,C), and by filler loading for all sizes (B, D). A and B show flexural strength, and C and D show flexural modulus. Each point in A and C represents quadruplicate measurements, each bar in B and D represents an average of 8 to 12 points. * indicated statistical significance at CI > 0.95

The translucency properties of the composites were evaluated in two ways: transmittance and depth of cure. The latter was evaluated both by the traditional mechanical method and Raman spectroscopy, measuring the degree of conversion at increasing depth.

As seen in Figure 5.4, the transmittance of the composites showed that the smaller particles had a much higher transmittance than the larger ones, where the 75 and 150 nm particles showed some wavelength dependence. For the fillers of 360 nm in diameter or larger, the transmittance was too low to measure accurately enough to reach a meaningful conclusion.

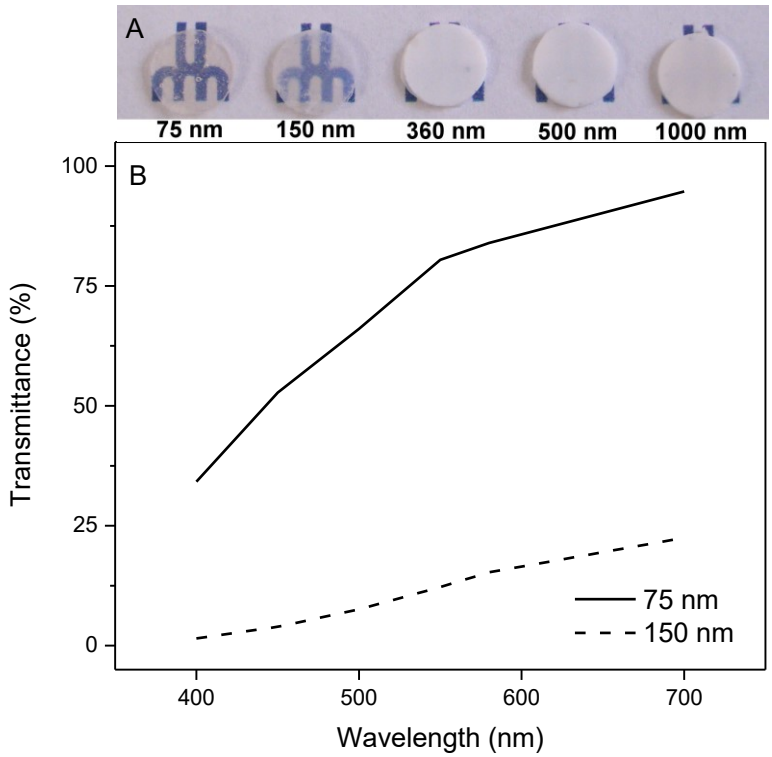

Figure 5.4 – A) Pictures of the 0.5 mm thick disks by filler size; B) transmittance measurements of the 75 nm and 150 nm filled disks.

Accordingly, the depth of cure showed a reciprocal relationship with filler size as shown in Figure 5.5A. The depth of cure dropped dramatically after the 75 nm filler, and remained at approximately the same level for the rest of the fillers. Filler loading had little effect of the depth of cure once filler was added after the initial addition (30 wt% in this case).

Both of the resins showed the same trend, but 7U3T had a markedly higher depth of cure. In order to account for the difference between the resins, the refractive indices of the 7B3T and 7U3T resins were measured to be 1.52 and 1.48, respectively, such that the UDMA resin more closely matches that of the silica filler (1.46) (*27*).

Furthermore, comparing the depth of cure as measured by mechanical means or by Raman spectroscopy (Figure 5.5A) shows that the values obtained were almost identical, such that the small difference can be attributed to the difference in measurement geometry

(side measurement for Raman spectroscopy versus center measurement for mechanical method).

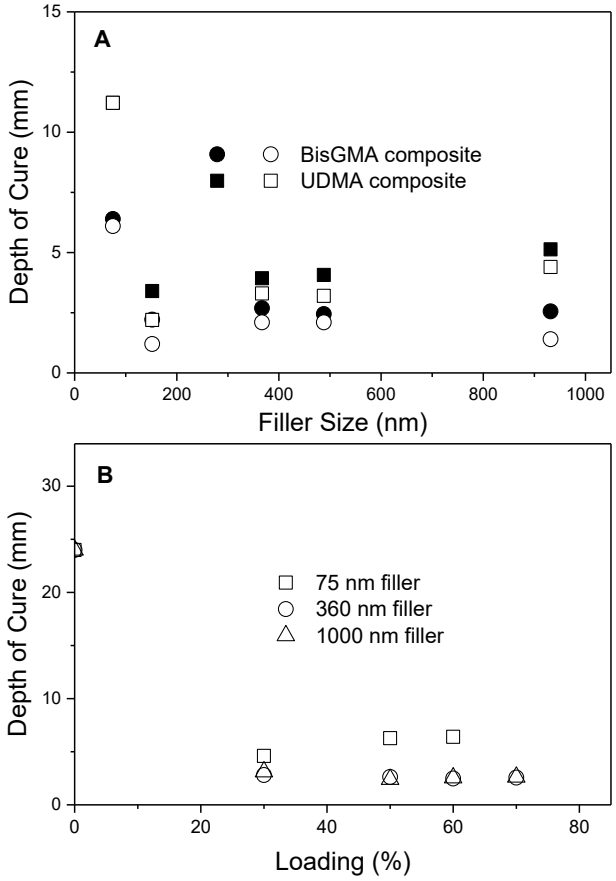

Figure 5.5 - A) Depth of cure of the composites according to their filler particle size at 60 wt% filler loading. Full symbols, mechanical measurements; empty symbols, Raman measurements. B) Depth of cure with varying filler loading using 7B3T based composites

5.4 **Discussion**

The maximum loading of the composites using particles of different sizes appears to be a function of two concurring phenomena: particle packing, and composite viscosity. When considering the packing of identical spherical particle, previous work and simulations have shown that the maximum theoretical packing is 74 vol% (*28*), however computer simulations and experimental results show that the maximum packing is closer to 64 vol% (*29*), depending on the system. The three largest particle sizes (360, 500, and 1000 nm) having a maximum loading of 70 wt% (~53.6 vol%) suggest that this is the upper limit for packing in

these composites, indicating a form of random loose packing (53.6-63.4 vol%) (*30*). This packing mode is consistent since excess resin is required to maintain the malleability of the unpolymerized composite pastes, where higher packing would likely render the composite friable.

The previously mentioned packing considerations set a hard limit on the packing of low dispersity spherical fillers, but as the particle size decreases, the effective filler surface area increases, leading to increased interactions between the filler and the resin. Such interactions then manifest macroscopically as higher viscosities (*31-32*). In turn, despite the smaller particles having the same theoretical packing limit as the large particles, the viscosity of the paste increases to a degree that renders such high loading impractical. For smaller particles (75 and 150 nm, in this case), the loading is therefore limited by the viscosity. Furthermore, when examining the differences between the 7B3T and 7U3T resins, the viscosity of the base resin clearly has an influence of the material viscosity, allowing the more fluid 7U3T resin to have a higher loading, though other resin-filler compatibility factors may be in play (*32*).

In terms of the mechanical properties, previous literature hypothesized that lower loading led to inferior mechanical strength (*17, 33-34*), but it had not been shown for fillers of identical composition and morphology. Results show that higher loading does indeed significantly increase both flexural strength and modulus (Figure 5.3). Such a phenomenon could be explained by the number of inter-particle contacts that serve to transmit and diffuse forces across the material; rather than the stress being concentrated at a specific point where it is more likely to break, that stress is transmitted and dispersed to many nearby particles through their physical contact. Lower loading would result in fewer interparticle contacts, and so lower yield stress.

Tests using different filler sizes with identical loading fractions show that the flexural strength does not differ significantly among filler sizes (Figure 5.2B-C), thus confirming the hypothesis, and agreeing with previous work on the topic (*35*). The observed variance in flexural modulus shows no clear trend, and is most likely due to bubble entrapment while polymerizing the composites. When maximum filler loading is used, however, larger particle sizes produce composites with superior flexural strength and modulus (Figure 5.3). Therefore, while conventional wisdom in dental materials is correct in that larger particles

result in mechanically stronger composites, this is purely due to the maximum allowable loading, and is not directly related to the filler size.

The translucency and depth curing properties of these materials were inversely affected by the particle size, such that smaller particles produced much higher depths of cure and transparencies (Figure 5.5A). This was expected due to the decreased light scattering and reflection that is exhibited by smaller particles. The biggest drop in depth of cure occurs between 75 and 150 nm, which corresponds to the Rayleigh scattering limit of the polymerization light's wavelength (400-600 nm). The UDMA-based composites also clearly show a greater depth of cure than the BisGMA-based composite. This is most likely due to the refractive index difference between the resin and the filler particles. Reflection and refraction effects that lead to turbidity or opacity in these composites are governed by the refractive index (*36*). If using fused silica for the value of the filler, it has a value of 1.46, leading to a difference of 0.06 with the BisGMA-based resin, but only 0.02 with the UDMA-based resin. This difference, however small, results in a far superior depth of cure with the UDMA-based resin (Figure 5.5). Therefore, the smallest particles produce the highest depth of cure, particularly when matched with refractive index matched resins.

Furthermore, in order to evaluate the influence of filler loading on depth of cure, particles of 1000, 360, and 75 nm in diameter were tested at different loading levels, which had no significant effect on the depth of cure. This follows scattering theory, such that once the particle concentration is high enough to exhibit multiple scattering, the scattering contribution no longer changes significantly, and the transmission of light and depth of cure remain mostly constant (Figure 5.5B).

When comparing the depth of cure as measured by the conventional spatula scraping method and the Raman spectroscopy, the results are very well matched (Figure 5.5A). Due to the exponential nature of light penetration, the conversion drops fairly rapidly when approaching the uncured bottom edge. For that reason, the conversion seems to change very little up to the full depth of cure of a given sample. The small divergence that is observed between the Raman and scraping measurements is simply due to the conical shape of the samples, where the depth of cure is higher in the middle than on the sides. These results indicate that the spatula method, while somewhat less accurate due to its inherent variability, can serve as a close approximation of the value measured by other means.

5.5 Conclusion

Low dispersity silica filler particles were synthesized, characterized, and tested in the formulation of dental composites with two monomer systems. Within the limitations of this study, with the use of monodisperse spherical silica fillers, the largest particles (350-1000 nm) produced superior flexural properties, as hypothesized, but only due to the superior loading permitted by their lower surface area. Conversely, smaller particles produced more transparent composites, which have a correspondingly higher depth of cure, particularly below the Rayleigh scattering limit (~ 100 nm in this case). Furthermore, the composites formulated with the BisGMA-based resin were stronger than the UDMA-based resin, but had inferior depths of cure. This study will allow a better understanding of how detailed filler compositions affect the properties of the final materials. A systematic understanding will further allow us to precisely tune the composite properties as desired. Studies on the influence of filler size on polymerization kinetics will allow us to further deepen our understanding of composite viscosity beyond that of maximum loading.

5.6 Supplementary Information

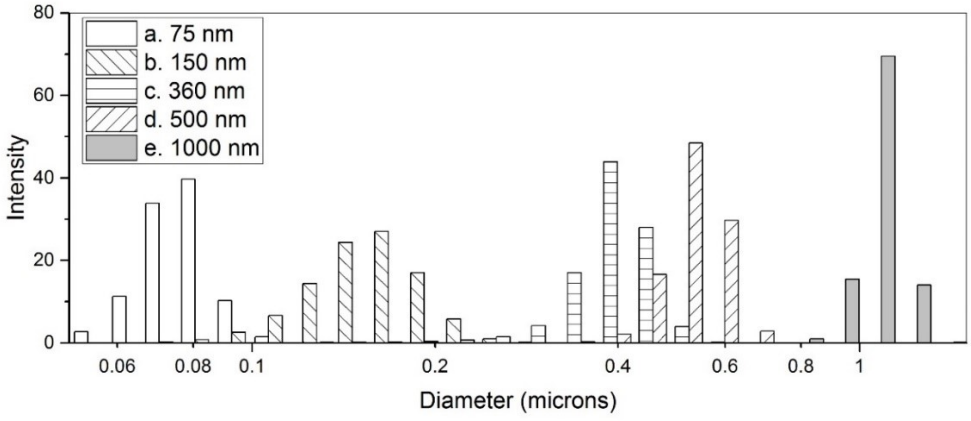

Figure S 5.1 - Laser diffraction data for the size distributions of the spheroidal silica fillers.

5.7 References

1. Shenoy, A., Is it the end of the road for dental amalgam? A critical review. *J Conserv Dent* **2008,** *11* (3), 99-107.
2. Lezaja, M.; Veljovic, D. N.; Jokic, B. M.; Cvijovic-Alagic, I.; Zrilic, M. M.; Miletic, V., Effect of hydroxyapatite spheres, whiskers, and nanoparticles on mechanical properties of

a model BisGMA/TEGDMA composite initially and after storage. *J Biomed Mater Res B Appl Biomater* **2013**.

3. Moraes, R. R.; Garcia, J. W.; Barros, M. D.; Lewis, S. H.; Pfeifer, C. S.; Liu, J.; Stansbury, J. W., Control of polymerization shrinkage and stress in nanogel-modified monomer and composite materials. *Dent Mater* **2011,** *27* (6), 509-519.
4. Dailing, E. A.; Lewis, S. H.; Barros, M. D.; Stansbury, J. W., Construction of monomer-free, highly crosslinked, water-compatible polymers. *J Dent Res* **2014,** *93* (12), 1326-1331.
5. Habib, E.; Wang, R.; Wang, Y.; Zhu, M.; Zhu, X. X., Inorganic Fillers for Dental Resin Composites: Present and Future. *ACS Biomat Sci & Eng* **2016,** *2* (1), 1-11.
6. Cramer, N. B.; Stansbury, J. W.; Bowman, C. N., Recent advances and developments in composite dental restorative materials. *J Dent Res* **2011,** *90* (4), 402-416.
7. Banerjee, S.; Ghosh, H.; Datta, A., Lamellar Micelles as Templates for the Preparation of Silica Nanodisks. *J Phys Chem C* **2011,** *115* (39), 19023-19027.
8. Banerjee, S.; Datta, A., Photoluminescent silica nanotubes and nanodisks prepared by the reverse micelle sol-gel method. *Langmuir* **2010,** *26* (2), 1172-1176.
9. Stöber, E.; Fink, A., Controlled Growth of Monodisperse Silica Spheres in the Micron Range. *J Coll Int Sci* **1968,** (26), 62-9.
10. Yukitani, W.; Hasegawa, T.; Itoh, K.; Hisamitsu, H.; Wakumoto, S., Marginal adaptation of dental composites containing prepolymerized filler. *Oper Dent* **1997,** (22), 242-248.
11. Kim, K.-H.; Ong, J. L.; Okuno, O., The effect of filler loading and morphology on the mechanical properties of contemporary composites. *J Prosthet Dent* **2002,** *87* (6), 642-9.
12. Lu, H.; Lee, Y. K.; Oguri, M.; Powers, J. M., Properties of a dental resin composite with a spherical inorganic filler. *Oper Dent* **2006,** *31* (6), 734-740.
13. Satterthwaite, J. D.; Maisuria, A.; Vogel, K.; Watts, D. C., Effect of resin-composite filler particle size and shape on shrinkage-stress. *Dent Mater* **2012,** *28* (6), 609-614.
14. Satterthwaite, J. D.; Vogel, K.; Watts, D. C., Effect of resin-composite filler particle size and shape on shrinkage-strain. *Dent Mater* **2009,** *25* (12), 1612-1615.

15. Elbishari, H.; Silikas, N.; Satterthwaite, J., Filler size of resin-composites, percentage of voids and fracture toughness: is there a correlation? *Dent Mat J* **2012,** *31* (4), 523-527.
16. Marghalani, H. Y., Effect of filler particles on surface roughness of experimental composite series. *J Appl Oral Sci* **2010,** *18* (1), 59-67.
17. Turssi, C. P.; Ferracane, J. L.; Vogel, K., Filler features and their effects on wear and degree of conversion of particulate dental resin composites. *Biomat* **2005,** *26* (24), 4932-7.
18. Arikawa, H.; Fujii, K.; Kanie, T.; Inoue, K., Light transmittance characteristics of light-cured composite resins. *Dent Mater* **1998,** *14* (6), 405-11.
19. Nakajima, M.; Arimoto, A.; Prasansuttiporn, T.; Thanatvarakorn, O.; Foxton, R. M.; Tagami, J., Light transmission characteristics of dentine and resin composites with different thickness. *J Dent* **2012,** *40 Suppl 2*, e77-82.
20. Azzopardi, N.; Moharamzadeh, K.; Wood, D. J.; Martin, N.; van Noort, R., Effect of resin matrix composition on the translucency of experimental dental composite resins. *Dent Mater* **2009,** *25* (12), 1564-8.
21. Emami, N.; Sjodahl, M.; Soderholm, K. J., How filler properties, filler fraction, sample thickness and light source affect light attenuation in particulate filled resin composites. *Dent Mater* **2005,** *21* (8), 721-730.
22. Lim, Y. K.; Lee, Y. K.; Lim, B. S.; Rhee, S. H.; Yang, H. C., Influence of filler distribution on the color parameters of experimental resin composites. *Dent Mater* **2008,** *24* (1), 67-73.
23. Salgado, V. E.; Cavalcante, L. M.; Silikas, N.; Schneider, L. F., The influence of nanoscale inorganic content over optical and surface properties of model composites. *J Dent* **2013,** *41 Suppl 5*, e45-53.
24. Antonucci, J. M.; Toth, E. E., Extent of Polymerization of Dental Resins by Differential Scanning Calorimetry. *J Dent Res* **1983,** *62* (2), 121-125.
25. Halvorson, R. H.; Erickson, R. L.; Davidson, C. L., The effect of filler and silane content on conversion of resin-based composite. *Dent Mat* **2003,** *19* (4), 327-333.
26. ISO, Polymer-based restorative material. In *Dentistry*, 2009; Vol. ISO 4049, p 28.

27. Malitson, I. H., Interspecimen Comparison of the Refractive Index of Fused Silica*,†. *J Optic Soc of Am* **1965,** *55* (10), 1205-1209.
28. Wang, R.; Habib, E.; Zhu, X. X., Application of close-packed structures in dental resin composites. *Dent Mater* **2017,** *33* (3), 288-293.
29. Song, C.; Wang, P.; Makse, H. A., A phase diagram for jammed matter. *Nature* **2008,** *453* (7195), 629-632.
30. Mohanty, K. K., Porous media: Fluid transport and pore structure. By F. A. L. Dullien, Academic Press, 574 pp., 1992. *AIChE Journal* **1992,** *38* (8), 1303-1304.
31. Darvell, B. W., *Materials Science for Dentistry*. Elsevier Science: 2009.
32. Klapdohr, S.; Moszner, N., New Inorganic Components for Dental Filling Composites. *Monatsh. Chem.* **2004,** *136* (1), 21-45.
33. Kim, K.-H.; Ong, J. L.; Okuno, O., The effect of filler loading and morphology on the mechanical properties of contemporary composites. *J Prosthet Dent* **2002,** *87* (6), 642-649.
34. Hu, X.; Marquis, P. M.; Shortall, A. C., Influence of filler loading on the two-body wear of a dental composite. *J of Oral Rehab* **2003,** *30* (7), 729-737.
35. Karabela, M. M.; Sideridou, I. D., Synthesis and study of properties of dental resin composites with different nanosilica particles size. *Dent Mater* **2011,** *27* (8), 825-835.
36. Schulz, H.; Burtscher, P.; Mädler, L., Correlating filler transparency with inorganic/polymer composite transparency. *Composites Part A: App Sci and Manuf* **2007,** *38* (12), 2451-2459.

Chapter 6 - **Conclusions and Future Work**

6.1 General Conclusions

The objective of this thesis was to improve the photocalorimetry method and better define how the different parts of dental resin composites affect the final properties of the material both before and after polymerization. The studies contained herein demonstrate that through systematic variation of the parameters involved, the role of each piece of these complex blends can be isolated to better understand the rules that determine their properties. The technique and models developed here will greatly accelerate the development and characterization of dental resin composites, at least partially bypassing the lengthy trial and error processes that are typically required to obtain clinically relevant composites.

6.1.1 Reliable Method for Photocalorimetric Measurements of Resin Curing

The variables involved in the photocalorimetry method were varied to assess their effect on the measurements, and on their reliability and repeatability. By observing the trends in the measured polymerization rate and final conversion with respect to protocol, temperature, mass, light intensity, and atmosphere, we were able to establish a robust and error-resistant protocol to allow us a better understanding of the photopolymerization processes being studied. Some variables, such as light intensity, followed the expected relationships with regards to polymerization kinetics. Others, such as mass, were not as straightforward, further justifying the need for such a study. This study will serve as a basis for all future work using photocalorimetry to ensure that they are reproducible and reliable, and will ensure consistency between studies.

6.1.2 Accurate Modeling of Composite Paste Viscosity and Conversion

Due to the complexity of commercial formulations, despite many studies examining their properties, very few previous studies have been able to establish anything more than qualitative causal relationships between each parameter and its effect. These studies involved either commercial materials whose full composition is not known, or had too few samples to be able to adequately portray the effect of the changes. In this thesis, spherical silica filler particles were synthesized with well-defined morphology and size, and were used to formulate experimental composites to systematically relate filler size and loading parameters to the resultant properties in the final materials. Our composites formulated with low

dispersity spherical silica particles of graded size (75 to 1000 nm) showed that the viscosity of these materials can be modeled and predicted using an extended version of the classic Krieger-Dougherty model. This modified model uses filler surface area in addition to loading to accurately predict the viscosity of these suspensions at different loading levels. The viscosity can in turn be used to model the conversion of composites, given an empirical resin constant and the conversion for resin alone; it was shown to be directly related to the logarithm of suspension viscosity. Furthermore, data and compositions from other work with shrinkage stress suggest that this shrinkage can also be predicted using this same EKD model. While this work was performed on BisGMA and UDMA resin blends, the fact that both yielded similar results suggests that only dramatic changes in molecular size or properties would affect this relationship. The model should therefore be applicable to a wide range of compositions.

6.1.3 Mechanical and Optical Properties of Cured Composites from Filler Size

The same formulations with spherical silica particles of graded sizes from the previous section were also used to evaluate the final mechanical and optical properties of these composites according to the filler size and loading. The filler loading was found to be the principal parameter that affects the mechanical properties of the composites, increasing strength with loading. While the smallest filler size (75 nm) had decreased mechanical performance compared to the larger sizes, when equally loaded, all others were within error, suggesting that filler size does not significantly influence mechanical performance of the composites. However, smaller particles have lower functional filler loading values due to their higher viscosity, resulting in poorer mechanical performance. Furthermore, as expected, very small filler particles were found to produce transparent composites, in particular for those of less than 150 nm, where Mie scattering is less prominent. Though this study was done in the context of dental composites, it can also be applied to other highly loaded polymer composites to design more refined formulations, yielding transparent and mechanically resistant materials.

6.1.4 Overall Conclusion

This thesis serves to advance the understanding of dental resin composite formulations for the design of new and better materials. Though the chemistry had advanced

significantly for these materials, this thesis now brings a much-needed understanding to the design of composites formulations. The filler has long been known to affect the rheological properties of the composites before polymerization and some of the properties after, however this relationship has now been better defined. Through the methodological optimizations developed herein, further research can more easily be performed with confidence in the integrity of the data obtained. Using standardized and well characterized methods, the relationships uncovered here now allow better predictions of composite properties at the design stage, saving time in material synthesis and formulation.

6.2 Perspectives

The work performed in the context of this thesis reached meaningful and useful conclusions, but also led to many more questions. The filler particles used in dental materials have so many parameters that the permutations are virtually endless, but the following are projects that would logically continue the work presented here.

6.2.1 High Dispersity and Multimodal Filler Particles

The work performed in chapters 4 and 5 was done with low dispersity silica particles for simplicity, and to eliminate morphology and dispersity as variables, however further studies should be done to see how both affect the relationships that were uncovered here. Dispersity is well known to affect particle packing, such that higher dispersity leads to denser packing, resulting in a higher maximum particle loading (*1*). As described in chapter 4, a higher maximum loading would result in lower viscosity pastes and in turn, theoretically, higher conversion values. Thus by using particles with the same average size, but different dispersities, it may be possible to develop an effective model of maximum loading for these highly loaded suspensions.

The next logical step to verify the applicability of the EKD model is to see if it still applies to multimodal filler distributions. Like dispersity, multimodality should allow higher maximum loading, decreasing the viscosity of the suspensions, and increasing conversion. The greatest difficulty to this application is that maximum filler loading is more difficult to define with multimodal fillers, though theoretical calculations may be applied for comparison purposes (*2-3*). Otherwise the maximum loading can be determined experimentally. Furthermore, since highly loaded composites have very high viscosity, this property becomes

very challenging to measure using traditional rheology methods; it would most likely be necessary to resort to Mooney viscosity (*4*) or other methods traditionally reserved for soft solids, such as compressive or tensile moduli, to adequately characterize highly loaded composites.

The final extension would be to use irregular particle morphologies. These would require surface area measurements (such as BET tests), since surface area cannot be calculated from first principles. This type of fillers is well known to have high maximum loading values, due both to their high dispersity and their superior packability. Once a valid model is obtained for high dispersity monomodal fillers, then it can be expanded to multimodal fillers, and finally to irregular particles.

6.2.2 Variations in Interfacial Energy and Reactivity

Another direct extension of the work in chapter 4 is to vary the surface functionalization of the filler particles to see the effect on both viscosity and conversion. Previous studies have shown that adding a fraction of octyltrimethoxysilane (OTMS) to the usual 3-MPS can mildly improve conversion in composites (*5*). The modification of surface properties will change the interfacial energy, which partly determines the viscosity of the paste (*c* parameter in the EKD model) and in turn the conversion of the composites. Qualitative experiments over the course of this thesis have demonstrated that composites filled with particles modified with OTMS in addition to 3-MPS have lower viscosities than those functionalized only with 3-MPS. Like the variations in resin monomers, this is expected to result in lower viscosity values. Although the work performed in chapter 4 directly related viscosity and conversion, in this case the interfacial reactivity would be lower due to the lower surface concentrations of γ-MPS. This change in methacrylate density may affect the relationship that was established with fillers functionalized only with γ-MPS. Thus, there would be a competition between the lower viscosity and lower methacrylate density, however, since the surface methacrylates account for only a small portion of the available groups, it would most likely still result in a higher conversion value due to the lower viscosity.

Polymer nanogel particles (see section **1.3.3**) that were previously shown to reduce shrinkage stress would also make an interesting extension to the models developed here. Since these are structurally similar in composition to the resin monomers themselves, their

contributions to viscosity and conversion may result in much more favorable values. These should have dramatically lower interaction energies, resulting in smaller viscosity changes with the addition of filler particles. This may also be helpful in explaining some of Liu *et al*'s observations regarding decreased shrinkage stress when adding nanogel particles to composite formulations (*6*).

6.2.3 Cellulose Nanocrystals as Ionomer Cement Components

Cellulose nanocrystals (CNCs) have seen increasing interest in the recent years for their very high mechanical properties, and biological origin. CNCs are obtained from the acid hydrolysis of cellulose fibers, resulting in only the small crystalline domains, where their dimensions depend on the source of cellulose initially used (wood, bacterial, plant). The most common protocol for producing CNCs involves hydrolysis using concentrated sulfuric acid, which leaves the surfaces of the nanocrystals with sulfate half-esters ($O\text{-}SO_3^-$), and counterion.

Due to their surface charge, CNCs are difficult to integrate into hydrophobic polymer matrices, such as those of dental resin composites. However, this ion coordination property could be exploited to integrate them into glass ionomer cements (see p.2). By placing the desired counterion on the surface of cellulose nanocrystals, their integration into glass ionomer cements should allow curing of the materials, and also bond the CNCs into the polymer matrix, conveying increased toughness and strength to the final material, thanks to their mechanical properties and high aspect ratio. Initial tests would evaluate whether a small percentage of nanocrystals have a positive influence, and could also test higher ratios, possibly replacing the alkaline glasses that are traditionally used as fillers in these materials.

6.3 References

1. Desmond, K. W.; Weeks, E. R., Influence of particle size distribution on random close packing of spheres. *Phys Rev E* **2014,** *90* (2), 022204.
2. Wang, R.; Habib, E.; Zhu, X. X., Application of close-packed structures in dental resin composites. *Dent Mater* **2017,** *33* (3), 288-293.
3. Wang, R.; Habib, E.; Zhu, X. X., Evaluation the filler packing structures in dental resin composites: from theory to practice. *Dent Mater* **Submitted 2017**.

4. ASTM, Standard Test Methods for Rubber—Viscosity, Stress Relaxation, and Pre-Vulcanization Characteristics (Mooney Viscometer). ASTM: 2015; Vol. D1646-15.
5. Wilson, K. S.; Zhang, K.; Antonucci, J. M., Systematic variation of interfacial phase reactivity in dental nanocomposites. *Biomaterials* **2005,** *26* (25), 5095-5103.
6. Liu, J.; Howard, G. D.; Lewis, S. H.; Barros, M. D.; Stansbury, J. W., A Study of Shrinkage Stress Reduction and Mechanical Properties of Nanogel-Modified Resin Systems. *Eur Polym J* **2012,** *48* (11), 1819-1828.

Appendices

Glossary

Brunauer-Emmett-Teller (BET) theory: a model of gas adsorption to solid surfaces, allowing measurements of surface area and surface porosity of solids.

Buccal surface: side of the teeth on the outside (in contact with the cheek).

Composite: Two phase blend made up of a continuous *resin* phase, and a discrete *filler* or *reinforcement* phase.

Compressive stress: force exerted on axially on a cylinder of material.

Conversion: fraction of double bonds that have reacted when the polymerization reaction occurs.

Diametral stress: force exerted diametrally (on the round side) on a cylinder of material.

Dispersity: size distribution of the material in question, defined as the particles weight average, divided by the size average. High dispersity materials will have a wider range of sizes, while low dispersity materials are all of very similar sizes. A value of 1 corresponds to particles that are all exactly the same size.

Filler: see reinforcement.

Flexural modulus: initial slope of the stress-strain graph in flexural stress tests, indicates stiffness of the material

Flexural strength: force exerted at the breaking point in flexural stress testing, indicates how much force the material can resist before breaking.

Flexural stress: stress exerted in three-point bending geometry, combining compressive and tensile forces.

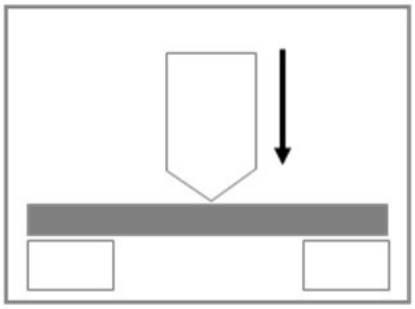

Lingual surface: inner surface of the teeth, (potentially) in contact with the tongue.

Marginal separation or leakage: separation between the dental restoration and the containing dental hard tissue. This gap can cause leakage, where bacteria can grow and cause restoration failure.

Monomodal: particles sizes are distributed around a single average or median value, usually in a Gaussian-like distribution.

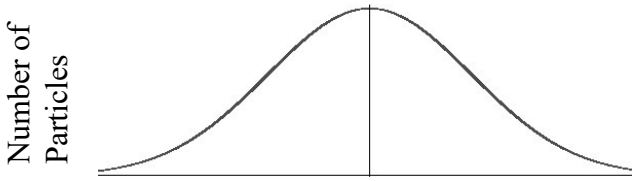

Multimodal: particle sizes are distributed over several main values, with several peak distributions.

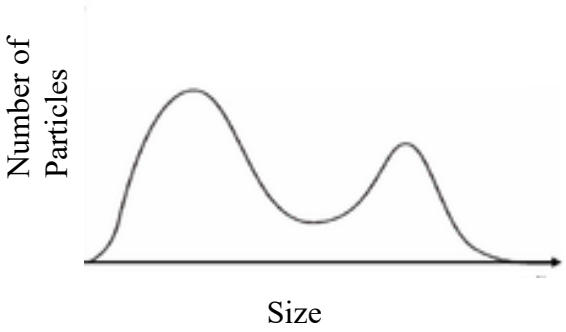

Occlusal surface: upper side of the tooth (for lower teeth) and lower side of the tooth (for upper teeth) where the jaw exerts most stress to masticate food

Radiopacity: opacity to X-rays, usually compared to an equivalent thickness of aluminum.

Reinforcement: solid particles added to a continuous (liquid) phase to convey improved mechanical performance to the resulting composite.

Resin: blend of monomers, radical initiators, and polymerization inhibitors that constitute the liquid phase of the composite.

Rheology: measurement of shear viscosity at different levels of stress by rotating two plates against one another.

Shrinkage, volumetric: volume reduction that occurs upon polymerization in free radical polymerizations

Shrinkage stress: force that is exercised upon the surrounding surfaces when volumetric shrinkage occurs.